# *Electronic Theses: Phenazine: a building block for multinuclear and heterometallic complexes, where the ligand acts as an electron acceptor and radical abstractor*

Vladimir Shuster

Thesis submitted to the
Faculty of Graduate and Postdoctoral Studies
in partial fulfillment of the requirements
for the M.Sc. degree in Chemistry

Department of Science
Faculty of Chemistry
University of Ottawa

# Abstract

Over the past decade, intensive academic and commercial interests have been paid on compounds possessing photochemical properties, namely for their preparation, chemical properties, high efficiency and potential low-cost.

Compounds having intense photochemical properties gained great interest due to wide range of potential applications. The sensitizers are one of the key components for high power-conversion efficiency in the dye sensitized solar cells (DSSCs). They are the core components in the organic light-emitting devices (OLEDs) due to their ability to emit light with the wavelengths largely red-shifted from their absorption wavelength. Ruthenium based sensitizers have been tagged "molecular light switches" because, although the fluorescence of these complexes in aqueous solutions is negligible, it increases of greater than 10000 fold in the presence of DNA. Many polypyridyl and dipyrido phenazine ruthenium complexes have achieved high power conversion efficiencies and therefore are of practical interest. Several research groups stated that the dipyrido phenazine ligand may be thought of as comprising two components: a bipyridyl unit and a phenazine unit. These two subunits behave essentially separately, with many molecular orbitals being localised over only one subunit and a redox properties of central phenazine moiety in the dipyrido phenazine ligand are important for the photochemical applications.

Therefore a phenazine ligand was selected as a model for the present investigation. The chemistry of phenazine ligand is mostly limited to the late transition metal and *f* - element complexes. Our laboratory has a rich backgroung in the aluminum and early transition metal chemistry. The aluminum chemistry and early transition metal chemistry are of great interest since aluminum and early transition metal complexes are environmentally friendlier and cheaper than the

late transition metal compounds. Another drawback of the ruthenium-based sensitizers is the lack of absorption in the red region of the visible spectrum, and also low molar extinction coefficients. An essential requirement for efficient conversion of solar energy is the good spectral match of the sensitizer absorption to the emission spectrum of solar radiation. In this regard, the ruthenium sensitizers' spectral response in the lower energy regions is not sufficient.

The current project has three parts. In the first part we collected and reviewed known literature regarding the certain classes of non-innocent ligands containing the six-membered carbon-nitrogen heterocycles and regarding the ligands potentially important for the photochemical applications. We also reviewed all available to the data information about the complexes supported by the phenazine ligand.

In the second part we have investigated interaction of alkylaluminum compounds and phenazine and observed reduction of phenazine accompanied by formation of dialuminum cage type compounds containing two formally mononegative phenazine ligand. The derivatization of phenazine has been also observed. It resulted in formation of compounds having a stable organic radical.

In a third part of our project we have explored interaction of phenazine or thiophenazine with the alkylaluminum compounds and chromium dichloride. The reaction in the three component system resulted in reduction of phenazine ligand and lead to the heterometallic Cr(II) - aluminum complexes containing a formally dinegative phenazine or thiophenazine ligands. When a large excess of triethylaluminum was taken, reduction of phenazine and chromium has been observed leading to the heterometallic multinuclear Cr(I) - aluminum complex containing a formally dinegative phenazine ligands and two chromium atoms in one complex in the rare oxidation state one.

# Acknowledgments

Firstly, I would like to acknowledge and express my deepest gratitude to my supervisor, Professor Sandro Gambarotta. Without his affording me this unique opportunity to join his group, this project would have never been realised and I would never have been able to acquire all the knowledge that he has transcribed from his experiences. The study in prof. Sandro Gambarotta group has provided me with more than what is needed for a successful and rewarding career. Furthermore, all this was packaged into an excellent research environment where a healthy teamwork spirit flourished. Within the group, I would like to acknowledge all my friends, Grigory Nikiforov, Sebastiano Licciulli, Chris Mason, Steven Horvath, Indu Vidyaratne and Elena Smolensky for their constant help, support, as well as their sharing of knowledge and experience.

I must thank Dr. Grigory Nikiforov for obtaining X-ray crystal structure data of my compounds (**2a**, **2b**, **2c**, **2d**, **3c** in chapter 2 and **3** and **4** in chapter 3) and Dr. Ilia Korobkov for obtaining X-ray crystal structure data of my compounds (**1a** in chapter 2 and **1** and **2** in chapter 3). I also wish to thank Dr. Grigory Nikivorov for the kind attention, valuable discussions and advises. I must be grateful to the University of Ottawa EPR team for measuring, analyzing my EPR data and important advises. In addition, many thanks are to Professor P. H. M. Budzelaar and Dr. Serge Gorelski for the DFT calculations.

# Table of contents

# List of Figures

# List of tables

## List of Abbreviations

| | |
|---|---|
| Ar | aromatic group |
| AF | antiferromagnetic |
| Bipy | 2,2′-bipyridyl |
| calcd | calculated |
| cat | cationic |
| Cp | cyclopentadienyl ($C_5H_5$) |
| Cp* | pentamethylcyclopentadienyl ($C_5Me_5$) |
| DEAC | diethylaluminum chloride |
| dimpy | 2,6-diiminepyridine |
| DFT | Density Functional Theory |
| DNA | Deoxyribo Nucleic Acid |
| DMP | 2,5-dimethylpyrrole |
| dppz | dipyrido[3,2-*a*:2′,3′-*c*]phenazine |
| ESI | Electro Spray Ionization (Mass Spectrometry) |
| EPR | Electron Paramagnetic Resonance |
| ESR | Electron Spin Resonance |
| Et | ethyl |
| $Et_2O$ | diethyl ether |
| $^{i}$Bu | iso-butyl |
| $^{i}$Pr | iso-propyl |
| HOMO | Highest Occupied Molecular Orbital |
| IR | Infrared |
| L | ligand |

| | |
|---|---|
| LC | ligand charge |
| LUMO | Lowest Unoccupied Molecular Orbital |
| MC | metal charge |
| Me | methyl |
| MLCT | Metal-to-Ligand Charge-Transfer |
| MPT | molybdopterin |
| $^{n}$Bu | butyl |
| NMR | Nuclear Magnetic Resonance |
| Ph | phenyl |
| phz | phenazine |
| Py | pyridine |
| R | alkyl group |
| SCE | Saturated calomel electrode |
| SOMO | semi occupied molecular orbital |
| sq | square |
| $^{t}$Bu | tert-Butyl |
| TEAL | triethylaluminum |
| THF | tetrahydrofuran |
| TIBA | tri-isobutylaluminum |
| TMA | trimethylaluminum |
| UV-Vis | Ultra Violet - Visible Spectroscopy |
| V | volt |
| XAS | X-Ray Absorption Spectroscopy |
| XRD | X-ray Diffraction |

# Chapter 1

## *Introduction*

## *Non innocent ligands*

Ligands are the "tools" of the organometallic chemist. They can be used to push or pull electron density, and to modify the available space around the metal, thus allowing tuning of reactivity at the metal centre in catalytic or stoichiometric reactions. They can link metal centres together in a multi nuclear assemblies and metalloorganic framework, possessing a desired physical properties. Ligands used in this way can be considered as "innocent," in the sense that their participation in the chemistry of a complex is exclusively ancillary. Sometimes, however, a ligand plays a more active ("non-innocent") role. Most often, this is an unwanted role, leading to complex decomposition, ligand degradation or side reactions. However, in many cases, ligand participation has been found to be crucial to catalytic activity, magnetic properties or especially to conductivity, semiconductivity and photo physical properties.

The term "non-innocent" was introduced in chemistry by Jørgensen in 1966. According to the definition by Jørgensen, a ligand is innocent if it allows the unambiguous determination of the oxidation state of the central metal atom.

This definition refers only to the ligand, but, in actuality, the innocent or non-innocent behaviour is related to the complex as a whole, [1] because, in order to draw conclusion about the nature of a ligand, consideration of molecular orbitals is necessary. The metal-centred and ligand-centred frontier orbitals in complexes containing "non-innocent" ligand should have small difference in energy, so electron transfer might occur easily within the molecule depending on the

conditions applied. In some cases, the ligand- and metal-centred orbitals can be so close that the complexes display "redox isomerism"; for example Pierpont has described a cobalt-dioxolene complex which switches between $Co^{II}$(sq) and $Co^{III}$(cat) forms as a function of temperature (Scheme 1).[2,3,4]

Some complexes with the "non innocent ligands" have even strong mixing between the ligand and metal frontier orbitals, such that assignment of oxidation states to individual metal and ligand components is difficult. [5]

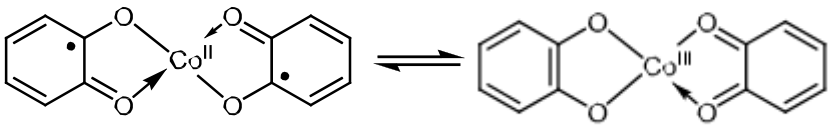


**Scheme 1.**

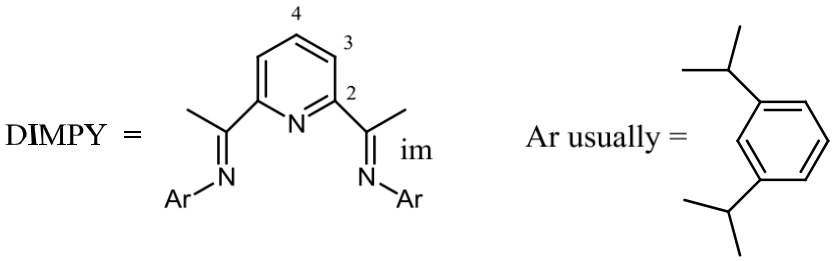


**Scheme 2.**

An example of electronic nature of "non innocent" ligand in complex is a difference between the nature of the metal - dimpy interaction and that of the same metal with a "classical" $\pi$ - acceptor like CO (dimpy ligand is on the Scheme 2).[6] In carbon monoxide, the $\pi$ * LUMO is concentrated on the carbon atom directly bound to the metal. As a result, there is a large overlap between metal *d* and ligand $\pi$ * orbitals, resulting in a mainly covalent back donation type interaction (Figure 1A). The dimpy $\pi$ * orbitals are very delocalized, and the direct d– $\pi$ * overlap is

much smaller. As a result, the interaction will have the character of an intramolecular single electron transfer (resulting in singlet biradical character, (Figure 1B), and the extent of transfer can be very sensitive to small changes in the relative orbital energies of the metal and ligand components. The dimpy ligand seems remarkable for the fluidity of its M–L interaction and its ability to temporarily store and later release electrons. This electronic flexibility results in considerable stabilization of unusually low valent oxidation states, which are in reality higher valent oxidation states in combination with ligand radical anions.

**Figure 1**. Schematic representation of orbital interactions in (A) metal–CO and (B) metal–dimpy complexes.

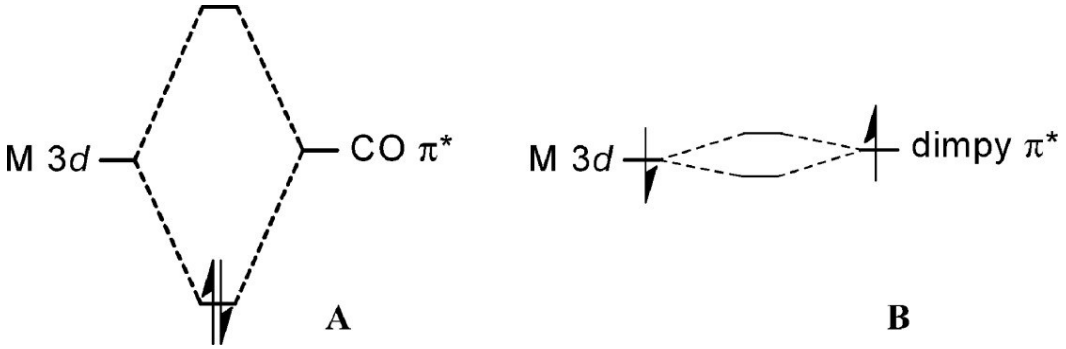


Transition metal complexes with the so-called "non-innocent" ligands have been known in coordination chemistry since the preparation and study of the planar dithiolene complexes of nickel, palladium and platinum nearly 40 years ago (Scheme 3).[7,8,9,10,11,12 ,13,14] However, the term "non-innocent" gained wide acceptance only in the 1990s, when such complexes attracted considerable attention. Hybrid DFT calculations supported by XAS and EPR experiments indicate a Ni(II) formal oxidation state and a diradical character of complex. Bonding description indicates the

presence of at most limited spin polarization (i.e. diradical character) of the dithiolene ligand, with the unpaired electrons located on the ligands (Scheme 3, structure B).[15,16]

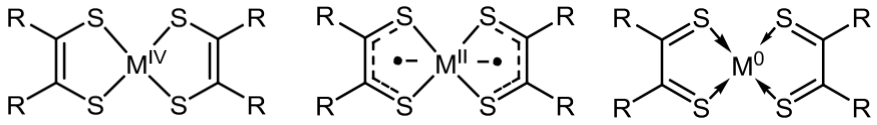


**A** **B** **C**

**Scheme 3**. Three possible resonance descriptions for the planar *bis*-dithiolene complexes with M = Ni, Pd, Pt.

Another representative example of complex with a non-innocent ligand is the $Ni(C_6H_4(NH)_2)_2$ obtained in 1966. [14] Wieghardt and coauthors confirmed that the $Ni(C_6H_4(NH)_2)_2$ has structure **C**; complex has Ni in a formal oxidation state two and unpaired electrons located on the ligands (Scheme 4).

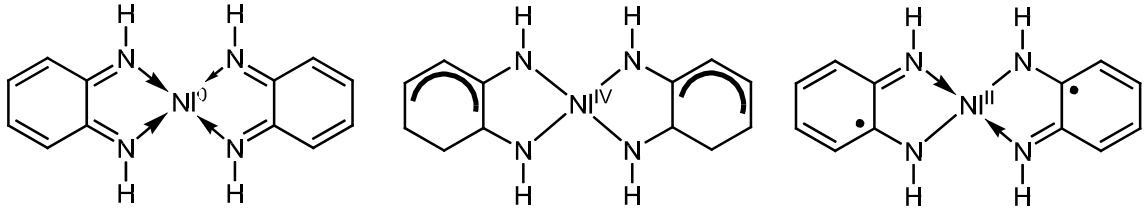


**A** **B** **C**

**Scheme 4**. Three possible resonance descriptions for the planar *o*-benzoquinonediimine nickel complexes.

Besides the consideration of molecular orbitals a conclusion about the nature of a ligand in such complexes can be drawn from the structural criteria. Oxidation and reduction of "non innocent" ligand can be followed from the changes in the bond lengths. For example, the length of the C-N single bond in *o*-phenylenediamine ligands [17] is ~ 1.46 Å. In *o*-diiminoquinones, both C=N bond lengths are ~ 1.31 Å, whereas these bond in the *o*-diiminobenzosemiquinonate radical have an intermediate value of ~ 1.36 Å. Table 1 lists approximate C=N and C2–$C_{im}$ bond lengths as a function of the number of electrons transferred to the dimpy ligand.[6]

**Table 1**. Variation of dimpy bond lengths (Å) as a function of electron transfer.

| No. electrons | $C_{im}$=$N_{im}$ | $C_{im}$–C2 | Ref. |
|---|---|---|---|
| 0 | 1.28 | 1.50 | 18,19 |
| 1 | 1.32 | 1.44 | 20,21 |
| 2 | 1.36 | 1.40 | 22 |
| 3 | 1.40 | 1.37 | 23 |

*C2 is attached to nitrogen in the central six membered ring of dimpy (Scheme 2).

As mentioned above, oxidation, reduction of ligands rather than metals as well as formation of radical species is very typical for complexes with non-innocent ligands. In redox reactions, such ligands can serve as an "electronic buffer" or "electron reservoir",[24] which reversibly accepts and donates electrons, whereas the oxidation state of the central metal atom remains unchanged.

In the next chapters, we will briefly present several classes of "non-innocent" ligands. Generally, many reviews have been devoted to various classes of “non-innocent” metal complexes: with oxygen-containing ligands based on pyrocatechols,[5,25,26] with dithiolene ligands,[27] with ligands based on aromatic diamines,[28],[29] *p*-quinones,[30] corroles,[31] *etc*.[32,33,34,35] We will mention only selected classes of ligands containing a conjugated carbon-nitrogen bonds, since we selected phenazine ligand for our investigation, which have conjugated carbon-nitrogen bonds and belong to the class of polycyclic aza-compounds containing (4n+2) $\pi$ electrons.

## *Selected classes of non-innocent ligands, Pterins and Flavins*

Pterins and flavins are important class of ligands containing conjugated carbon-nitrogen bonds in a six membered heterocycles (Scheme 5). These ligands permit metal coordination preferentially at the O4 -N5 chelating cites (Scheme 6). They are redox-active cofactors in their own right,[36,37] which can even function as $O_2$ activating species in enzymes without direct support by metal centers, [37] although a redox activity of pterins and flavins is substantially enhanced after metal ion binding. [38], [39], [40] In complexes with these ligands, there is a strong

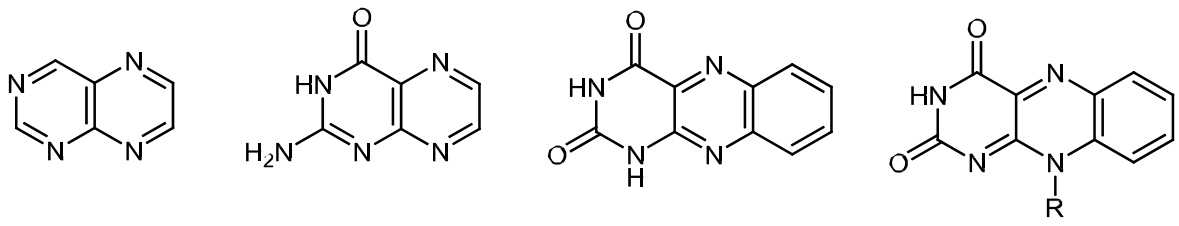

**Pteridine** **Pterin** **Alloxazine** **Flavins**

**Scheme 5.**

interaction between the transition metal atom and the ligand. [41] [42] In particular, UV-Vis and photoelectron spectroscopy demonstrated that the resonance description involving partial structures A and B (Scheme 6) is preferable to the alternative structure C which implies a complete transfer of two electrons to the molybdenum center (a fragment of the complex is shown in Scheme 6).[42]

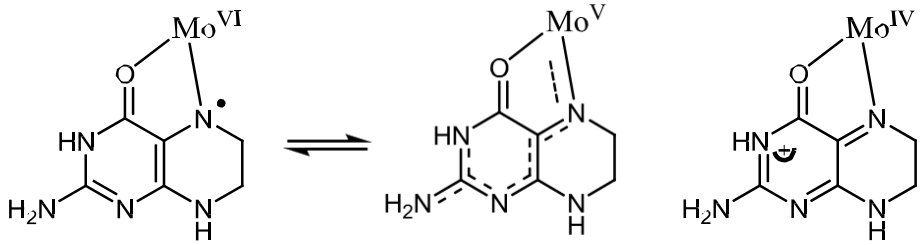


**A** **B** **C**

**Scheme 6.**

A considerable metal → ligand charge transfer and stabilisation of ruthenium, copper and rhenium complexes with the reduced ligand were established by cyclic voltammetry and UV-Vis spectroscopy in the visible region.[43] Iridium,[44] copper,[45,46,47,48] iron(II),[46] cobalt(II) [46] and zinc [47] complexes with pterin and pteridine were studied by spectroscopic and electrochemical methods and characterised by X-ray diffraction.

The molybdopterin (MPT) is a catalytic centre of enzymes that transfer an oxygen atom to or from the substrate (Scheme 7). These enzymes catalyse a wide range of reactions and are present in virtually all living systems. Several of these enzymes have been structurally characterised and each catalytic centre shown to involve a single metal atom bound to one or two MPT groups, plus other donor atoms. Spectroscopic information indicates that the oxygen atom transfer reaction takes place

at the metal centre, the oxidation state of which changes from

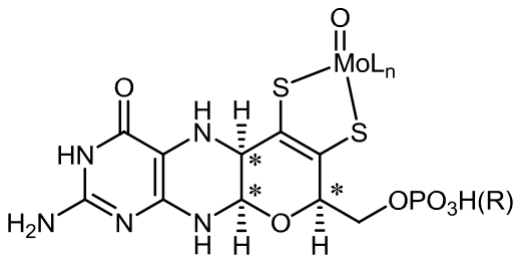


**Scheme 7**. Structure of "molybdopterin" (MPT), the ligand that coordinates molybdenum or tungsten at the catalytic centre of the oxotransferase enzymes; chiral centres are indicated by *; R =H or a dinucleotide.[49]

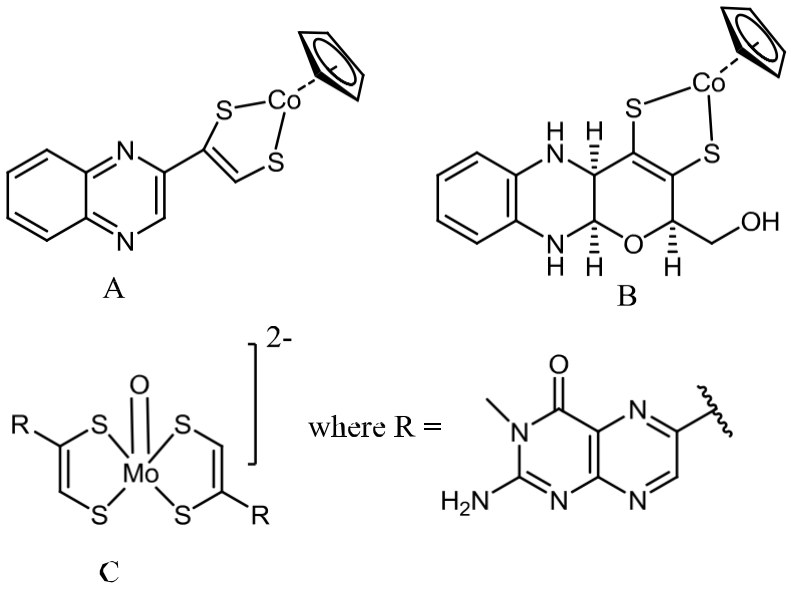


**Scheme 8**. (A) [CpCo{$S_2C_2H$(quinoxalin-2-yl)}] [50] ; (B) [CpCo(dt)] compound containing a pyranoquinoxaline analogue of MPT [51]; and (C) one of the $[Mo(O)(dt)_2]^{2-}$ complexes synthesised by Davies et al.[52],[53]

Mo(VI) to Mo(IV) (or vice-versa). This chemistry has been replicated by low molecular weight analogues of these centres. However, challenges remain in understanding the coordination chemistry of these centres, not the least of these is the role of the pterin and pyran ring that, together with the dithiolene, form MPT.[54,55 56,57]

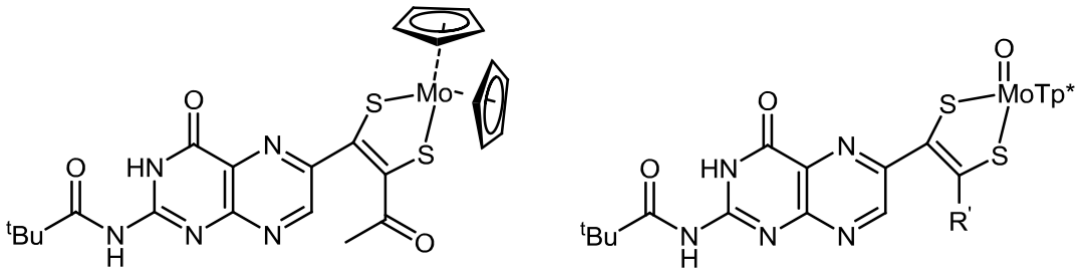


**Scheme 9**. [$Cp_2Mo(dt)$] and [Tp*Mo(O)(dt)] (Tp* = the hexamethylated tris(pyrazolylborate) ligand, R′ = phenyl or difluorophenyl) complexes containing a dithiolene ligand related to MPT.[58,59]

As an initial step towards the synthesis of MPT, general strategies for the synthesis of asymmetrically substituted dithiolenes have been developed and series of complexes have been synthesized (Scheme 8 and Scheme 9). The $E_{1/2}$ values for the Co(II)/Co(III) and Mo(V)/Mo(IV) redox couple were shown to be modulated by the nature of the substituent (R) on the dithiolene.

## *Selected classes of non-innocent ligands, 2,6-diiminopyridine (dimpy) and related ligands*

Chemistry of complexes supported by the dimpy ligand in intensively developed during the last 15 years. Metal complexes with dimpy ligand catalyze a wide variety of reactions, ranging from polymerization [60] and hydrogenation [61] to aldehyde homologation, [62] electrocatalysis [63] and hydrosilylation of olefins,[64] as well as the cyclization of enynes and diynes. [65] The ligand shows a unique tendency to become involved in chemical reactions.

Conjugated carbon-nitrogen ligands including 2,6-diiminepyridine (dimpy) (Scheme 2), and its derivatives (I – VIII, Scheme 10) have long been recognized as "non-innocent".[6] Their $\pi$-systems can easily accept one or more electrons, leading to formation of stable complexes where the metal has a deceptively low *formal* oxidation state, while the actual electronic structure is best viewed as containing a higher-valent metal bound to a negatively charged ligand ("electronic non-innocence").

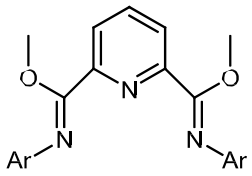

I, ref. [66]

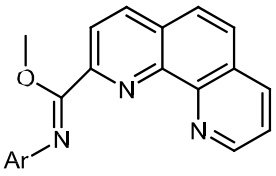

II, ref.[67]

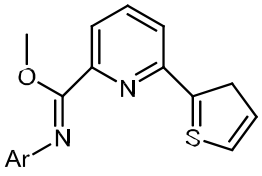

III, ref.[68]

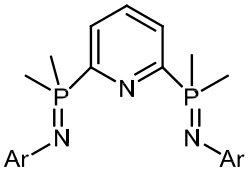

IV, ref.[69],[70]

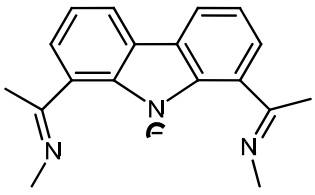

VI, ref.[72]

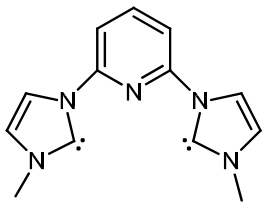

VII, ref. [73]

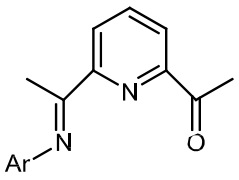

VIII, ref.[74]

**Scheme 10.**

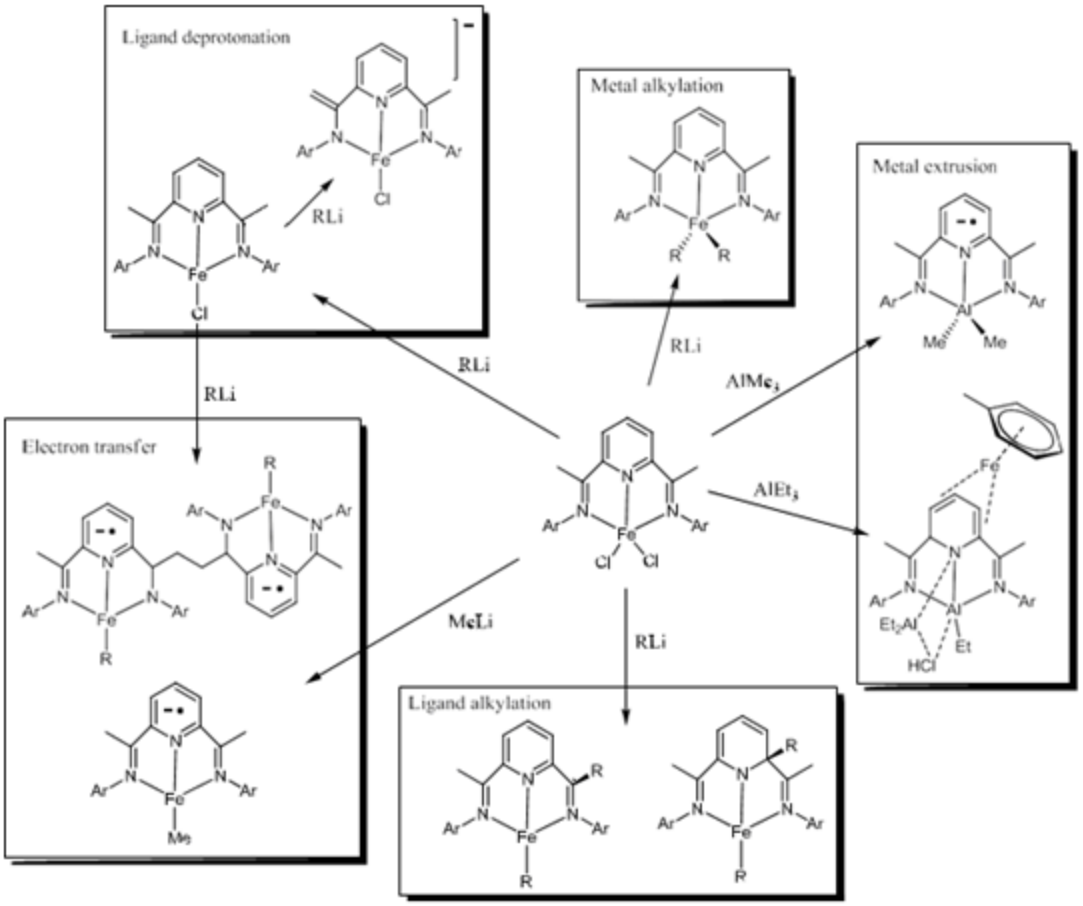


**Scheme 11**. Metal- and ligand-centred reactivity of (dimpy)$FeCl_2$ (R = $CH_2SiMe_3$). Scheme is taken from ref. [6] Metal alkylation ref.[75] Ligand deprotonation refs.[76,78] Electron transfer [77] and ligand alkylation ref.[78] Metal extrusion refs.[79,80]

The reaction of transition-metal chloride complexes of the dimpy ligand with alkylating agents has been studied extensively, mainly with the aim to generate transition-metal alkyls as immediate precursors of polymerization catalysts (Example of iron is given in Scheme 11). While in some cases simple metal alkylation is indeed observed, more often one finds also reduction of the metal centre leading to ligand radical anion complexes or alkyl attack at the ligand. One might have expected alkyl

attack at the imine function, but that is certainly not the only reaction observed. In fact, alkyl addition has been observed at nearly all positions of the ligand (Scheme 4),[81,78] although the single example of C4 alkylation was isolated as a dimer.[82,83] Calculations support the idea that much of this chemistry can be interpreted in terms of radical formation induced by the electronic non-innocence of the dimpy ligand. Also, for both transition metals and main group metals ligand alkylation can be reversible,[78,81,79,80,84,85] and the various isomers can be surprisingly close in energy.[79,80]

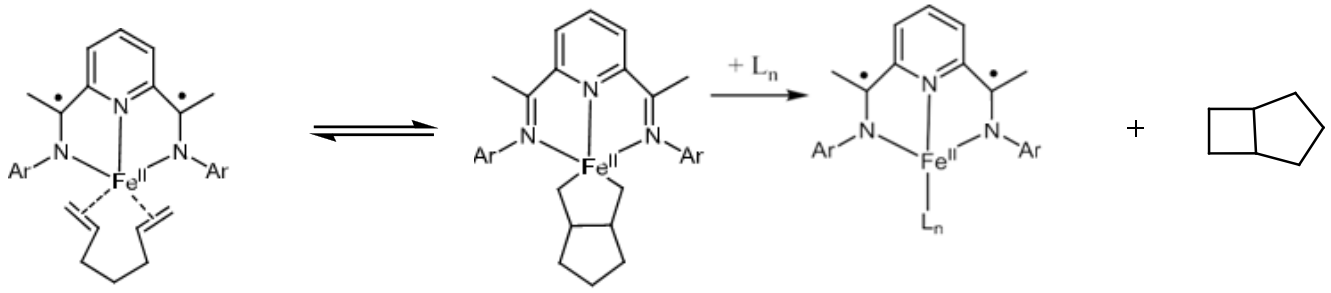


**Scheme 12**. Catalytic [2$\pi$ + 2$\pi$] cycloaddition promoted by bis(imino)pyridine iron.

The iron complex (dimpy)Fe($N_2$)$_2$can be used in a number of reactions, such as the hydrogenation and hydrosilylation of olefins,[64] as well as the cyclization of enynes and diynes [65] (Scheme 12). A combination of spectroscopic techniques and density functional theory calculations established that this formally iron(0) compound (with a neutral ligand) has the physical oxidation state of an intermediate spin iron(II) compound, where the metal has transferred two electrons to the dimpy ligand.[86,87]

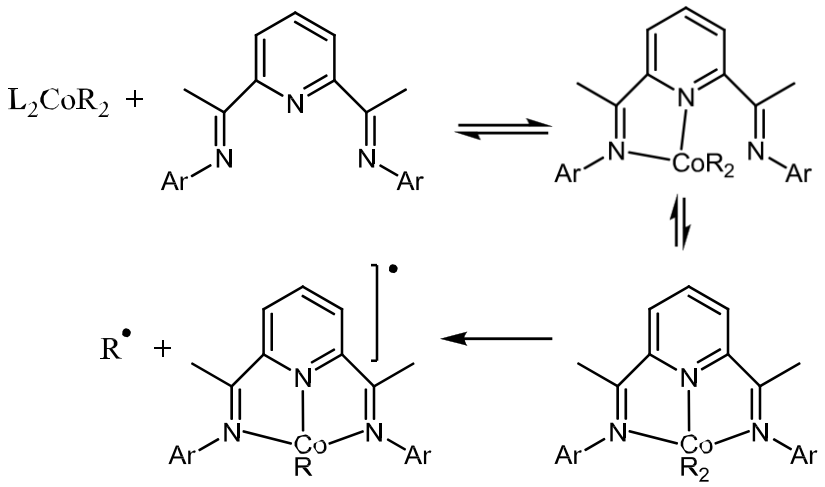

**Scheme 13**. L = Pyridine, TMEDA; R = $CH_2SiMe_3$.

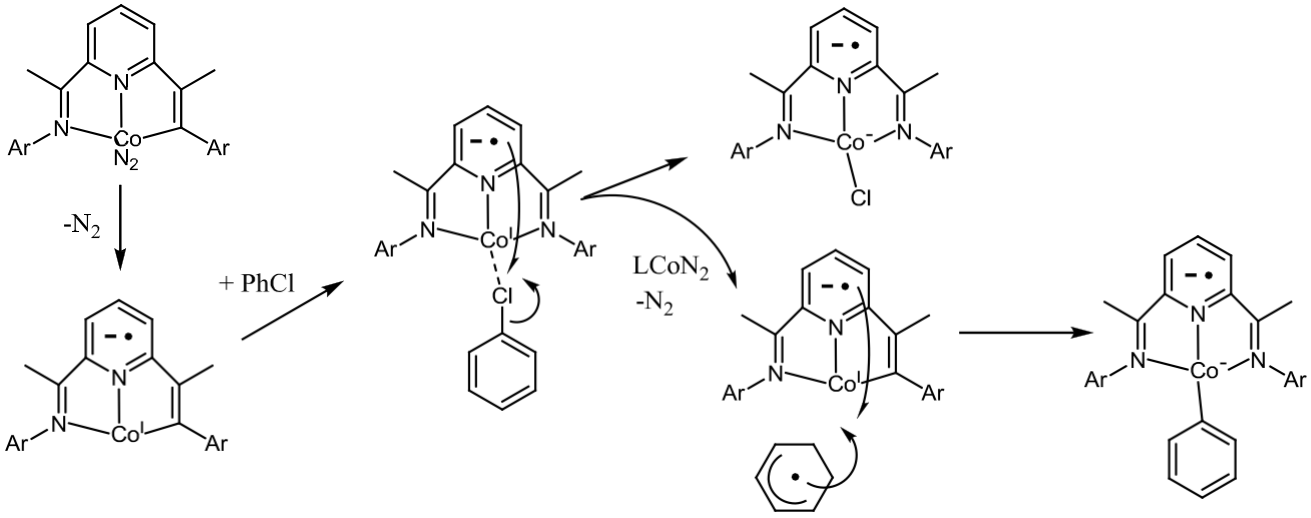

**Scheme 14**. Radical- type oxidative addition at (dimpy)Co fragments.

The neutral dimpy ligand, coordinated to the metal, is capable of abstracting an electron from a metal-carbon bonding orbital, thus leading to the loss of an organic radical (Scheme 13).

Where that radical then ends up depends on the solvent used, nature of the central metal atom, and distribution of unpaired electron density over the ligand. [88,89]

The binuclear oxidative addition of ArCl to (dimpy)Co($N_2$) is rationalized in Scheme 14. Authors [89] believe that the reaction is best explained by a radical process (analogous mechanisms have been proposed for alkyl halide addition to cobalt(II).[90] The aryl halide could displace $N_2$ from (dimpy)Co($N_2$) and then undergo C-Cl cleavage to release the free aryl radical, which would independently react with a second (dimpy)Co($N_2$) molecule. Alkyl halides RX (X=Cl, Br, I, R = benzyl, Me) also react with the (dimpy)Co($N_2$) in the similar way.

## *Selected classes of non-innocent ligands, bipyridyl and polypyridyl ligands, photochemical properties of these ligands*

The bipyridine, phenantroline and related polypyridine ligands are extensively studied over the last hundred years and various oxidative and reductive transformations are described for complexes supported by this class of ligands.

The simple bipyridyl ligand and more complex polypyridyles might be described as "non innocent" ligands.[35] For instance, $[Cr(bipy)_3]^{3+}$ is involved in a series of reduction reactions,[91] with the metal-and ligand centred orbitals (which are comparable in energy in that complex) involved in redox processes. The metal atom of $[Cr(bipy)_3]^{3+}$ is reduced in the first step to form $[Cr^{II}(bipy)_3]^{2+}$, and the successive two electron reduction occurs at the $\pi^*$ orbital of the ligand to give a species described as $[Cr^{II}(bipy)_2(bipy^{\bullet -})]^{+}$ {or as $[Cr^{III}(bipy)(bipy^{\bullet -})_2]^{+}$}. The complex $Ti(bipy)_3$ was first prepared by Herzog in 1960 [92] and later it has been studied by several authors in connection with

the metal oxidation state and nature of a ligand.[93,94,95] Analysis of the EPR, NMR, electronic spectra and chemical behavior of the complex led to the conclusion that the ligands in $Ti(bipy)_3$ carries a considerable negative charge.

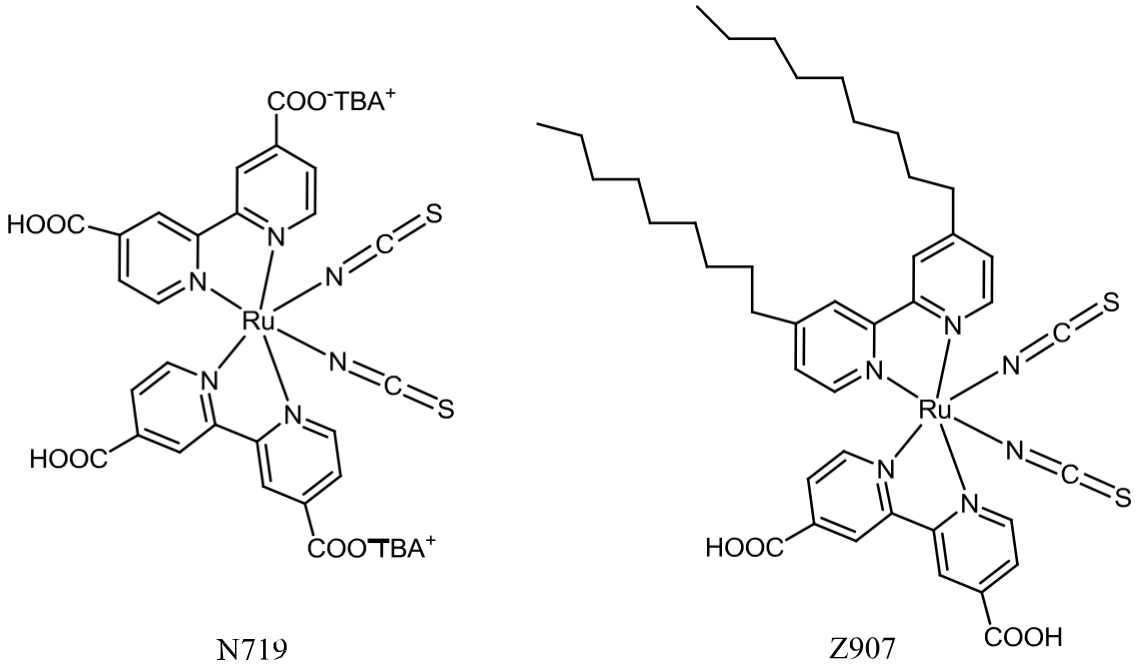


**Scheme 15.**

Ruthenium and osmium based polypyridyl complexes have gained considerable attention because of their intense fluorescence properties. Sensitizers having the general formula $ML_2(X)_2$, where L stands for 2,2′-bipyridyl-4,4′-dicarboxylic acid, M = Ru or Os, and X presents a halide, cyanide, thiocyanate, acetyl acetonate, thiacarbamate or water substituent, are particularly promising.[96,97] The classic sensitizer dye employed in dye sensitized solar cell is a ruthenium(II) bipyridyl dye, cis-bis(isothiocyanato)-bis(2,20-bipyridyl-4,40-dicarboxylato)-ruthenium(II), which is usually referred to as "N3", or in its partially deprotonated form (a di-tetra butylammonium salt) as "N719" (Scheme 15). The incorporation of carboxylate groups allows ligation to the $TiO_2$ film

surface *via* the formation of bidendate and ester linkages, while the (NCS) groups enhance the

absorption of visible light. The highest solar-to-electrical conversion efficiency to date (about 12%) has been obtained with the combination of polypyridine complexes of Ru such as "N719" and the iodide triiodide mixture dissolved in a low viscosity solvent such as 3-methoxypropionitrile. Addition of long alkyl units to the bipyridine ring of the Ru-dye, as in the dye "Z907" (Scheme 15) increases significantly the hydrophobicity of the bound titania surface. This in turn reduces the

amount of water adsorption and better stability of the solar cells.[98]

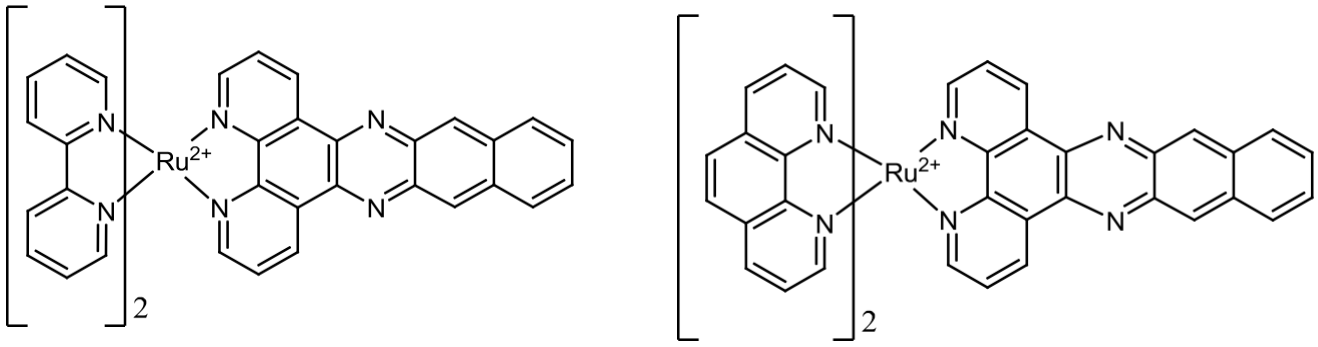


**Scheme 16**. Ruthenium(II) complexes with selected simple extended ligands based on the dppz chromophore.

Another important ligand is dipyrido[3,2-*a*:2′,3′-*c*]phenazine (dppz), which belong to the polypirydil ligands. Ruthenium (II),[99,100,101] rhenium (I),[99,100,101] copper(I)[99,100,101] and iridium (III)[100] based complexes containing dppz and its derivatives (Scheme 16) have been intensively explored because of their intense photochemical properties and fluorescence upon association with DNA. Ruthenium (II) complexes with the dppz have been tagged "molecular light switches" because, although the fluorescence of these complexes in aqueous solutions is negligible, it increases of greater than 10000 fold in the presence of DNA.[102] Complexes of dppz are also useful

as components in organic light-emitting devices (OLEDs) because their emission color is largely red-shifted from their absorption wavelength.[103],[104]

The properties of dppz suggest that reduction of the ligand, or complexes containing these ligands, leads to the formation of a radical anion with a charge located on the phenazine portion of the ligand.[99,105,106,107,108,109] Various studies using cyclic voltammetry,[110,111,106] UV/vis [110,111,106] and emission spectroscopies, [110,111] nanosecond transient absorption spectroscopy [111,112] and EPR [106] also established that the emitting state resulted from a charge transfer from the ruthenium centre to the dppz ligand, in effect producing $[Ru^{III}(bpy)^2(dppz^{\bullet -})]^{2+}$ as the MLCT state. The spectrum of the dppz anion radical matched that of the nanosecond transient absorption of excited state $[Ru(bpy)_2(dppz)]^{2+}$, suggesting that the electron is localized on the dppz $^{\bullet -}$ radical anion in this excited state.[111]

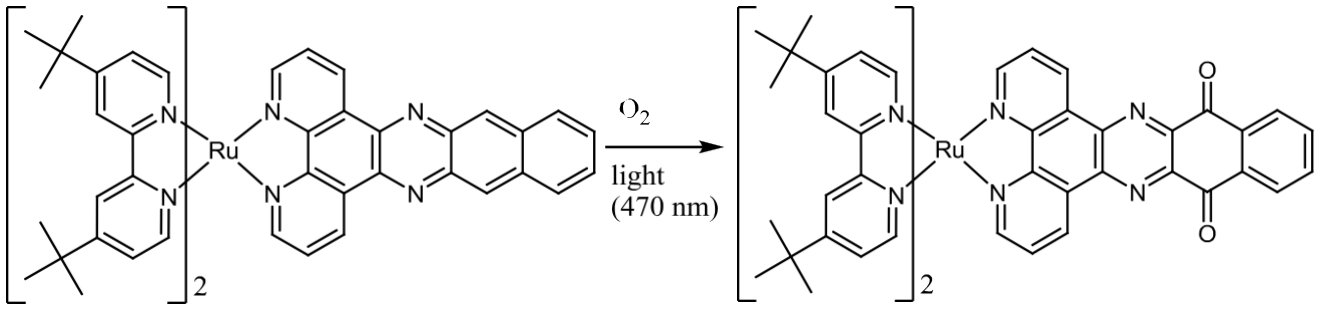


**Scheme 17.**

The "non innocent" nature of dppz is illustrated by oxidation of ruthenium polypyridyl complex. Irradiation of a complex in the presence of oxygen leads to the oxidation of a benzodipyridophenazine ligand to a quinine (Scheme 17).[113] Authors [113] postulate that the oxidation process involves singlet oxygen which is created by triplet sensitisation from the excited ruthenium

$^3$MLCT state. The polypyridylruthenium complexes are able to create singlet oxygen which can be used in organic transformations, which can also be exploited for the preparative catalytic oxidation of citronellol.[114] Other example is electrochemical reduction of complex $[Ru(L)(bipy)_2](ClO_4)_2$, [bipy = 2,2′-bipyridyne; L = 7-methoxy-5-(4-methoxyphenyl)-2,3-bis(4-methoxyphenylimino)-3,5-dihydro-2H-phenazin-1-one] (Scheme 18).[115] Complex showed a reversible reductive response near -0.35 V.

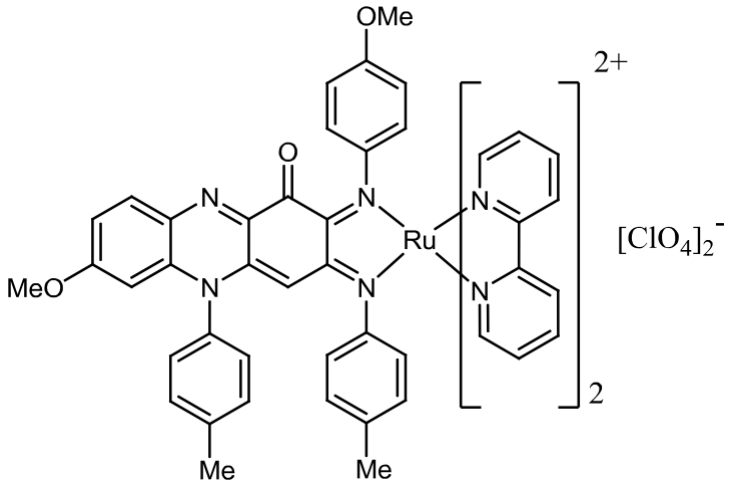


**Scheme 18.**

Exhaustive electrolysis of $[Ru(L)(bipy)_2](ClO_4)_2$ at –0.60 V produced a blue solution The EPR spectroscopy confirmed contribution of a large free radical [116] (ligand) to the SOMO of complex. Hence, authors [115] concluded that upon reduction of $[Ru(L)(bipy)_2](ClO_4)_2$, an electron is added to the ketonic function of the phenazine ligand to result in a free radical-containing phenazine ligand $L^{\bullet -}$.

Apart from ruthenium(II), several other metal centres produce a light-switch complex when coordinated to dppz, as described in the recent review.[101] For example, $[Cr(phen)_2dppz]^{3+}$ exhibits

metal-centred phosphorescence in solution that is quenched by DNA. Likewise, the emission of $[Ir(bpy)_2dppz]^{3+}$ is quenched by DNA. On the other hand, $[Os(phen)_2dppz]^{2+}$ has no emission in water, and is a red-emitting light-switch DNA probe ($\lambda$ max = 738 nm), albeit one which has very low quantum yield when bound to DNA and considerably shorter lifetimes than $[Ru(phen)_2dppz]^{2+}$.

The luminescence properties of several Pt(II) complexes with various extended aromatic ligands are described by interplay of LC, MC, and MLCT states in organic solvents. [Pt(dppz)(4-aminopyridine)$_2$]$^+$ is non-emissive in aqueous solution, but develops emission on binding to DNA, although with different properties than the emission in $CH_3CN$. [101,117]

After ruthenium, rhenium is the metal that has been most intensively studied in the excited state with dppz and polypyridyles as ligands. [101,118] Several rhenium(I) complexes also exhibit light-switch behaviour. *fac*-$[Re(dppz)(CO)_3(py)]^+$, *fac*-$[Re(dppz)(CO)_3(4\text{-Mepy})]^+$, and *fac*-$[Re(dppz)(CO)_3(4,4'\text{-bpy})]^+$ are light switch complexes that show no significant emission in aqueous solution and have their emission enhanced on binding to DNA. In these complexes the emission was arises predominantly from dppz-based $\pi\,\pi^*$ states with some MLCT character.

As stated above, the complexes supported by the dppz ligand, containing a phenazine moiety, have intense photochemical and fluorescence properties. Moreover, a redox properties of central phenazine moiety in the dipyrido[3,2-*a*:2′,3′-*c*]phenazine (dppz) ligand are important for the photochemical applications as concluded in [112]. Authors [99,119] stated that dppz ligand may be thought of as comprising two components: a bipy unit and a phenazine unit (Scheme 19). These two subunits behave essentially separately, with many molecular orbitals (MOs) being localised over only one subunit. DFT calculations of $[Ru(bipy)_2(dppzoxad)]^{2+}$ (dppzoxad = 2-(11-dipyrido[3,2- *a*:2′,3′-*c*]phenazine)-5-phenyl-1,3,4-oxadiazole) (Scheme 20) support assignment

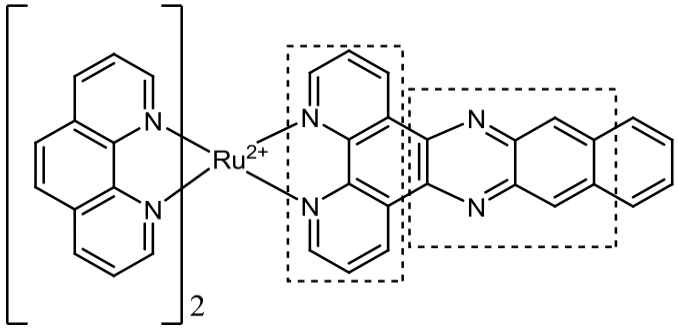

**Scheme 19.**

of $t_{2g}$(Ru) orbital being the HOMO and significant phenazine andoxadiazole character of the LUMO orbital with less amplitude on the phen portion of the ligand. [99] The electrochemical behaviour of complexes $[Ru(bipy)_2(dppzoxad)](CF_3SO_3)_2 \cdot 2MeCN \cdot H_2O$ and $[Re(dppzCN)(CO)_3Cl]$ (dppzCN = 11-cyanodipyrido[3,2-*a*:2′,3′-*c*]phenazine) (Scheme 20) suggests that they form radical anion species with electrons populating a phenazine-based SOMO; this is supported by the resonance Raman spectra of $[Re(dppzCN)(CO)_3Cl]^-$ and calculations on the reduced species.

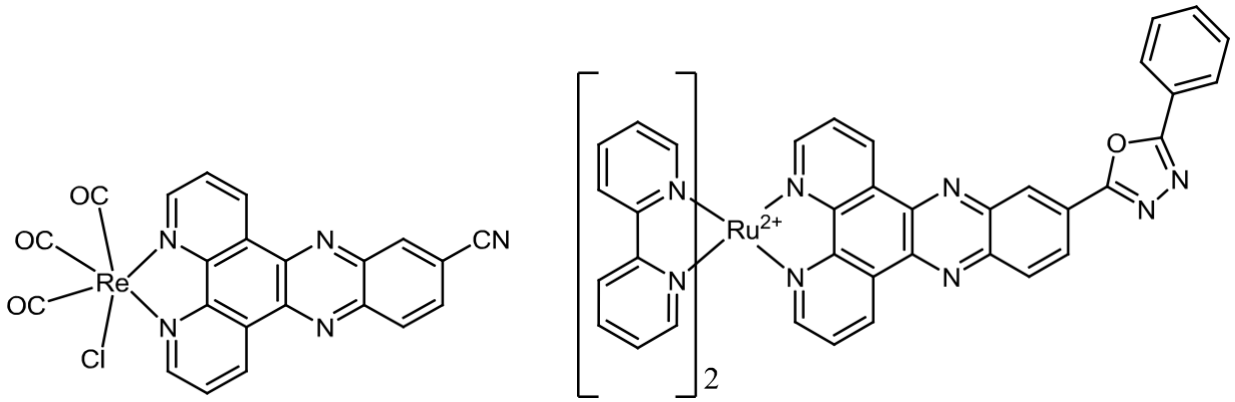

**Scheme 20.**

Therefore a simple phenazine ligand had been chosen for the present investigation. The next two chapters will describe known complexes containing a neutral phenazine ligand and complexes containing phenazine radical anions and negatively charged phenazine ligand.

## *Phenazine as a neutral donor ligand*

Phenazine (phz) is well known as an electron donating ligand. It contains two nitrogen donor sites capable to coordinate to the Lewis acidic centre and participate in hydrogen-bonding interactions. Various donor-acceptor adducts containing the neutral phenazine have been prepared and characterized. The neutral phenazine forms a stable donor acceptor complex with $I_2$: phz · $I_2$ (phz = phenazine), [120] and pyromellitic dianhydride phz · $C_{10}H_2O_6$. [121]

**Figure 2**. Propeller-like arrangement of hydronium ion and phenazine ligands in compound $[Cu_2L_3][(H_3O)_2(phz)_3]\cdot(CH_3COCH_3)_2\cdot(H_2O)_2$.

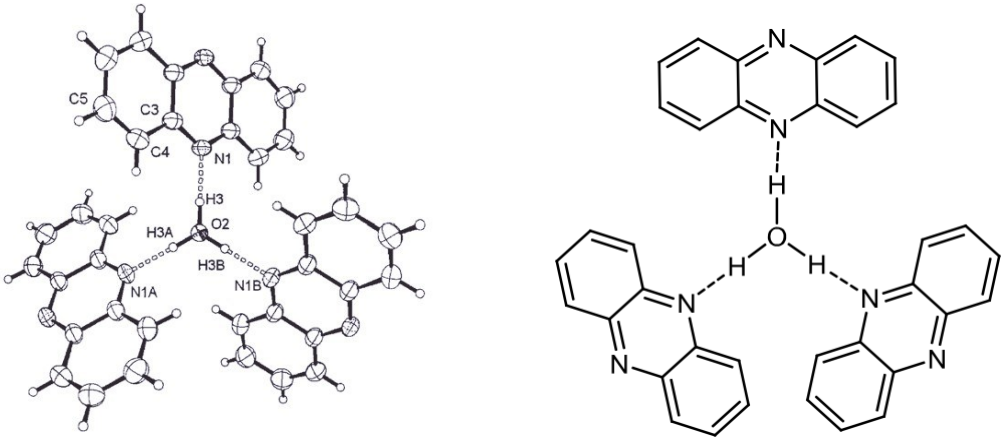

Complexes $[Cu_2L_3][(H_3O)_2(phz)_3]\cdot(CH_3COCH_3)_2\cdot(H_2O)_2$ and $[Cu_2L_3][(H_3O)_2(phz)_3]$ ($H_2L$ = chloroanilic acid, phz = $C_{12}H_8N_2$) [122] are containing hydronium ion coordinated to phenazine through the hydrogen atoms (Figure 2). Another example of a phenazine complex, where phenazine is interacting with hydrogen atoms of coordinated water, is $[CuL(H_2O)(phz)]$ ($H_2L$ = chloroanilic acid). The host phenazine molecule is intercalated between the infinite chains $[CuL(H_2O)]_\infty$ and is connected to the chain *via* hydrogen bonding with the coordinated water molecule.[123]

A large number of metal complexes containing formally neutral phenazine moiety is reported. They have been prepared in order to create supramolecular assemblies or metallo organic frameworks of different configuration for the various purposed including development of synthetic receptors, [124] systems for ion- or molecule exchange,[123] magnetic materials. [122,123,131,132] and optical meterials.[127]

The neutral phenazine donor molecule coordinates to one metal centre through one nitrogen atom and acts as monodentante bridging ligand in such complexes. Such property of phenazine is responsible for utilisation of it as a "linking ligand". Additionally, phenazine can form a columnar stack through the $\pi$-$\pi$ interaction. This phenomenon is used for construction of various multilayer assemblies and metallo-organic frameworks.

Examples of such complexes are briefly discussed below. The reaction of $Fe(C_5H_4GaMe_2)_2$ with phenazine results in the formation of the supramolecular polyferrocene $[Fe(C_5H_4GaMe_2)_2 \cdot (\mu\text{-phz})]$, which consists of polymer chains arranged parallel to each other and aligned parallel to the crystallographic *a*-*c*-diagonal. Each chain is surrounded by four other polymer chains (Figure 3). [125]

**Figure 3**. Part of the solid state structure of $[Fe(C_5H_4GaMe_2)_2 \cdot (\mu\text{-phz})]_\infty$.

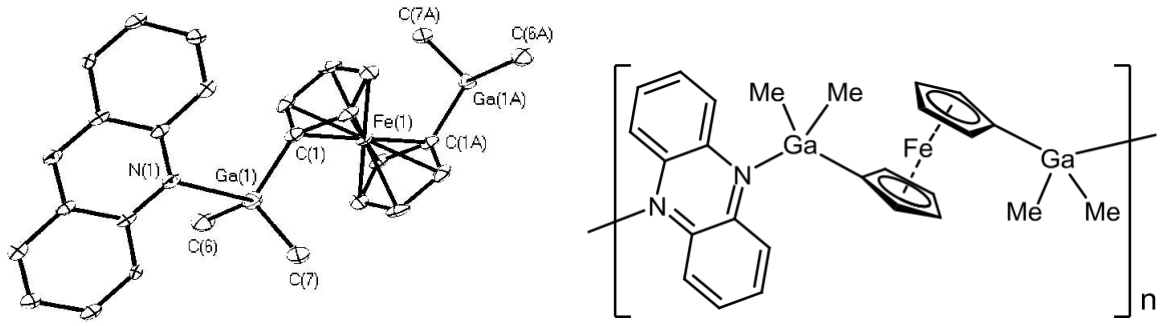


Reaction of $[Ru_2(OCC_2H_5)_4(H_2O)_2](BF_4)$ with phenazine resulted in the polymeric $[Ru_2(OCC_2H_5)_4(\mu\text{-phz})](BF_4)$ with the structure consisting of infinite non linear $[- Ru_2(OCC_2H_5)_4 - (phz) - ]_\infty$ chains.[126]

Cupper complexes with the phenazine molecule are the most studied due to variety of stoichiometries and structural formats displayed. Figure 4 shows the schematic molecular packing of some Cu(I) phenazine complexes. The phenazine always coordinates to Cu(I) through the nitrogen atoms.[127,128] A characteristic feature common to compounds **A**, **B** and **D** is the coexistence of a $\pi$-$\pi$ phenazine stacking structure and a one-dimensional chain or two-dimensional sheet structure. Neighbouring one-dimensional chains in **A** or **D** are connected to each other through $\pi$-$\pi$ interaction, phz-phz separations of 3.47 Å are not that short but indicate significant $\pi$-$\pi$ interaction. On the other hand, **C** is constructed from one-dimensional chains which are interconnected through $[PFO_3]^{2-}$ bridges. The resulting two-dimensional sheet also contains $\pi$-$\pi$ phenazine stacking, with phz ··· phz 3.31 Å indicating a strong $\pi$-$\pi$ interaction. Such a structural constraint induces a perturbation on the electronic state of the compound, a perturbation which is thought to be responsible for the conducting property observed in **C**

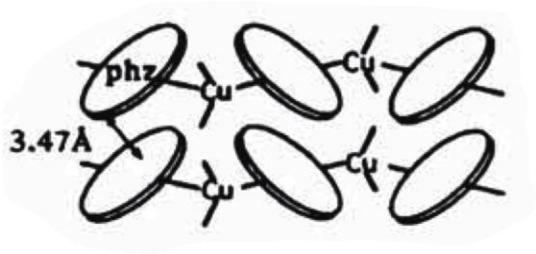


[Cu($\mu$-phz)($NO_3$)] (**A**)

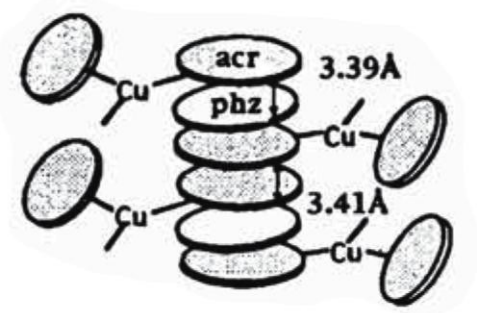


[{Cu(Acr)$_2$($NO_3$)}$_2$(phz)($H_2O$)] (**B**)

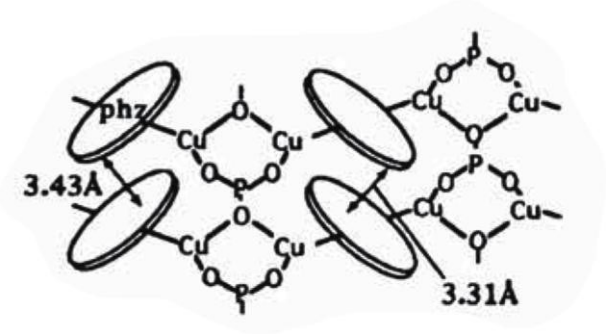


[$Cu_2$($\mu$-phz)($PFO_3$)] (**C**)

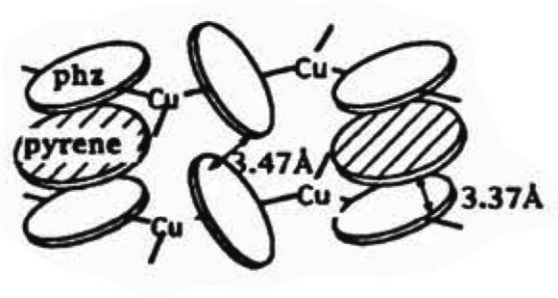


[{Cu($\mu$-phz)(MeCN)}$_2$($C_{10}H_{10}$)($PF_6$)$_2$] (**D**)

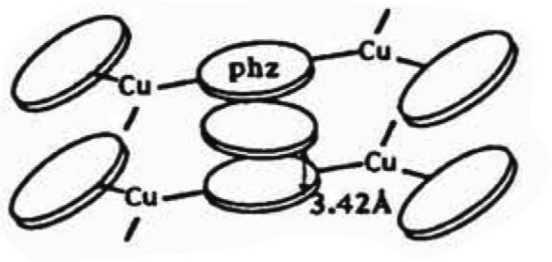


[{$Cu_2$($\mu$-Phz)$_3$($MeOH$)$_2$}(phz)($PF_6$)$_2$] (**E**)

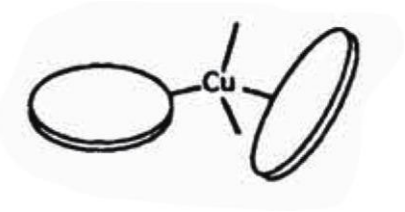


[Cu($\mu$-phz)$_2$($NO_3$)] (**F**)

**Figure 4**. Schematic molecular-packing diagram of some Cu(I) phenazine compounds (phz = phenazine, acr = acrydine). Pictures are taken from ref. 129.

The most remarkable feature in compound **D** is the intercalation of pyrene molecules into a phenazine stack. Since the intercalation takes place between every other phenazine stack in the one-

dimensional chain and the stack without intercalation is of course composed of phenazine molecules only, it is reasonable to consider that an iodine atom can easily penetrate the crystal. Dicopper complexes $[Cu_2(\mu\text{-phz})_3(MeOH)_2](phz)(PF_6)_2$ (**E**) and $[Cu(\mu\text{-phz})_2(H_2O)](ClO_4)$ and $[Cu(\mu\text{-phz})_2(NO_3)]$, (**F**) crystallizes as infinite stacks of the cupper (I) complex cations. [128]. The relatively high conductivity of compound **E** indicates the partial charge transfer to/from the phenazine moiety, which causes relatively high electron mobility of this compound. [129]

**Figure 5**. Top views of the packing arrangement of complexes $[Cu_2(\mu\text{-Br})_2(\mu\text{-phz})]$ and $[Cu_2(\mu\text{-Cl})_2(\mu\text{-phz})]$. Pictures are taken from ref. 130.

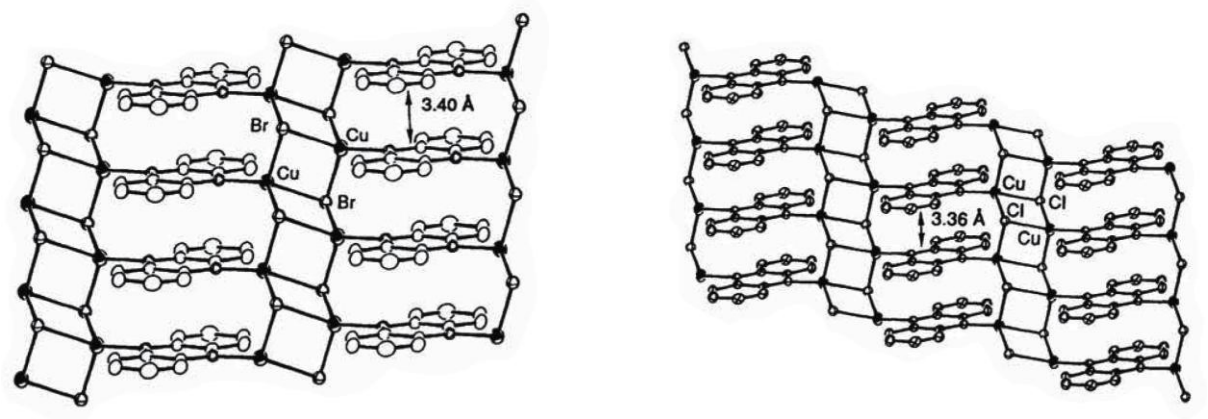


$[Cu_2(\mu\text{-Br})_2(\mu\text{-phz})]$ $[Cu_2(\mu\text{-Cl})_2(\mu\text{-phz})]$

Compounds $[Cu_2(\mu\text{-Br})_2(\mu\text{-phz})]$ and $[Cu_2(\mu\text{-Cl})_2(\mu\text{-phz})]$ have two-dimensional sheets containing phz molecules between polymeric stair frameworks of CuBr and CuCl, respectively (Figure 5). The interplanar spacings of adjacent phz molecules for $[Cu_2(\mu\text{-Br})_2(\mu\text{-phz})]$ and $[Cu_2(\mu\text{-Cl})_2(\mu\text{-phz})]$ are 3.40 Å and 3.36 Å, respectively. The copper atoms of the $Cu_2I_2$ rhomboid in

$[Cu_2(\mu\text{-}I)_2(\mu\text{-phz})]$ are bridged by phz molecules to give an infinite linear chain and the phz molecules overlap between the infinite chains with an interplanar spacing of 3.46 Å. [130]

**Figure 6**. Perspective view of the packing arrangement of $[Ag_2(\mu\text{-phz})(ClO_4)_2]$. Picture is taken from ref. 128.

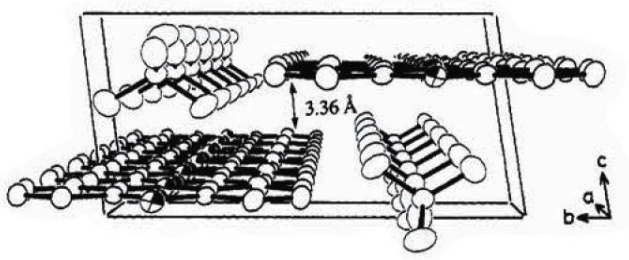


Complex $[Cu(hfac)_2(\mu\text{-phz})]$ (Hhfac = 1,1,1,5,5,5-hexafluoropentane-2,4-dione) consist of a one-dimensional chain structure $[Cu(hfac)_2(\mu\text{-phz})]_\infty$ with the bridging phenazine moieties coordinated to the Cu(II) centers through the nitrogen atoms. This complex showed antiferromagnetic interaction with $J/k_B$ = -0.031(6) K estimated from the Bonner–Fisher model.[131]

The silver cations and phenazine in the $[Ag_2(\mu\text{-phz})(ClO_4)_2]$ forms an infinite linear chain, while the $[Ag_2(\mu\text{-phz})(NO_3)_2]$ forms a planar infinite sheet in the direction of the *b* and *c* axes (Figure 6). [128] The 2D-sheets $(AgSCN)_n$ in $[\{Ag(SCN)\}_2(\mu\text{-phz})]$ are linked by the planar phenazine ligands creating distorted polygons consisting $[Ag_6(SCN)_4(\mu\text{-phz})_2]$ with enough space to accommodate the phenyl rings of the phenazine ligand forming 3D-network structure.[132]

Interaction of $\{[LPt(4\text{-ethynylpyridyl})_2)_2(cis\text{-}Pt(PEt_3)_2)]Ag_2\}(OSO_2CF_3)_6$, where and L = cyclobis[(cis-(dppp)], with phenazine results in formation of host-guest assemblies containing the $[(\mu^3\text{-}Ag)_2\text{-}(\mu\text{-phz})]$ moiety coordinated to the acetylene groups (Scheme 21).[124]

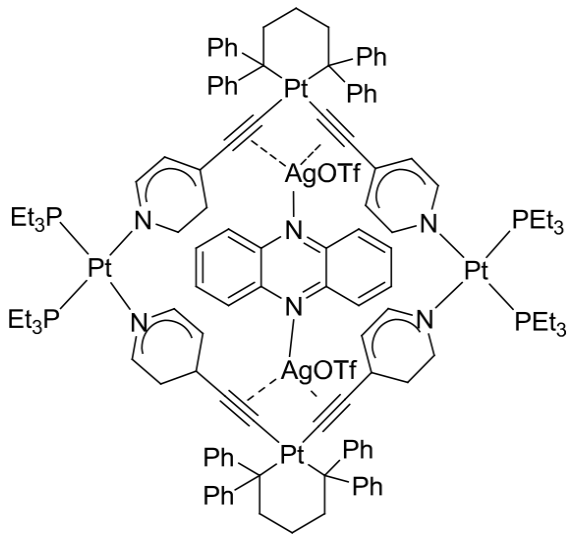


**Scheme 21**. Summary of the significant geometric features of {LPt(4-ethynylpyridyl)$_2$)$_2$(*cis*-Pt(PEt$_3$)$_2$)$_2$[($\mu^3$-Ag)$_2$-($\mu$-phz)]}(OSO$_2$CF$_3$)$_6$ host-guest complex (OTf = OSO$_2$CF$_3$, L = cyclobis[(cis-(dppp)]).

In conclusion, the electronic nature of discussed complexes was not investigated, although conductivity, magnetic and optical properties of Cu(I) complexes supported by the "formally neutral phenazine ligand" indicate a substantial charge transfer from Cu(I) to phenazine moiety and vice-versa in agreement with the "non innocent" nature of phenazine ligand in these complexes.

## *Reduction of phenazine by the main group substrates*

Polycyclic aza-compounds (*e.g.* pyrazine, quinoxaline, phenazine) containing (4n+2) $\pi$ electrons can be reduced by various reducing agents forming 4n$\pi$ dianions. Reduction of phenazine is producing the formally antiaromatic system with 16-$\pi$ electrons, which can be stabilized by the

alkali, alkaline earth metals or by coordination to the *f*-element. The reduction can be achieved electrochemically,[133] the phenazine has a reduction potential -0.364 V vs SCE [134] and phenazine could be reduced more easily than fluorenone (-1.30 V vs SCE)[135], azobenzene (-1.35 to -1.41 V vs SCE), [136] and benzanthracene, (first and second reduction potentials of -1.58 and -1.93 V vs SCE).[134b] Therefore phenazine has been extensively used to probe the reducing properties of various substrates as will be discussed below.

A various derivatives of phenazine have been reduced by the metallic lithium or sodium forming anionic species in solution, the reduced species were monitored by means of proton and carbon NMR. [137, 138] Authors [137] suggest that a significant portion of the charge in the reduced species resides on the nitrogen atoms, as based on the MO calculations and the proton and carbon NMR spectroscopy. It is notable that the anionic derivative of phenazine can be obtained from the 5,10-dihydrophenazine and alkyl lithium. The only one structure containing the formally mononegative terminal phzH (phz = Phenazine) coordinated to the lithium center is reported for the lithium complex $Li_2(\mu\text{-}Cl)(\eta^2\text{-}NC_{12}H_8NH)(THF)_4$ [*, 139]

Phenazine was reduced by activated magnesium metal in THF. The reaction was reported to be rather complex; reduction yield initially a radical anion complex, the final reaction products are complexes containing formally dianion of phenazine $[Mg(\mu\text{-}\eta^2\text{-}C_{12}H_8N_2)(THF)_2]$ and $[(MgBr)_2(\mu\text{-}\eta^2\text{-}C_{12}H_8N_2)(THF)_6]\cdot[MgBr_2(THF)_4]$ [140] (Scheme 22).

[*] Here and below, a reduced phenazine ligand in complexes will be presented as $NC_{12}H_8NH$ and $C_{12}H_8N_2$, since the nature of coordinated reduced phenazine is essentially unclear from the literature data.

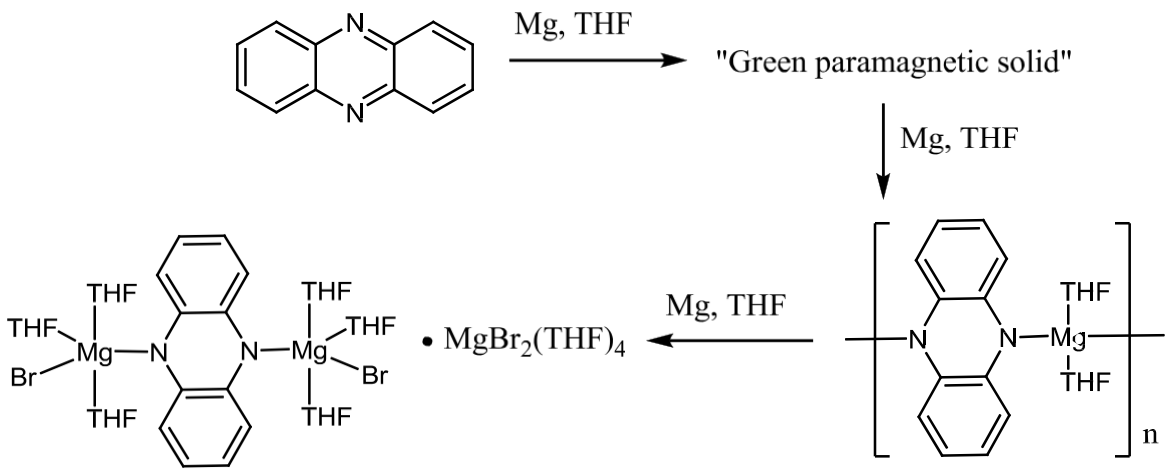


**Scheme 22.**

The neutral phenazine reacts with the aluminum hydrides producing either dyhydrophenazine by reduction with the $LiAlH_4$ in ether (Scheme 23)[141] or a reduced radical species. Namely, the reduction of phenazine by the $AlH_3$ (or $AlD_3$) at room temperature in THF is accompanied by the formation of radicals $[(AlH_3)_2(\mu\text{-}\eta^2\text{-}C_{12}H_8N_2)]^{\bullet -}$ or $[(AlD_3)_2(\mu\text{-}\eta^2\text{-}C_{12}H_8N_2)]^{\bullet -}$ (Scheme 24).[142]

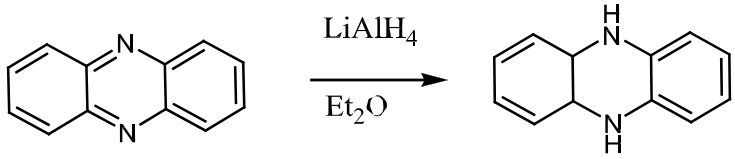


**Scheme 23**.

Structures of paramagnetic products from the reaction of $AlH_3$ and the phenazine have been identified by detailed ESR studies and the reaction pathway was rationalized applying the single

electron transfer mechanism (SET) (Scheme 24).[143] It should be pointed out that the intermediate complexes and the reaction products were characterized only by the ESR spectroscopy and none of compounds were isolated in the solid state.

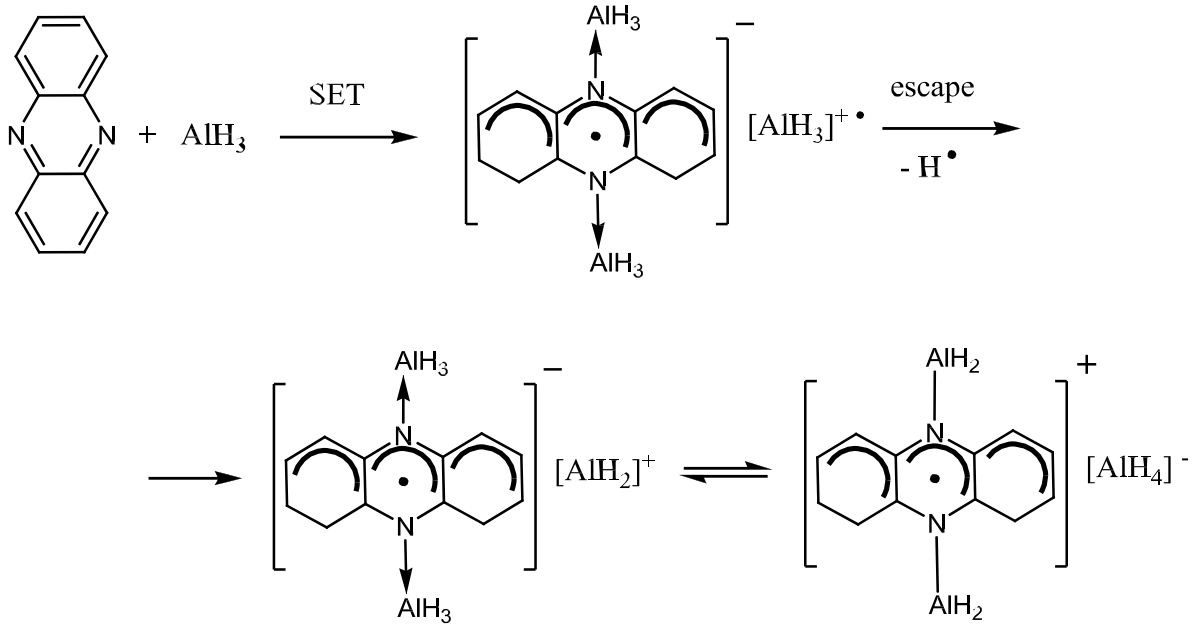


**Scheme 24**. SET – single electron transfer.

Reduction of phenazine by the sodium metal in the presence of $AlMe_3$ in THF solution is leading to the green solution and resulted in deposition of aluminum metal. Application of ESP spectroscopy allowed identification of intermediate radical complex $[(AlMe_2)_2(\mu\text{-}\eta^2\text{-}C_{12}H_8N_2)]^{\bullet +}$ and the reaction mechanism was rationalized as shown in Scheme 25.[144]

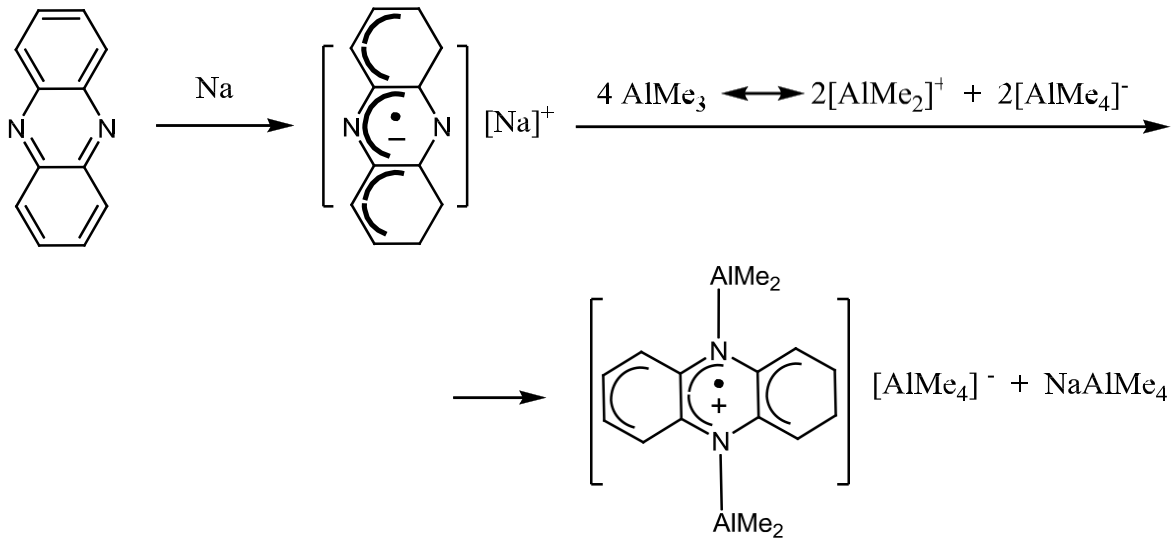


**Scheme 25**.

W.Kaim [144] stated that the complexes exist in solution as ion pairs, because the hyperfine coupling constants strongly depend on the temperature and coordination solvent applied. From the other side an ionic pairing in the radical complexes is different from the classic ion pairing due to substantial charge compensation by the coordination of radical species and stronger binding of counter ions than in the classical ion pairs.

## *Transition metal complexes with the reduced phenazine*

Chemistry of transition metal complexes containing a reduced phenazine is growing rapidly since the discovery of first example $[(C_5Me_5)_2La]_2(\mu\text{-}\eta^2\text{:}\eta^2\text{-}C_{12}H_8N_2)$ in 1994 by Schumann and coworkers (Scheme 26).[145] The phenazine dianion is normally bridging two lanthanide or uranium moieties. A large group of lanthanide and uranium complexes containing the bridging phenazine dianion between the two metal centres have been reported.

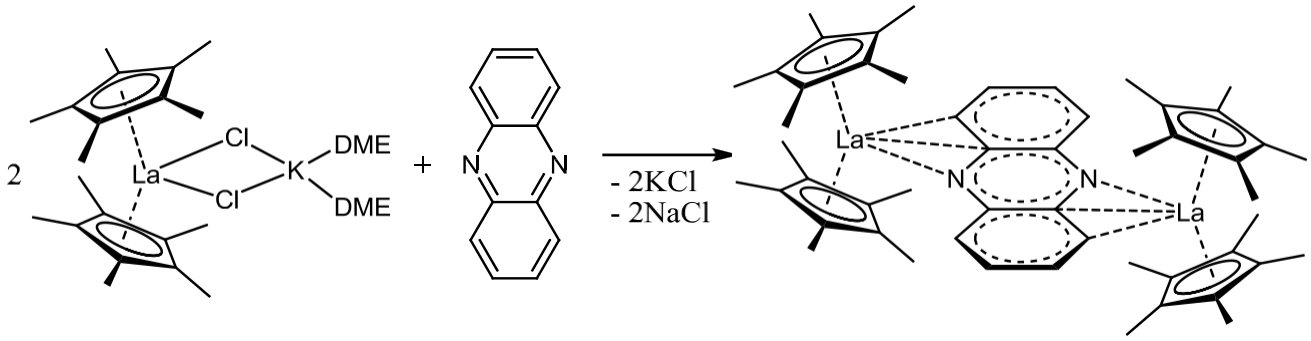


**Scheme 26**.

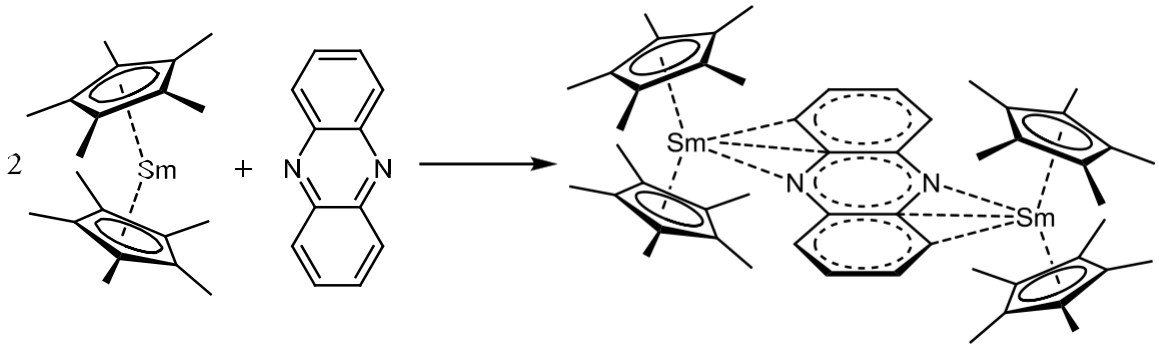


**Scheme 27.**

Sm(II) complex $(C_5Me_5)_2Sm$ and Yb(II) complex $(C_5Me_5)_2Yb(Et_2O)$ immediately reacts with the phenazine with formation of $[(C_5Me_5)_2Ln]_2(\mu\text{-}\eta^3\text{:}\eta^3\text{-}C_{12}H_8N_2)$ [146,147, 148] (Ln = Sm, Yb) (Scheme 27). Authors [146] compared the structure of $[(C_5Me_5)_2Sm]_2(\mu\text{-}\eta^3\text{:}\eta^3\text{-}C_{12}H_8N_2)$ and that of the magnesium complex, $[(MgBr)_2(\mu\text{-}\eta^2\text{-}C_{12}H_8N_2)(THF)_6]\cdot[MgBr_2(THF)_4]$, which also contains a phenazine dianion.[140] The magnesium complex is significantly different from the samarium system. In magnesium complex the phenazine dianion is essentially $\sigma$ bonded to the magnesium and functions as an amido ligand, while the interaction of samarium with the ring system appears to be

allylic. The same approach can be used to describe state of bridging phenazine ligand in other lanthanide complexes $[Cp'_2Ln]_2(\mu\text{-}\eta^3\text{:}\eta^3\text{-}C_{12}H_8N_2)$. ($Cp' = C_5Me_5$, $C_5Me_4H$; Ln = La, Sm, Yb, Lu).

The effective magnetic moment of $[(C_5Me_5)_2Yb]_2(\mu\text{-}\eta^3\text{:}\eta^3\text{-}C_{12}H_8N_2)$ shows that each $(C_5Me_5)_2Yb^{III}$ fragment behaves as an isolated paramagnet linked by a dianionic diamagnetic bridging phenazine with no magnetic exchange occurring between the spin carriers to 5 K. At low temperature the $[(C_5Me_5)_2Yb]_2(\mu\text{-}\eta^3\text{:}\eta^3\text{-}C_{12}H_8N_2)$ undergo antiferromagnetic coupling. A spin polarization model is advanced to account for the electronic exchange coupling.[148]

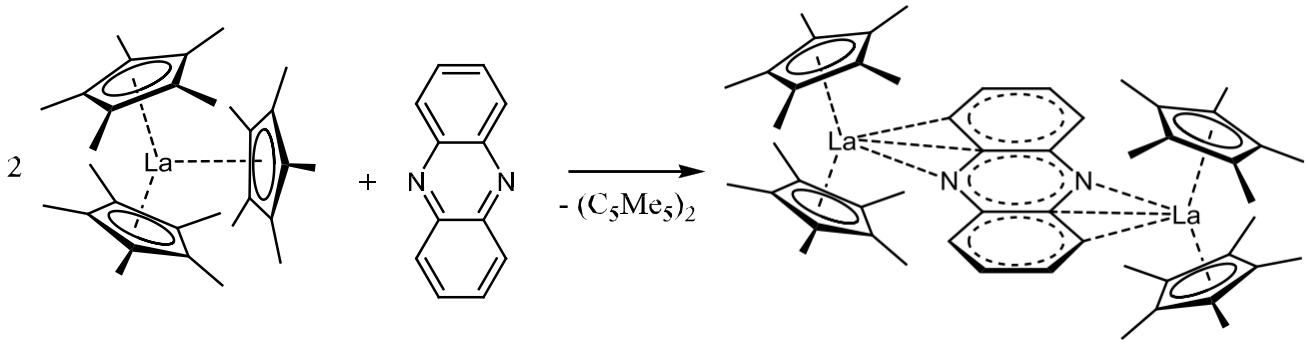


**Scheme 28.**

The dinitrogen complexes $[(C_5Me_4H)_2Ln(THF)]_2(\mu\text{-}\eta^2\text{:}\eta^2\text{-}N_2)$ (Ln = Y, La, Lu) readily reacts with phenazine to yield complexes $[(C_5Me_4H)_2Ln]_2(\mu\text{-}\eta^3\text{:}\eta^3\text{-}C_{12}H_8N_2)$ [147, 149 , 150] with the structure similar to that of $[(C_5Me_5)_2Ln]_2(\mu\text{-}\eta^3\text{:}\eta^3\text{-}C_{12}H_8N_2)$. [146-148] Interaction of lanthanum complex $(C_5Me_5)_3La$ with the phenazine has been used to better estimate the reduction potential of the $(C_5Me_5)_3La$ (Scheme 28). Complex $(C_5Me_5)_3La$ is not as reducing as $(C_5Me_5)_2Sm$, it does not reduce benzanthracene, which has first and second reduction potentials of -1.58 and -1.93 V vs SCE.[134b] However, $(C_5Me_5)_3La$ does reduce phenazine (reduction potential -0.364 V vs SCE [134]) with formation of $[(C_5Me_5)_2La]_2(\mu\text{-}\eta^3\text{:}\eta^3\text{-}C_{12}H_8N_2)$. Reaction between $(C_5Me_5)_3Sm$ and phenazine

also produces $[(C_5Me_5)_2Sm]_2(\mu\text{-}\eta^3\text{:}\eta^3\text{-}C_{12}H_8N_2)$. [151] $(C_5Me_5)_3Sm$ is stronger reductant than the $(C_5Me_5)_3La$ and it reduces diazobenzene and cyclooctatetraene.

The monomethylcyclopentadienyl tetraphenyl borate complexes $[(C_5Me_5)_2Ln]_2[(\mu\text{-}\eta^6\text{:}\eta^1\text{-}Ph)_2BPh_2]$ (Ln= Yb, Sm) are also reactive toward the phenazine with formation of $[(C_5Me_5)_2Ln]_2(\mu\text{-}\eta^3\text{:}\eta^3\text{-}C_{12}H_8N_2)$ containing the formally dianionic bridging phenazine (Scheme 29). [152,153]

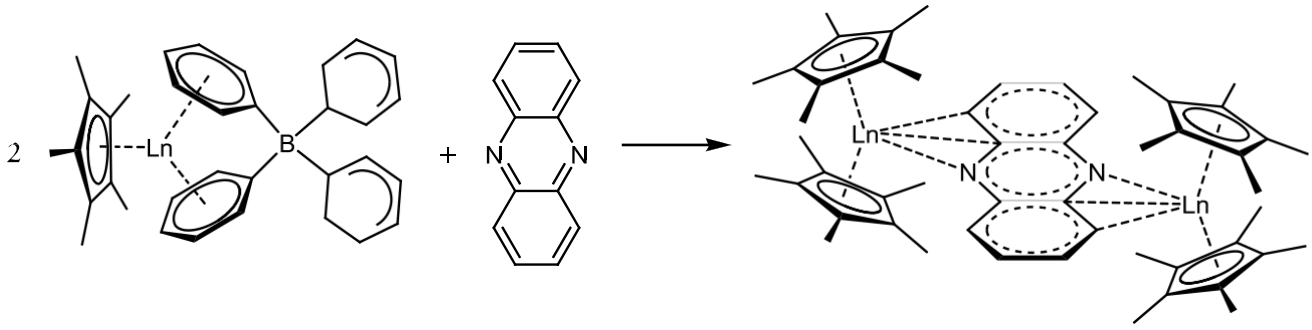


**Scheme 29**. Ln = Yb, Sm.

The reactivity of the tetraphenylborate salt of the rare earth metallocene cations $[(C_5Me_5)_2Y]_2[(\mu\text{-}\eta^6\text{:}\eta^1\text{-}Ph)_2BPh_2]$ has been investigated with substrates that undergo reduction with *f* element complexes to probe metal-substrate interactions prior to reduction. The reaction of $[(C_5Me_5)_2Y]_2[(\mu\text{-}\eta^6\text{:}\eta^1\text{-}Ph)_2BPh_2]$ with phenazine in benzene produces a radical product $[(C_5Me_5)_2Y]_2(\mu\text{-}\eta^3\text{:}\eta^3\text{-}C_{12}H_8N_2)[BPh_4]$ and its EPR spectrum strongly supports the presence of the radical monoanion $(phz)^{\bullet -}$ (Scheme 30).

The slow conversion of $[(C_5Me_5)_2Y]_2(\mu\text{-}\eta^3\text{:}\eta^3\text{-}C_{12}H_8N_2)[BPh_4]$ to $[(C_5Me_5)_2Y]_2(\mu\text{-}\eta^3\text{:}\eta^3\text{-}C_{12}H_8N_2)$ can be described by a second one-electron reduction of the phenazine radical anion by $[BPh_4]^-$ (Scheme 30).[154]

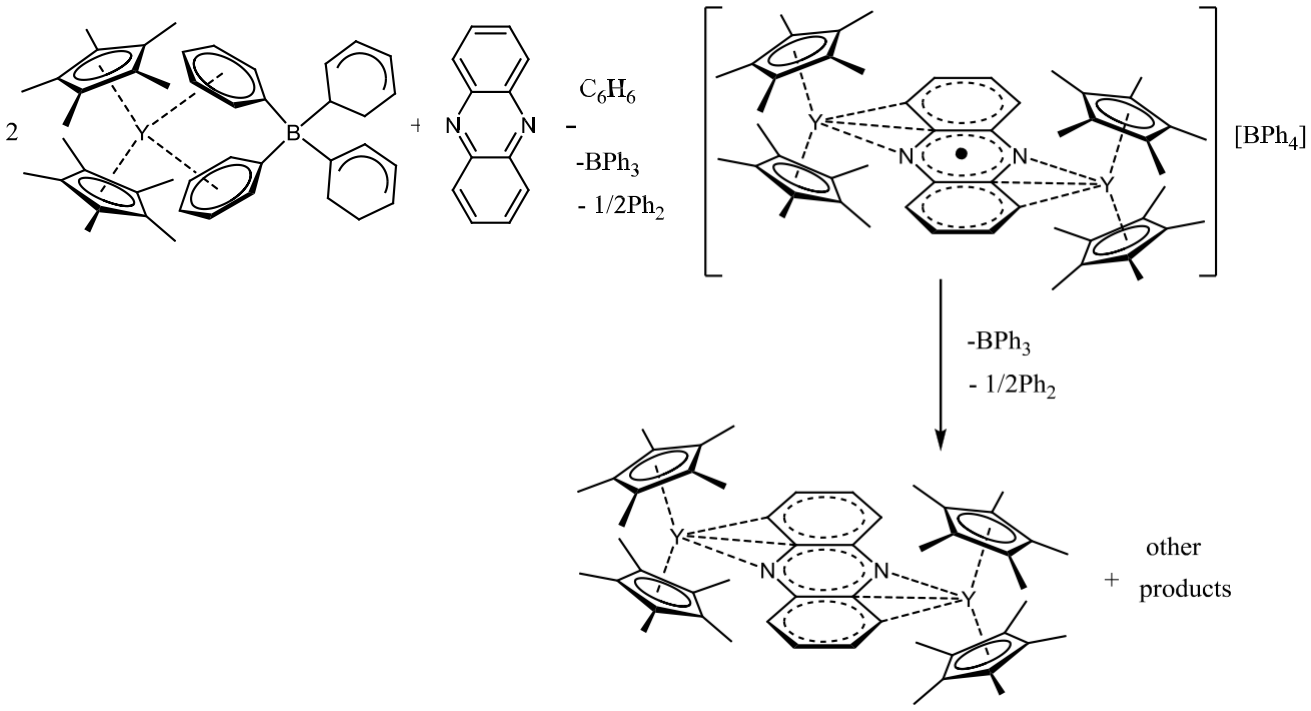


**Scheme 30**.

Complex $[(C_5Me_5)(C_8H_8)U]_2(\mu\text{-}\eta^3\text{:}\eta^3\text{-}C_8H_8)$ functions as a two-electron reductant with phenazine to make bimetallic heteroleptic tetravalent complex $[C_5Me_5(C_8H_8)U]_2(\mu\text{-}\eta^1\text{:}\eta^1\text{-}C_{12}H_8N_2)$ formally containing one $(C_5Me_5)^{1-}$ ligand, one $(C_8H_8)^{2-}$ ligand and ½ $(C_{12}H_8N_2)^{2-}$ per uranium (Scheme 31). [155] Complex $[(C_5Me_5)(C_8H_8)U]_2(\mu\text{-}\eta^3\text{:}\eta^3\text{-}C_8H_8)$ also reduces PhEEPh (E = S, Se, Te) substrates and does not reduce anthracene, acenaphthylene, or benzanthracene, which have higher reduction potential than the phenazine.

Authors [155] stressed that the uranium center of $[C_5Me_5(C_8H_8)U]^{1+}$ unit coordinates to the phenazine dianion in a $\eta^1$-bonding mode, not previously seen in *f* element chemistry. [145-154] In the lanthanide complexes, the phenazine dianion bridges the metals using three adjacent atoms in an aza-allyl mode on each side.

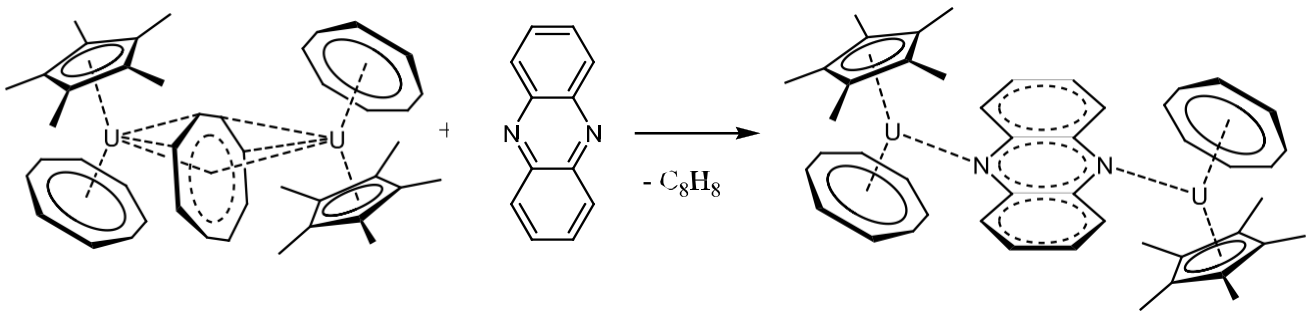


**Scheme 31.**

Interaction of $Mo(PMe_3)_6$ with phenazine does not resembles the lanthanide chemistry and proceeds in a totally different manner (Scheme 32).[156] Phenazine reacts with $Mo(PMe_3)_6$ to give ($\eta^6$-$C_6$-$C_{12}H_8N_2$)$Mo(PMe_3)_3$, $[Mo(PMe_3)_3]_2$($\mu$-$\eta^6$,$\eta^6$-$C_6$-$C_{12}H_8N_2$) and ($\eta^4$-$C_4$-$C_{12}H_8N_2$)$_2Mo(PMe_3)_2$, in which the phenazine exhibits novel coordination modes *via* only the carbon atoms (Scheme 32). Comparison of the reactivity of the phenazine, acridine and anthracene complexes respectively ($\eta^6$-$C_6$-$C_{12}H_8N_2$)$Mo(PMe_3)_3$, ($\eta^6$-$C_6$-Acr)$Mo(PMe_3)_3$ and ($\eta^6$-An)$Mo(PMe_3)_3$ (Acr = acridine, An = anthracene) demonstrates that incorporation of nitrogen substituents into the central ring promotes oxidative addition of $H_2$. The phenazine ligand is hydrogenated at elevated temperatures. Thus, ($\eta^6$-$C_6$-$C_{12}H_8N_2$)$Mo(PMe_3)_3$ releases a mixture of 5,10-dihydrophenazine and 1,2,3,4-tetrahydrophenazine upon treatment with $H_2$ in benzene at 95 °C (Scheme 33).[156]

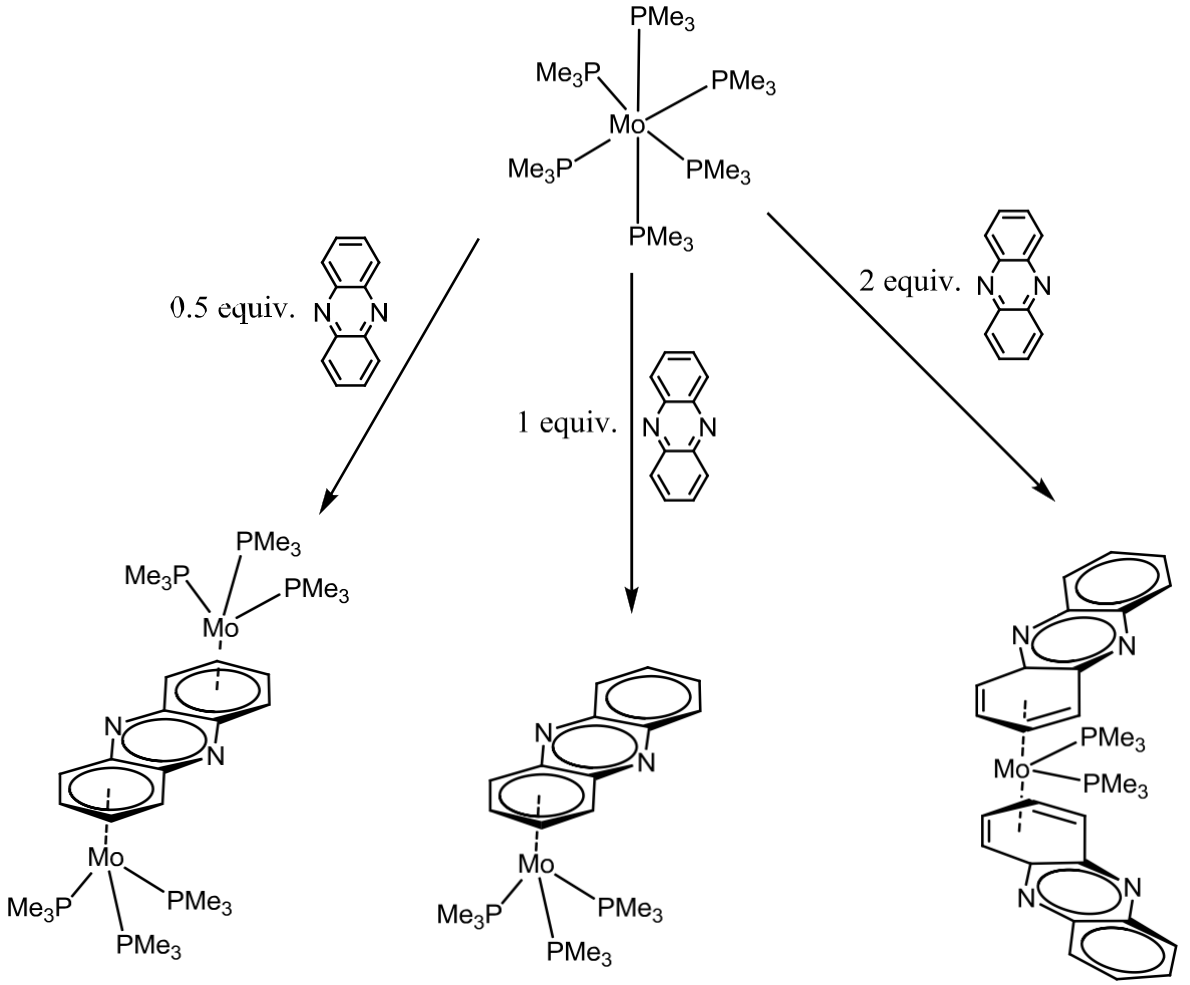


**Scheme 32.**

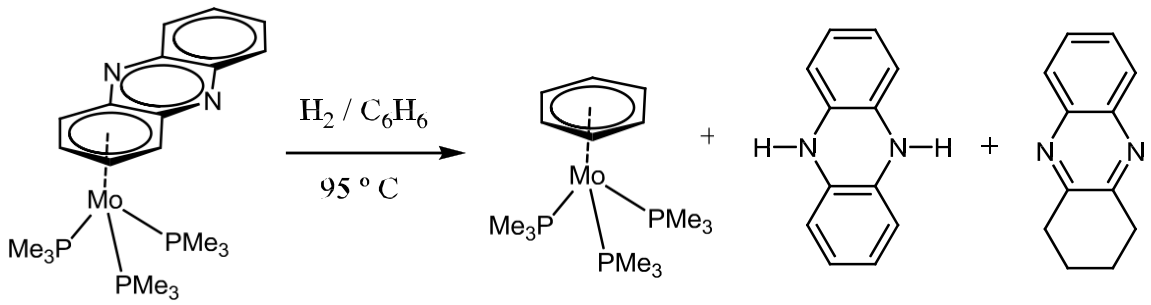


**Scheme 33.**

Chemistry of phenazine and low valent transition metal substrates continues to grow rapidly during the last years. The last report present reaction of phenazine with $[Ru_3(CO)_{12}]$ in THF. [157] The starting compounds produced the $[Ru_3(\mu\text{-H})(\mu_3\text{-}\{(C_6H_4)(C_6H_3)N_2\})(CO)_9]$ (**A**), $[Ru_4(\mu_4\text{-}\{(C_6H_4)(C_6H_3)N_2H\})(\mu\text{-CO})(CO)_{10}]$ (**B**), and $[Ru_6(\mu_5\text{-}\{(C_6H_4)(C_6H_3)N_2H\})(\mu\text{-CO})_3(CO)_{12}]$ (**C**), that arise from a C−H oxidative addition and a C-to-N prototropy.

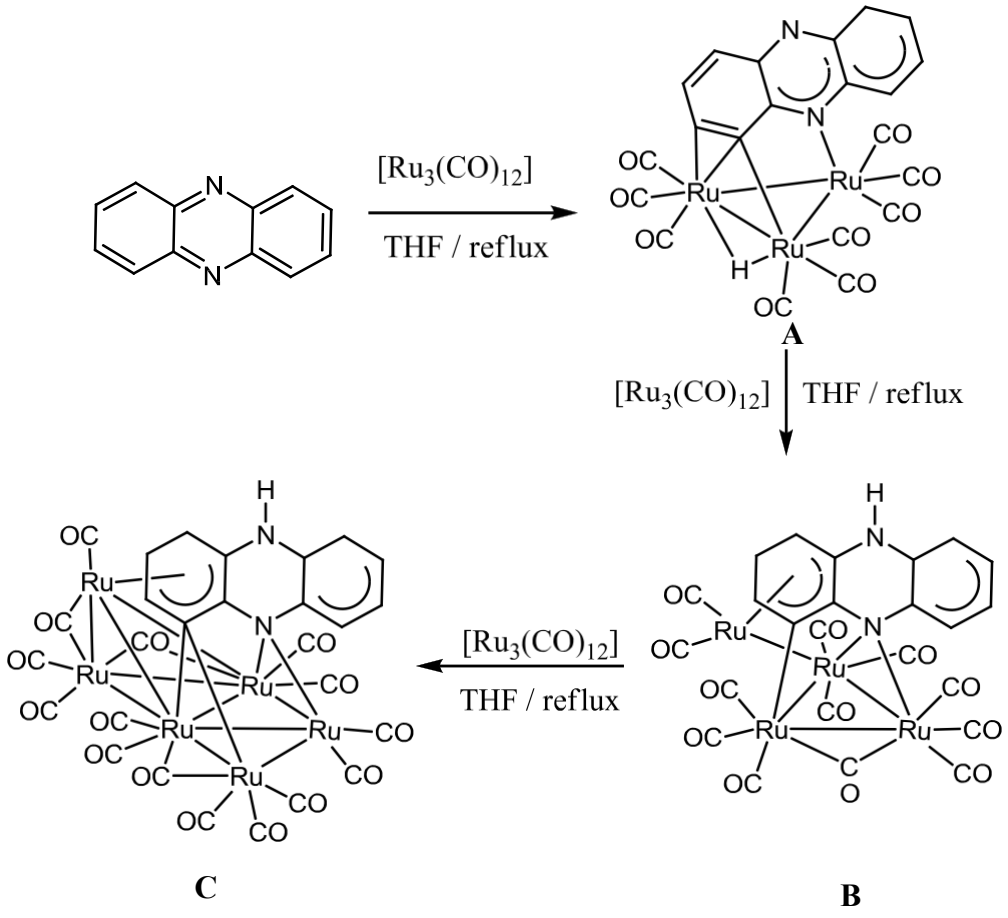


**Scheme 34**. The reaction of $[Ru_3(CO)_{12}]$ with an equimolar amount of phenazine in THF at reflux temperature.

It was stated that compound **A** arises from the oxidative addition of a phenazine C−H bond (along with other processes such as CO ligand substitution), while compound **B** results from compound **A** through a combination of an $Ru(CO)_n$ fragment addition and a prototropic process that transfers the hydride H atom to the uncoordinated N atom of the C-metalated phenazine ligand. Authors [157] proposed that the long distance transfer of the hydride H atom of **A** to the uncoordinated N atom of the C-metalated phenazine ligand leading to **B** cannot be an intramolecular process. Therefore, such a transfer should occur intermolecularly, either directly (the hydride atom is transferred to the free N atom of a different molecule) or through a proton transporter (water, THF solvent, or free phenazine) and should be accompanied by the addition of a $Ru(CO)_n$ fragment A subsequent incorporation of two $Ru(CO)_n$ to the tetranuclear compound **B** leads to the hexanuclear derivative **C**, which maintains the same C-metalated NH phenazine tautomer as **B**. [157]

In conclusion, the available literature data revealed that phenazine can be reduced to the corresponding dianion with a variety of substrates. Reaction of neutral phenazine with the magnesium or *f*-element compounds produces dinuclear complexes containing the bridging phenazine dianion. The bonding situation in the lanthanide complexes is complex and the phenazine moiety bridges the metal centres using three adjacent atoms in an aza-allyl mode on each side. Although the room temperature effective magnetic moment of $[(C_5Me_5)_2Yb]_2(\mu\text{-}\eta^3\text{:}\eta^3\text{-}C_{12}H_8N_2)$ is in agreement with the presence of dianionic diamagnetic bridging phenazine, at low temperature the $[(C_5Me_5)_2Yb]_2(\mu\text{-}\eta^3\text{:}\eta^3\text{-}C_{12}H_8N_2)$ undergo antiferromagnetic coupling and spin polarization model is advanced to account for the electronic exchange coupling.[148] Reduction of neutral phenazine by magnesium [140] and *f* elements [154] is proceeded *via* intermediates containing a radical anion of phenazine, illustrating a “non innocent” behaviour of phenazine ligand in these complexes, however

only one intermediate of this type $[(C_5Me_5)_2Y]_2(\mu\text{-}\eta^3\text{:}\eta^3\text{-}C_{12}H_8N_2)[BPh_4]$ has been fully characterized to the date.[154] The examples of chemical transformation of coordinated phenazine are provided in the literature for the case of hydrogenation of molybdenum complex $(\eta^6\text{-}C_6\text{-}C_{12}H_8N_2)Mo(PMe_3)_3$ producing a mixture of 5,10-dihydrophenazine and 1,2,3,4-tetrahydrophenazine [156] and for interaction of phenazine and $[Ru_3(CO)_{12}]$ leading to long distance transfer of the hydride H atom from a carbon atom of phenazine to the nitrogen atom of another phenazine molecule [157] illustrating a chemical "non innocence" of phenazine ligand".

## References


[1] C. K. Jørgensen, *Coord. Chem. Rev*., **1966**, *1*, 164.

[2] R. S. da Silva, S. I. Gorelsky, E. S. Dodsworth, E. Tfouni, A. B. P. Lever, *Dalton Trans*., **2000**, 4078.

[3] A. B. P. Lever, H. Masui, R. A. Metcalfe, D. J. Stufkens, E. S. Dodsworth, P. R. Auburn, *Coord. Chem. Rev*., **1993**, *125*, 317.

[4] P. R. Auburn, E. S. Dodsworth, M. Haga, W. Liu, W. A. Nevin, A. B. P. Lever, *Inorg. Chem*., **1991**, *30*, 3502.

[5] M. D. Ward, J. A. McCleverty, *Dalton Trans*., **2002**, 275.

[6] Q. Knijnenburg, S. Gambarotta, P. H. M. Budzelaar, *Dalton Trans*., **2006**, 5442.

[7] G. N. Schrauzer, V. Mayweg, *J. Am. Chem. Soc*., **1962**, *84*, 3221.

[8] A. Davison, N. Edelstein, R. H. Holm, A. H. Maki, *J. Am. Chem. Soc*., **1963**, *85*, 2029

[9] A. Davison, N. Edelstein, R. H. Holm, A. H. Maki, *Inorg. Chem*., **1963**, *2*, 1227.

[10] H. B. Gray, R. Williams, I. Bernal and E. Billig, *J. Am. Chem. Soc*., **1962**, *84*, 3596.

[11] E. Billig, R. Williams, I. Bernal, J. H. Waters and H. B. Gray, *Inorg. Chem*., **1964**, *3*, 663.

[12] J. A. McCleverty, *Progr. Inorg. Chem*., **1968**, *10*, 49.

[13] E. I. Stiefel, J. H. Waters, E. Billig, H. B. Gray, *J. Am. Chem. Soc*., **1965**, *87*, 3016.

[14] A. L. Balch, R. H. Holm, *J. Am. Chem. Soc*., **1966**, *88*, 5201.

[15] R. K. Szilagyi, B. S. Lim, T. Glaser, R. H. Holm, B. Hedman, K. O. Hodgson, E. I. Solomon, *J. Am. Chem. Soc*., **2003**, *125*, 9158.

[16] (a) K.D. Karlin, E.I. Stiefel (Eds.), *Prog. Inorg. Chem*., **2004**, 52; (b) S.J.N. Burgmayer, *Progr. Inorg. Chem*. **2004**, *52*, 491.

[17] D. Herebian, E. Bothe, E. Bill, T. Weyhermuiller, K. Wieghardt, *J. Am. Chem. Soc*., **2001**, *123*, 10012.

[18] G. J. P. Britovsek, V. C. Gibson, B. S. Kimberley, P. J. Maddox, S. J. McTavish, G. A. Solan, A. J. P. White and D. J. Williams, *Chem. Commun*., **1998**, 849.

[19] B. L. Small, M. Brookhart, A. M. A. Bennett, *J. Am. Chem. Soc*., **1998**, *120*, 4049.

[20] H. Sugiyama, I. Korobkov, S. Gambarotta, A. Möller, P. H. M. Budzelaar, *Inorg. Chem*., **2004**, *43*, 5771.

[21] B. de Bruin, E. Bill, E. Bothe, T. Weyhermüller, K. Wieghardt, *Inorg. Chem*., **2000**, *39*, 2936.

[22] D. Reardon, F. Conan, S. Gambarotta, G. P. A. Yap, Q. Wang, *J. Am. Chem. Soc*., **1999**, *121*, 9318.

[23] D. Enright, S. Gambarotta, G. P. A. Yap, P. H. M. Budzelaar, *Angew. Chem., Int. Ed*., **2002**, *41*, 3873.

[24] S. J. N. Burgmayer, H. L. Kaufmann, G. Fortunato, P. Hug, B. Fischer, *Inorg. Chem*., **1999**, *38*, 2607.

[25] S. G. Pierpont, *Coord. Chem. Rev*., **2001**, *216-217*, 99.

[26] S. G. Pierpont, *Coord. Chem. Rev*., **2001**, *219-221*, 415.

[27] M. Fourmigué, *Acc. Chem. Res*., **2004**, *37*, 179.

[28] A. Mederos, S. Dominguez, R. Hernardez-Molina, J. Sanchiz, F. Brito, *Coord. Chem. Rev*., **1999**, *193-195*, 913.

[29] A. Mederos, S. Dominguez, R. Hernandez-Molina, J. Sanchiz, F. Brito, *Coord. Chem. Rev*., **1999**, *193-195*, 857.

[30] E. Uhlig, *Z. Chem*., **1989**, *29*, 305.

[31] A Ghosh, E Steene, *J. Inorg. Biochem*., **2002**, *91*, 423.

[32] A. Vlcek Jr., *Chemtracts*, **1998**, *11*, 352.

[33] J. A. McCleverty, M. D. Ward, C. J. Jones, *Comments Inorg. Chem*., **2001**, *22*, 293.

[34] N. Mezailles, F. Mathey, P. Le Floch, *Progr. Inorg. Chem*., **2001**, *49*, 455.

[35] K P Butin, E K Beloglazkina, N V Zyk, *Rus. Chem. Rev*., **2005**, *74*, 531.

[36] C. Lorente, A.H. Thomas, *Acc. Chem. Res*., **2006**, *39*, 395.

[37] (a) C. Walsh, *Acc. Chem. Res*. **1980**, *13*, 148; (b) T.C. Bruice, *Acc. Chem. Res*., **1980**, *13*, 256.

[38] (a) W. Kaim, B. Schwederski, O. Heilmann, F. Hornung, *Coord. Chem. Rev*., **1999**, *182*, 323; (b) P. Hemmerich, J. Lauterwein, in: G.L. Eichhorn (*Ed*.), *Inorganic Biochemistry*, Elsevier, Amsterdam, **1973**, 1168.

[39] M. J. Clarke, *Comments Inorg. Chem*. **1984**, *3*, 133.

[40] S. Fukuzumi, T. Kojima, *J. Biol. Inorg. Chem*. **2008**, *13*, 321.

[41] B. Fisher, J. Strahle, M. Viscontini, *Helv. Chim. Acta*, **1991**, *74*, 1544.

[42] S. J. N. Burgmayer, M. R. Arkin, L. Bostick, S. Dempster, K. M. Everett, H. L. Layton, K. E. Paul, C. Rogge, A. L. Rheingold, *J. Am. Chem. Soc*., **1995**, *117*, 5812.

[43] C. Bessenbacher, C. Vogler, W. Kaim, *Inorg. Chem*., **1989**, *28*, 4645.

[44] O. Heilmann, F. M. Hornung, W. Kaim, J. Fiedler, *Faraday Trans*., **1996**, *92*, 4233.

[45] T. Kohzuma, A. Odani, Y. Morita, M. Takani, O. Yamauchi, *Inorg. Chem*., **1988**, *27*, 3854.

[46] Y. Funahashi, H. Hara, H. Masuda, O. Yamauchi, *Inorg. Chem*., **1997**, *36*, 3869.

[47] M. Mitsumi, J. Toyoda, K. Nakasuji, *Inorg. Chem*., **1995**, *34*, 3367.

[48] D-H. Lee, N. N. Murthy, Y. Lin, N. S. Nasir, K. D. Karlin, *Inorg. Chem*., **1997**, *36*, 6328.

[49] M.J. Romão, *Dalton Trans*., **2009**, 4053.

[50] E.M. Armstrong, M.S. Austerberry, J.H. Birks, R.L. Beddoes, M. Helliwell, J.A. Joule, C.D. Garner, *Heterocycles*, **1993**, *35*, 563.

[51] B. Bradshaw, A. Dinsmore, D. Collison, C.D. Garner, J.A. Joule, *Perkin Trans. 1*, **2001**, 3232.

[52] E.S. Davies, G.M. Aston, R.L. Beddoes, D. Collison, A. Dinsmore, A. Docrat, J.A. Joule, C.R. Wilson, C.D. Garner, *Dalton Trans*., **1998**, 3647.

[53] E.S. Davies, R.L. Beddoes, D. Collison, A. Dinsmore, A. Docrat, J.A. Joule, C.R. Wilson, C.D. Garner, *Dalton Trans*., **1997**, 3985.

[54] F. J. Hine, A. J. Taylor, C. D. Garner, *Coord. Chem. Rev*., **2010**, *254*, 1570.

[55] W. Kaim, B. Schwederski, *Coord. Chem. Rev*., **2010**, *254*, 1580.

[56] R. Hille, in: H. Sigel, A. Sigel (Eds.), *Metal Ions in Biological Systems*, vol. *39*, Marcel Dekker, Inc., New York, **2002**, p. 187.

[57] M. J. Romao, *Dalton Trans*., **2009**, 4053.

[58] R.S. Pilato, K.A. Eriksen, M.A. Greaney, E.I. Stiefel, S. Goswami, L. Kilpatrick, T.G. Spiro, E.C. Taylor, A.L. Rheingold, *J. Am. Chem. Soc*., **1991**, *113*, 9372.

[59] S.J.N. Burgmayer, M. Kim, R. Petit, A. Rothkopf, A. Kim, S. BelHamdounia, Y. Hou, A. Somogyi, D. Habel-Rodriguez, A. Williams, M.L. Kirk, *J. Inorg. Biochem*., **2007**, *101*, 1601.

[60] (a) B. L. Small, M. Brookhart, A. M. A. Bennett, *J. Am. Chem. Soc*., **1998**, *120*, 4049; (b) G. J. P. Britovsek, V. C. Gibson, B. S. Kimberley, P. J. Maddox, S. J. McTavish, G. A. Solan, A. J. P. White, D. J. Williams, *Chem. Commun*., **1998**, 849.

[61] (a) Q. Knijnenburg, A. D. Horton, H. van der Heijden, T. M. Kooistra, D. G. H. Hetterscheid, J. M. M. Smits, B. de Bruin, P. H. M. Budzelaar, A.W.Gal, *J. Mol. Catal. A*., **2005**, *232*, 151; (b) S. C. Bart, E. Lobkovsky, P. J. Chirik, *J. Am. Chem. Soc*., **2004**, *126*, 13794.

[62] E. L. Dias, M. Brookhart, P. S. White, *J. Am. Chem. Soc*., **2001**, *123*, 2442.

[63] (a) G. Chiericato, C. R. Arana, C. Casado, I. Cuadrado, H. D. Abrũna, *Inorg. Chim. Acta*, **2000**, *300*, 32; (b) J. H. Jiang, A. Kucernak, *Electrochim. Acta*, **2002**, *47*, 1967.

[64] S. C. Bart, E. Lobkovsky, P. J. Chirik, *J. Am. Chem. Soc*., **2004**, *126*, 13794.

[65] K. T. Sylvester, P. J. Chirik, *J. Am. Chem. Soc*. **2009**, *131*, 8772.

[66] (a) N. Kleigrewe, W. Steffen, T. Blömker, G. Kehr, R. Fröhlich, B. Wibbeling, G. Erker, J.-C. Wasilke, G. Wu, G. C. Bazan, *J. Am. Chem. Soc*., **2005**, *127*, 13955; (b) W. Steffen, T. Blömker, N. Kleigrewe, G. Kehr, R. Fröhlich, G. Erker, *Chem. Commun*., **2004**, 1188.

[67] W.-H. Sun, S. Jie, S. Zhang, W. Zhang, Y. Song, H. Ma, J. Chen, K. Wedeking, R. Fröhlich, *Organometallics*, **2006**, *25*, 666.

[68] C. Bianchini, G. Mantovani, A. Meli, F. Migliacci, *Organometallics*, **2003**, *22*, 2545.

[69] K. Kreischer, J. Kipke, M. Bauerfeind, J. Sundermeyer, *Z. Anorg. Allg. Chem*., **2001**, *627*, 1023.

[70] S. Al-Benna, M. J. Sarsfield, M. Thornton-Pett, D. L. Ormsby, P. J. Maddox, P. Brès, M. Bochmann, *Dalton Trans*., **2000**, 4247.

[71] G. J. P. Britovsek, V. C. Gibson, S. Mastroianni, D. C. H. Oakes, C. Redshaw, G. A. Solan, A. J. P. White, D. J. Williams, *Eur. J. Inorg. Chem*., **2001**, 431.

[72] D. S. McGuinness, V. C. Gibson, J.W. Steed, *Organometallics*, **2004**, *23*, 6288.

[73] G. J. P. Britovsek,V.C. Gibson,O.D. Hoarau, S. K. Spitzmesser, A. J. P. White, D. J. Williams, *Inorg. Chem*., **2003**, *42*, 3454.

[74] S. Fernandes, R. M. Bellabarba, A. F. G. Ribeiro, P. T. Gomes, J. R. Ascenso, J. F. Mano, A.R. Dias, M. M. Marques, *Polym. Int*., **2002**, *51*, 1301.

[75] J. Cámpora, A. M. Naz, P. Palma, E. Álvarez, M. L. Reyes, *Organometallics*, **2005**, *24*, 4878.

[76] M. W. Bouwkamp, E. Lobkovsky, P. J. Chirik, *Inorg. Chem*., **2006**, *45*, 2.

[77] H. Sugiyama, I. Korobkov, S. Gambarotta, A. Möller, P. H. M. Budzelaar, *Inorg. Chem*., **2004**, *43*, 5771.

[78] J. Scott, S. Gambarotta, I. Korobkov, P. H. M. Budzelaar, *J. Am. Chem. Soc*., **2005**, *127*, 13019.

[79] M. Bruce, V. C. Gibson, C. Redshaw, G. A. Solan, A. J. P. White, D. J. Williams, *Chem. Commun*., **1998**, 2523.

[80] Q. Knijnenburg, J. M. M. Smits, P. H. M. Budzelaar, *Organometallics*, **2006**, *25*, 1036.

[81] D. Reardon, F. Conan, S. Gambarotta, G. P. A. Yap, Q. Wang, *J. Am. Chem. Soc*., **1999**, *121*, 9318.

[82] D. Enright, S. Gambarotta, G. P. A. Yap, P. H. M. Budzelaar, *Angew. Chem., Int. Ed*., **2002**, *41*, 3873.

[83] T. M. Kooistra, D. G. H. Hetterscheid, E. Schwartz, Q. Knijnenburg, P. H. M. Budzelaar, A. W. Gal, *Inorg. Chim. Acta*, **2004**, *357*, 2945.

[84] I. Korobkov, S. Gambarotta, G. P. A. Yap, P. H. M. Budzelaar, *Organometallics*, **2002**, *21*, 3088.

[85] G. K. B. Clentsmith, V. C. Gibson, P. B. Hitchcock, B. S. Kimberley, C. W. Rees, *Chem. Commun*., **2002**, 1498.

[86] S. C. Bart, K. Chłopek, E. Bill, M. W. Bouwkamp, E. Lobkovsky, F. Neese, K. Wieghardt, P. J. Chirik., *J. Am. Chem. Soc*., **2006**, *128*, 13901.

[87] Q. Knijnenburg, S Gambarotta, P. H. M. Budzelaar, *Dalton Trans*. **2006**, 5442.

[88] D. Zhu, F. F. B. J. Janssen, P. H. M. Budzelaar, *Organometallics* **2010,** *29*, 1897.

[89] (a) D. Zhu, P. H. M. Budzelaar, *Organometallics*, **2010**, *29*, 5759; (b) V. C. Gibson, M. J. Humphries, K. P. Tellmann, D. F. Wass, A. J. P. White, D. J. Williams, Chem. Commun., 2001,

2252–2253; (c) T. M. Kooistra, Q. Knijnenburg, J. M. M. Smits, A. D. Horton, P. H. M. Budzelaar, A. W Gal, *Angew. Chem. Int. Ed*., **2001**, 40, 4719-4722.

[90] (a) J. Halpern, J. P. Maher, *J. Am. Chem. Soc*., **1965**, *87*, 5361; (b) P. B. Chock, J. Halpern, *J. Am. Chem. Soc*., **1969**, *91*, 582. (c) L. G. Marzilli, P. A. Marzilli, J. Halpern, *J. Am. Chem. Soc*., **1971**, *93*, 1374.

[91] M. C. Hughes, D. J. Macero, *Inorg. Chem*., **1976**, *15*, 2040.

[92] S. Herzog, R. Taube, *Z. Anorg. Allg. Chem*. **1960**, *306*, 159.

[93] J. Quirk, G. Wilkinson, *Polyhedron*, **1982**, *1*, 209.

[94] A. Flamini, A.M. Giuliani, *Inorg. Chim. Acta*, **1986**, *112*, L7.

[95] (a) R. Pappalardo, *Inorg. Chim. Acta*, **1968**, *2*, 209; (b) E. König, S. Herzog, *J. Inorg. Nucl. Chem*., **1970**, *32*, 613; (c) E. König, S. Herzog, *J. Inorg. Nucl. Chem*., **1970**, *32*, 601; (d) Y Kaizu, T. Yazaki, Y Torii, H. Kobayashi, *Bull. Chem. Soc. Jap*., **1970**, *43*, 2068; (e) I. Hanazaki, S. Nagakura, *Bull. Chem. Soc. Jap*., **1971**, *44*, 2312; (f) E. König, E. Lindner, *Spectrochim. Acta*, **1972**, *28A*, 1393.

[96] M. Grätzel, *J. Photochem. Photobiol*. C, **2003**, *4*, 145.

[97] A. Bencini, V. Lippolis, Coord. *Chem. Rev*., **2010**, *254*, 2096.

[98] K Kalyanasundaram, M. Grätzel, *Current Opinion in Biotechnology*, **2010**, *21*, 298.

[99] N. J. Lundin, P. J. Walsh, S. L. Howell, J. J. McGarvey, A. G. Blackman, K. C. Gordon, *Inorg. Chem*. **2005**, *44*, 3551.

[100] N. J. Lundin, P. J. Walsh, S. L. Howell, A. G. Blackman, K. C. Gordon, *Chem. Eur. J*. **2008**, *14*, 11573.

[101] A. W. McKinleya, P. Lincoln, E. M. Tuite, *Coord. Chem. Rev*., **2011**, *255*, 2676.

[102] V. W.-W. V. Yam, K. K.-W. Lo, K.-K. Cheung, R. Y.-C. Kong, *Dalton Trans*., **1997**, 2067.

[103] G. David, P. J. Walsh, K.C. Gordon, *Chem. Phys. Lett*., **2004**, *383*, 292.

[104] K. C. Gordon, P. J. Walsh, E.M. McGale, *Curr. Appl. Phys*., **2004**, *4*, 331.

[105] F. Baumann, W. Kaim, M. G. Posse, N. E. Katz, *Inorg. Chem*., **1998**, *37*, 658.

[106] J. Fees, W. Kaim, M. Moscberosch, W. Matheis, J. Klima, M. Krejcik, S. Záliš, *Inorg. Chem*., **1993**, *32*, 166.

[107] J. Fees, M. Ketterle, A. Klein, J. Fiedler, W. Kaim, *Dalton Trans*., **1999**, 2595.

[108] A. Klein, W. Kaim, E. Waldhoer, H.-D. Hausen, *Perkin Trans. 2*, **1995**, 2121.

[109] A.Klein, T. Scheiring, W. Kaim, *Z. Anorg. Allg. Chem*., **1999**, *625*,1177.

[110] M.N. Ackermann, L.V. Interrante, *Inorg. Chem*., **1984**, *23*, 3904.

[111] E. Amouyal, A. Homsi, J.-C. Chambro, J.-P. Sauvage, *Dalton Trans*., **1990**, 1841.

[112] C. G. Coates, L. Jacquet, J. J. McGarvey, S. E. J. Bell, A. H. R. Al-Obaidi, J. M. Kelly, *J. Am. Chem. Soc*., **1997**, *119*, 7130.

[113] S. Rau, M. Schwalbe, S. Losse, H. Görls, C. McAlister, F. M. MacDonnell, J. G. Vos, *Eur. J. Inorg. Chem*., **2008**, 1031.

[114] (a) G. Albano, V. Balzani, E. C. Constable, M. Maestri, D. R. Smith, *Inorg. Chim. Acta*, **1998**, *277*, 225; (b) M. C. DeRosa, R. J. Crutchley, *Coord. Chem. Rev*. **2002**, *233*, 351; (c) F. Gao, H. Chao, F. Zhou, Y.-X. Yuan, B. Peng, L.-N. Ji, *J. Inorg. Biochem*. **2006**, *100*, 1487; (d) S. Meyer, D. Tietze, S. Rau, B. Schäfer, G. Kreisel, *J. Photochem. Photobiol*. *A*, **2007**, *186*, 248.

[115] P. Banerjee, G. Mostafa, A. Castiñeiras, S. Goswami, *Eur. J. Inorg. Chem*., **2007**, 412.

[116] A. K. Deb, S. Goswami, *Dalton Trans*., **1989**, 1635.

[117] R. McGuire Jr., M. C. McGuire, D. R. McMillin, *Coord. Chem. Rev*., **2010**, *254*, 2574.

[118] A. Coleman, C. Brennan, J. G. Vos, M. T. Pryce, *Coord. Chem. Rev*., **2008**, *252*, 2585.

[119] J. Fees, M. Ketterle, A. Klein, J. Fiedler, W. Kaim, *Dalton Trans*., **1999**, 2595.

[120] T. Uchida, K. Kimura, *Acta Cryst. C*, **1984**, *C40*, 139.

[121] N. Karl,W. Ketterer, J.J. Stezowski, *Acta Cryst. B*, **1982**, *B38*, 2917.

[122] T.-T. Luo, Y. - H. Liu, H. - L. Tsai, C. - C. Su, C. - H. Ueng, K. - L. Lu, *Eur. J. Inorg. Chem*., **2004**, 4253.

[123] S. Kawata, S. Kitagawa, H. Kumagai, C. Kudo, H. Kamesaki, T. Ishiyama, R. Suzuki, M. Kondo, M. Katada, *Inorg. Chem*., **1996**, *35*, 4449.

[124] J. A. Whiteford, P. J. Stang, S. D. Huang, *Inorg. Chem*., **1998**, *37*, 5595.

[125] A. Althoff, P. Jutzi, N. Lenze, B. Neumann, A. Stammler, H. –G. Stammler, *Organometallics*, **2002**, *21*, 3018.

[126] F. A. Cotton, Y. Kim, T. Ren, *Inorg. Chem*., **1992**, *31*, 2723.

[127] M. Munakata, T. Kuroda-Sowa, M. Maekawa, A. Honda, S. Kitagawa, *Dalton Trans*., **1994**, 2771.

[128] M. Munakata, S. Kitagawa, N. Ujimaru, M. Nakamura, M. Maekawa and H. Matsuda, *Inorg. Chem*., **1993**, *32*, 826.

[129] T. Kuroda-Sowa, M. Munakata, H. Matsuda, S. Akiyama, M. Maekawa, *Dalton Trans*. **1995**, 2201.

[130] M. Munakata, T. Kuroda-Sowa, M. Maekawa, A. Honda, S. Kitagawa, *Dalton Trans*., **1994**, 2771.

[131] T. Kogane, N. Koyama, T. Ishida, T. Nogami, *Polyhedron*, **2007**, *26*, 1811.

[132] S. E. H. Etaiw, D. M. A. El-Aziz, M. Sh. Ibrahim, A. S. B. El-din, *Polyhedron*, **2009**, *28*, 1001.

[133] R.C. Kaye, H.I. Stonehill, *J. Chem. Soc*., **1952**, 3240.

[134] (a) O. N. Nechaeva, Z. V. Pushkareva, *Zh. Obshch. Khim*. **1958**, *28*, 2693; (b) E. de Boer, *Adv. Organomet. Chem*. **1964**, *2*, 115.

[135] A. Behrendt, C. G. Screttas, D. Bethell, O. Schiemann, B. R. Stelle, *J. Chem. Soc., Perkin Trans. 2*, **1998**, 2039.

[136] F. G. Thomas, K. G. Boto, *The Chemistry of the Hydrazo, Azo, and Azoxy Groups*; S. Patai, Ed.; Wiley: New York, **1975**; Chapter *12*.

[137] A. Minsky, Y. Cohen, M. Rabinovitz, *J. Am. Chem. Soc*., **1985**, *107*, 1501.

[138] Y. Cohen, A. Y. Meyer, M. Rabinovitz, *J. Am. Chem. Soc*., **1986**, *108*, 7039;

[139] L.M. Engelhardt, G.E. Jacobsen, A.H. White, C.L. Raston, *Inorg. Chem*. **1991***, 30*, 3978.

[140] P.C. Junk, C.L. Raston, B.W. Skelton, A.H. White, *Chem. Comm*., **1987**, 1162.

[141] a) L. Birkofer, A. Birkofer, *Chem. Ber*., **1952**, *85*, 286 - 289; b) F. Bohlmann, *Chem. Ber*. **1952**, *85*, 390 - 394; c) G. R. Clemo, H. McIlwain, *J. Chem. Soc*., **1934**, 1991 - 1993.

[142] W. Kaim, *J. Am. Chem. Soc*., **1984**, *106*, 1712 - 1716.

[143] (a) J. K. Kochi, "*Organometallic Mechanisms and Catalysis*"; Academic Press: New York, **1978**; Chapter 17 and references therein; (b) L. Eberson, *Adv. Phys. Org. Chem*., **1982**, 18, 79 - 185. (c) E. C. Ashby, *Pure Appl. Chem*., **1980**, *52*, 545 - 569.

[144] W. Kaim, *J. Organomet. Chem*., **1981**, *215*, 337 - 348.

[145] J. Scholz, A. Scholz, R. Weimann, C. Janiak, H. Schumann, *Angew. Chem., Int. Ed*. **1994**, *33*, 1171.

[146] W. J. Evans, S. L. Gonzales, J. W. Ziller, *J. Am. Chem. Soc*., **1994**,*116*, 2600.

[147] W. J. Evans, S. E. Lorenz, J. W. Ziller, *Inorg. Chem*., **2009**, *48*, 2001.

[148] D. J. Berg, J. M. Boncella, R. A. Andersen, *Organometallics*, **2002**, *21*, 4622.

[149] W. J. Evans, D. S. Lee, J. W. Ziller, N. Kaltsoyannis, *J. Am. Chem. Soc*., **2006**, *128*, 14176.

[150] S. E. Lorenz, B. M. Schmiege, D. S. Lee, J. W. Ziller, W. J. Evans, *Inorg. Chem*., **2010**, *49*, 6655.

[151] W. J. Evans, K. A. Miller, D. S. Lee, J. W. Ziller, *Inorg. Chem*., **2005**, *44*, 4326.

[152] W. J. Evans, T. M. Champagne, J. W. Ziller, *Organometallics*, **2007**, *26*, 1204.

[153] W. J. Evans, J. R. Walensky, T. M. Champagne, J. W. Ziller, A. G. DiPasquale, A. L. Rheingold, *J. Organomet. Chem*., **2009**, *694*, 1238.

[154] M. R. MacDonald, J. W. Ziller, W. J. Evans, *Inorg. Chem*., **2011**, *50*, 4092.

[155] W. J. Evans, M. K. Takase, J. W. Ziller, A. G. DiPasquale, A. L. Rheingold, *Organometallics* **2009,** *28,* 236.

[156] A. Sattler, G. Zhu, G. Parkin, *J. Am. Chem. Soc*., **2009**, *131*, 7828.

[157] J. A. Cabeza, P. García-Álvarez, V. Pruneda, *Organometallics*, **2012**, *31*, 941.

## Chapter 2

# *Radical Cleavage of Al-C Bonds Promoted by Phenazine: from non-Innocent Ligand to Radical Abstractor.*

In this chapter we describe the complex reactivity of phenazine with $AlR_3$ (R = Me, Et, $^{i}$Bu) and the formation of stable organic radical species. Phenazine may act as both regular neutral donor and a reduced ligand engaging in electron transfer reaction with a wide variety of elements including lanthanides and actinides. However, the reactivity with alane or $AlMe_3$ as reported by Heunish in 1972 [1] and Kaim in 1984 [2] on the basis of EPR evidences seems to suggest the formation of stable radical species. [1, 2] In addition, we have reported that the reaction of organo aluminum Ziegler-Natta activator with the "dimpy" ligands, having the nitrogen containing aromatic ring, affords a very unusual divalent Al synthon (trivalent Al coupled to a radical anion) possibly indicating that this type of ligands may also promote radical Al-C bond cleavage.[3] Furthermore, when the phenazine moiety becomes part of larger aromatic systems, including those containing the Ru(bipy) moieties, photochemical activation of dioxygen is being observed.[4] Given the importance of these rather complex frames vis-à-vis ability to trigger water splitting via formation/extraction of radical hydrogen atoms, we became interested in establishing the ability of phenazine to promote cleavage of chemical bonds in radical fashion.

## *Results and Discussion.*

Reaction of phenazine with $AlMe_3$ affords immediate color change upon mixing. The expected coordination adduct $[AlMe_3]_2(\mu\text{-}\eta^1\text{:}\eta^1\text{-}C_{12}H_8N_2)$ (**1a**) was obtained as red crystalline material only if a rapid work up is carried out to isolate the complex (Scheme 35).

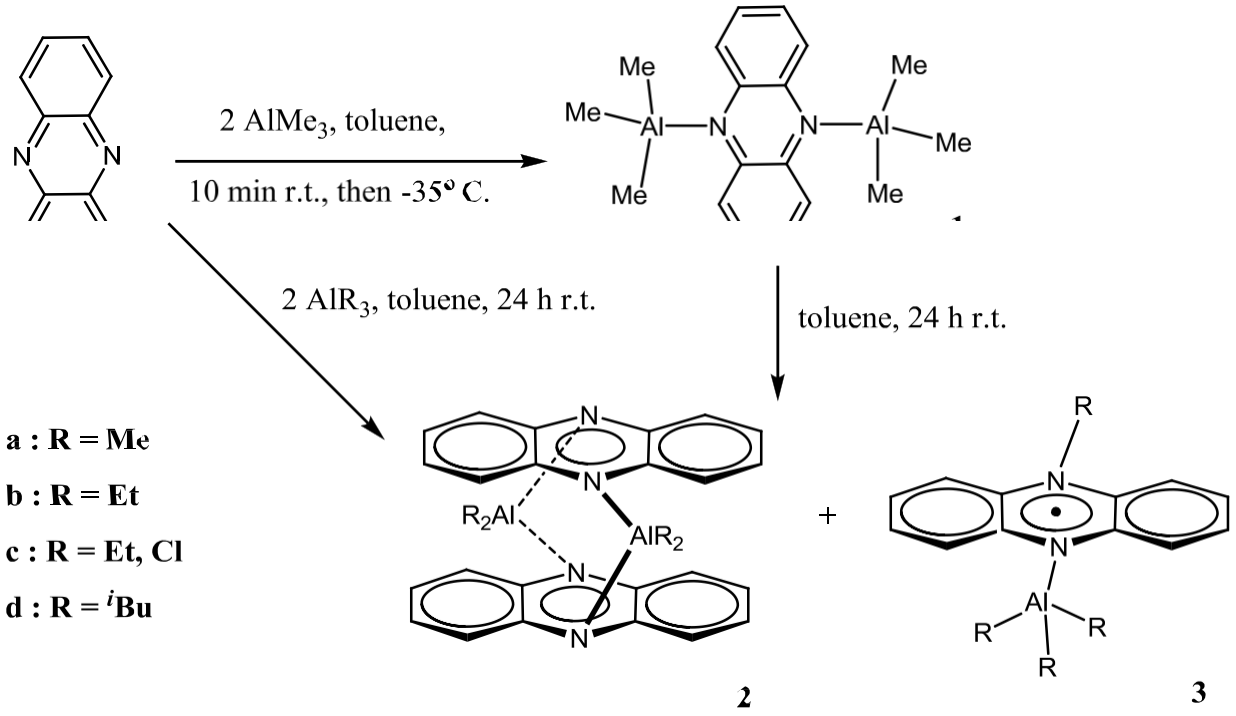


**Scheme 35**. Preparation of alkyl aluminum phenazine complexes.

The structure **1a** shows the expected coordination of two aluminate groups $\sigma$-bonded to each of the two phenazine N atoms (Figure 7). The complex is diamagnetic and shows the expected features in the NMR spectra.

**Figure 7**. X-ray Structure of complex $[AlMe_3]_2(\mu\text{-}\eta^1\text{:}\eta^1\text{-}C_{12}H_8N_2)$ (1a). Thermal ellipsoids are drawn at the 50% probability level.

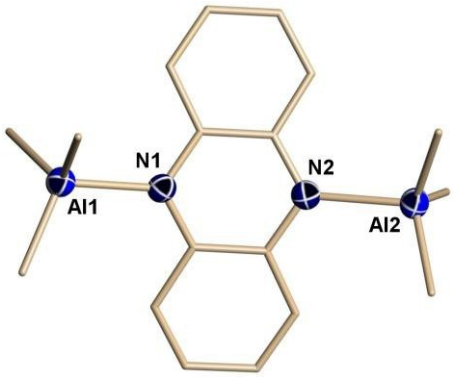


**Table 2**. Selected Bond Distances (Å) and Angles (°) for complex $[AlMe_3]_2(\mu\text{-}\eta^1\text{:}\eta^1\text{-}C_{12}H_8N_2)$ (**1a**).

| | | | |
|---|---|---|---|
| Al(1)-N(1) | 2.144(4) | N(1)-C(1) | 1.359(5) |
| Al(2)-N(2) | 2.147(4) | N(1)-C(7) | 1.354(5) |
| Al(1)-C(13) | 1.970(5) | C(13)-Al(1)-C(15) | 107.9(2) |
| Al(1)-C(14) | 1.975(5) | C(13)-Al(1)-C(14) | 118.2(2) |
| Al(1)-C(15) | 1.968(5) | C(15)-Al(1)-C(14) | 113.3(2) |
| N(1)-C(1)-C(2) | 120.0(4) | C(13)-Al(1)-N(1) | 101.6(2) |
| N(1)-C(1) | 1.359(5) | C(15)-Al(1)-N(1) | 111.8(2) |
| N(1)-C(7) | 1.354(5) | C(14)-Al(1)-N(1) | 103.3(2) |

We noticed that if the reaction mixture, from which **1a** can be isolated, is instead allowed to stand at room temperature for a few hours, the red color turned dark-green (Scheme 35). A new diamagnetic complex $[AlMe_2]_2(\mu\text{-}\eta^1\text{:}\eta^1\text{-}C_{12}H_8N_2)_2$ (**2a**) was isolated as dark-green crystals. Isostructural compounds were obtained in the case of similar reactions carried out with $Et_3Al$,

(**2b**), $Et_2AlCl$ (**2c**) and *i*-$Bu_3Al$ (**2d**). The NMR spectra of all the compounds gave the expected features and integration ratios. The only exception was **2d** and for which analytically pure crystalline material could not be isolated due to persistent contamination by paramagnetic oily material.

In all the complexes the crystal structures showed dinuclear arrangements where the two phenazine moieties are slightly folded (angle between two phenyl wings are in the range 158.1° to 161.7°), arranged parallel to each other and linked at the nitrogen atoms by two $R_2Al$ units (Figure 8).

**Table 3**. Selected Bond Distances (Å) and Angles (°) for complex $[AlMe_2]_2(\mu\text{-}\eta^1\text{:}\eta^1\text{-}C_{12}H_8N_2)_2$ (**2a**).

| | | | |
|---|---|---|---|
| Al(1)-N(4) | 1.970(2) | N(2)-C(7) | 1.388(5) |
| Al(1)-N(2) | 1.976(4) | N(2)-Al(1)-C(25) | 114.78(18) |
| Al(1)-C(25) | 1.963(4) | N(2)-Al(1)-N(4) | 86.99(14) |
| Al(1)-C(26) | 1.960(4) | N(4)-Al(1)-C(25) | 116.81(18) |
| N(2)-C(6) | 1.396(5) | N(4)-Al(1)-C(26) | 114.07(17) |

**Table 4**. Selected Bond Distances (Å) and Angles (°) for complex $[AlEt_2]_2(\mu\text{-}\eta^1\text{:}\eta^1\text{-}C_{12}H_8N_2)_2$ (**2b**).

| | | | |
|---|---|---|---|
| Al(1)-N(1) | 1.978(3) | N(1)-Al(1)-N(2a) | 87.03(14) |
| Al(1)-N(2a) | 1.979(4) | N(1)-Al(1)-C(13) | 114.82(17) |
| Al(1)-C(15) | 1.970(4) | C(15)-Al(1)-C(13) | 106.61(18) |
| Al(1)-C(13) | 1.974(4) | C(15)-Al(1)-N(1) | 115.04(17) |
| N(1)-C(1) | 1.397(5) | C(15)-Al(1)-N(2a) | 115.12(18) |

| | | | |
|---|---|---|---|
| N(1)-C(7) | 1.389(5) | C(13)-Al(1)-N(2a) | 117,70(17) |

**Figure 8**. X-ray Structures of complexes $[AlMe_2]_2(\mu\text{-}\eta^1\text{:}\eta^1\text{-}C_{12}H_8N_2)_2$ (**2a**), $[AlEt_2]_2(\mu\text{-}\eta^1\text{:}\eta^1\text{-}C_{12}H_8N_2)_2$ (**2b**), $[AlEt_{1.6}Cl_{0.4}]_2(\mu\text{-}\eta^1\text{:}\eta^1\text{-}C_{12}H_8N_2)_2$ (**2c**) and $[Al^iBu_2]_2(\mu\text{-}\eta^1\text{:}\eta^1\text{-}C_{12}H_8N_2)_2$ (**2d**). Thermal ellipsoids are drawn at the 50% probability level.

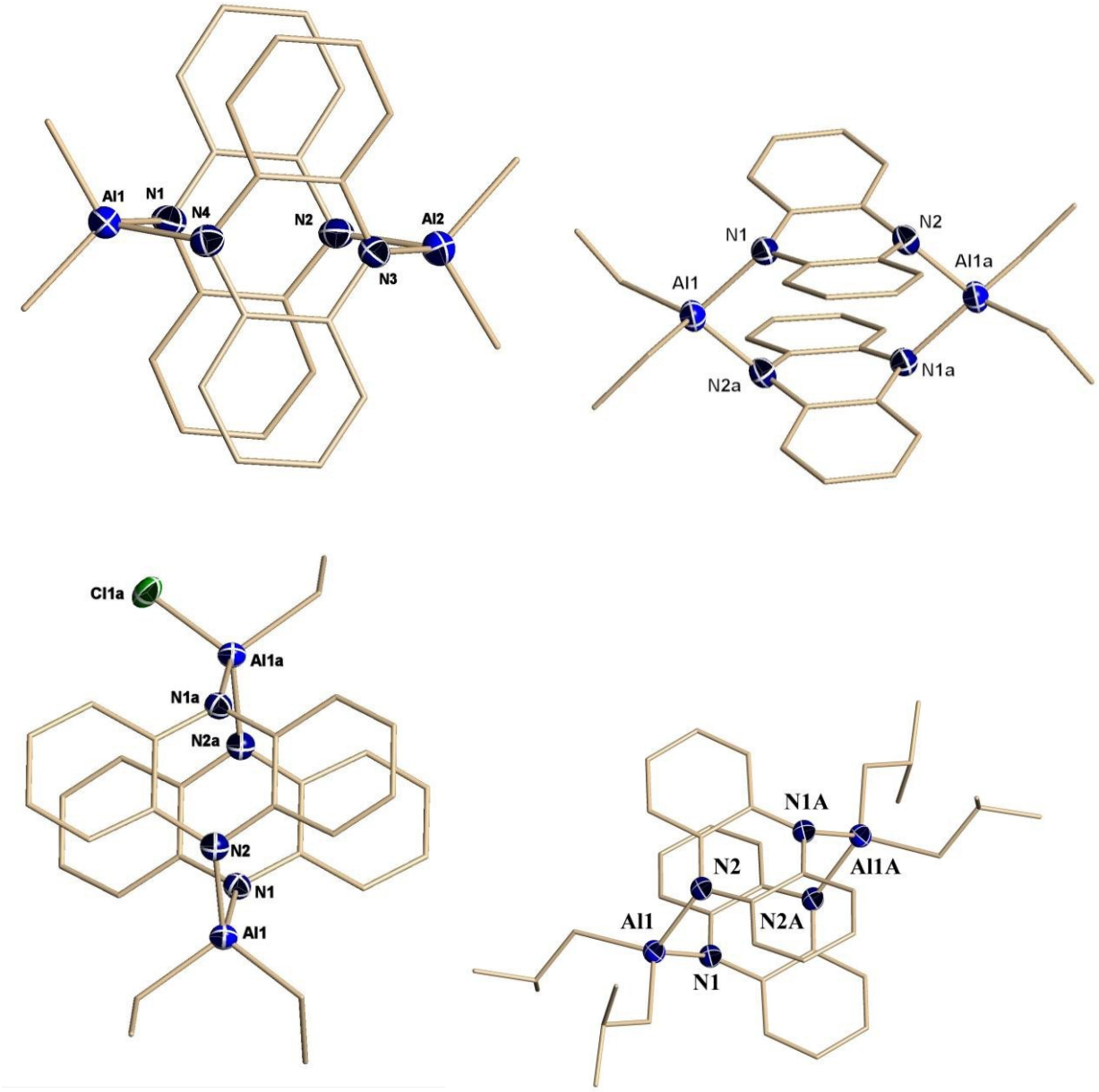

**Table 5.** Selected Bond Distances (Å) and Angles (°) for complex $[AlEt_{1.6}Cl_{0.4}]_2(\mu\text{-}\eta^1\text{:}\eta^1\text{-}C_{12}H_8N_2)_2$ (**2c**).

| | | | |
|---|---|---|---|
| Al(1)-N(1) | 1.966(2) | N(1)-Al(1)-N(2a) | 87.52(9) |
| Al(1)-N(2a) | 1.965(2) | N(1)-Al(1)-C(1) | 116.7(6) |
| Al(1)-C(1) | 1.978(16) | N(1)-Al(1)-Cl(1) | 119.6(6) |
| Al(1)-Cl(1) | 2.01(2) | C(1)-Al(1)-Cl(1) | 102.8(8) |
| N(1)-C(3) | 1.390(3) | C(3)-N(1)-C(9)-C(14) | 19.3(3) |

**Table 6**. Selected Bond Distances (Å) and Angles (°) for complex $[Al^iBu_2]_2(\mu\text{-}\eta^1\text{:}\eta^1\text{-}C_{12}H_8N_2)_2$ (**2d**).

| | | | |
|---|---|---|---|
| Al(1)-N(1) | 1.990(3) | N(2a)-Al(1)-N(1) | 85.12(12) |
| Al(1)-N(2a) | 1.991(3) | N(1)-Al(1)-C(13) | 113.50(15) |
| Al(1)-C(13) | 1.993(4) | N(1)-Al(1)-C(17) | 119.94(15) |
| Al(1)-C(17) | 1.989(4) | C(13)-Al(1)-C(17) | 104.92(17) |
| N(1)-C(7) | 1.387(5) | C(7)-N(1)-C(1) | 115.1(3) |
| N(1)-C(1) | 1.396(4) | | |
| N(2)-C(6) | 1.392(5) | | |
| N(2)-C(12) | 1.396(5) | | |

The geometry surrounding aluminum is distorted tetrahedral in **2a - 2d**, due to the small bite N-Al-N angles (e.g. in **2a**: N(2)-Al(1)-N(4) = 86.99(14)˚; N(3)-Al(2)-N(1) = 86.71(14)˚) and larger C-Al-C angles (e.g. in **2a**: C(26)-Al(1)-C(25) 106.1(2)˚ and C(28)-Al(2)-C(27) 106.36(19)˚) (for other complexes see Tables 4 to 6 and Figure 8). The aluminum-nitrogen bond distances in **2a - 2d** (1.966(2) Å to 1.993(4) Å; Tables 4 to 6) are similar to those in N-donor aluminum complexes carrying the monoanionic ligand e.g. in $LAlCl_2$,[5] $LAlMe_2$ and LAlMeCl [6] (L = $\beta$-diketiminate ligand) or in aluminum amido complexes $(2,6\text{-}i\text{Pr}_2C_6H_3)N(SiMe_3)AlMe_2$,

(Al – N 1.823(2) Å),[7] [K·THF(2,6-*i*Pr$_2$C$_6$H$_3$N(SiMe$_3$)Al(C≡CPh)$_3$)]$_2$ (Al – N 1.836(2) Å) [8] and are shorter than in the complex **1a** (2.144(4) Å and 2.147(4) Å) consistent with the stronger interaction between the aluminum center and the formally anionic phenazine moieties.

The nitrogen-carbon bond distances of the formally monoanionic phenazine ligand (1.388(5) Å to 1.396(5) Å in **2a**, N(1)-C(1)=1.397(5) Å and N(1)-C(7)= 1.389(5) Å in **2b**, N(1)-C(3)=1.390(3) Å and N(1)-C(9)=1.395(3) Å in **2c**, 1.387(5) Å to 1.396(5) Å in **2d**) are longer than those in the formally neutral phenazine ligand in **1a** (1.349(5) to 1.359(5) Å) and are similar to those in the magnesium complex [MgBr$_2$(C$_{12}$H$_8$N$_2$)(THF)$_6$]·[MgBr$_2$(THF)$_4$] [9] (1.396(8) Å and 1.384(7) Å) containing the phenazine dianion.

Complexes **2a**–**d** appears to be indefinitely stable at room temperature under inert atmosphere. Crystalline complexes did not change appearance upon storing in a sealed ampoule over several months

The proton NMR spectra of **2a**–**c** display the resonances of the phenazine ligand and of the alkyl groups of AlR$_2$ moieties, with relative intensities in agreement with the [AlR$_2$]$_2$(C$_{12}$H$_8$N$_2$)$_2$ formulations. The chemical shifts of the phenazine rings [7.1 and 6.4 ppm (**2a**), 6.9 and 6.5 ppm (**2b**), 6.9 and 6.5 ppm (**2c**)] are all in similar ranges. However, the resonances of **2a**–**c** are significantly shifted to lower fields relative to those of **1a** (8.1 and 7.5 ppm) which contains a formally neutral phenazine ligand attached to the aluminum centre. From the other side, resonances of formally dinegative phenazine in complexes [(C$_5$Me$_5$)$_2$La]$_2$($\mu$-$\eta^2$:$\eta^2$-C$_{12}$H$_8$N$_2$) (6.19 and 5.29 ppm) [10] and [(C$_5$Me$_5$)$_2$Y]$_2$($\mu$-$\eta^3$:$\eta^3$-C$_{12}$H$_8$N$_2$), (6.07 ppm and 4.88 ppm) [11] are at significantly lower frequencies than those of **2a** – **2c** due to increase of proton shielding by increase of the negative charge on the ligand. The $^{13}$C NMR resonances of phenazine in **2a** – **2c** (140.5, 125.5, 124.0 **2a**, 140.5, 125.5, 123.5 **2b** and 140.5, 123.5 **2c**) are also shifted to lower

frequency relative to free phenazine (143.5, 130.4 and 129.7 respectively) due to presence of negative charge on the phenazine moiety.

The resonance of the methyl group in **2a** is observed at 1.1 ppm and which is significantly shifted with respect to $\{AlMe_3\}_2$ [12] and to the same unit in **1a** (-0.31 ppm and -0.3 ppm respectively). This is likely an effect of the negative charge on the phenazine ligand. The chemical shift of the ethyl resonances of the $\{AlEt_2\}$ moiety in **2b** [0.2 ppm ($CH_2$) and 1.1 ppm ($CH_3$)] is weakly affected by the coordination to phenazine, the resonances of free $AlEt_3$ being at 1.39 and 1.11 ppm. [13] The proton resonances of the ethyl group in **2c** (0.1 ppm ($CH_2$) and 1.5 ppm ($CH_3$)) are shifted relative to those of **2b** as a probable result of the inductive effect of the chlorine atom bonded to the aluminum centre.

The connectivity of **2a-d** is intriguing and implies that each phenazine moiety exists in the form of a radical mono-anion. This is of course under the assumption that the aluminate residue contains trivalent aluminum. In turn, this implies that a strong antiferromagnetic (AF) coupling is present within the molecule causing the diamagnetism. To clarify this issue, the electronic structure of complexes **2** and **3** has been investigated by means of DFT calculations. Calculations were carried out on model complex **2a** in both a singlet and triplet states. Two different functionals (bp86 and b3-lyp [14]) have been utilized for calculations and in both scenarios, the triplet state was significantly higher in energy than the singlet. The observed diamagnetism is well explained by the broken-symmetry b3-lyp analysis results with a configuration showing AF coupling between the unpaired alpha and beta electrons on the two units. The coupling is represented by the $S^2$ value: 0 would be perfect pairing, 1 would be perfect separation; for this complex we obtain $S^2 = 0.27$. For comparison, the (dimpy)CoMe complex gives $S^2 \approx 0.8$ using the same formalism and has thus more biradical character. [15a] In the broken-

**Figure 9**. Highest occupied $\alpha$ and $\beta$ orbitals of **2a**, as calculated at the unrestricted b3-lyp level (first four pictures) and the bp86 method (last two pictures).

α:

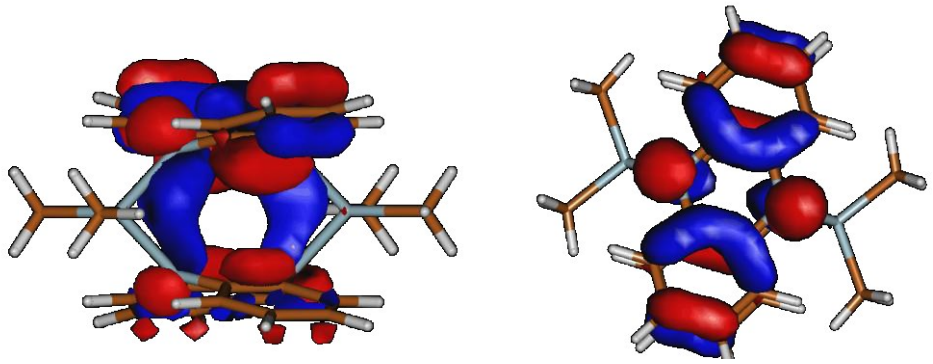

β:

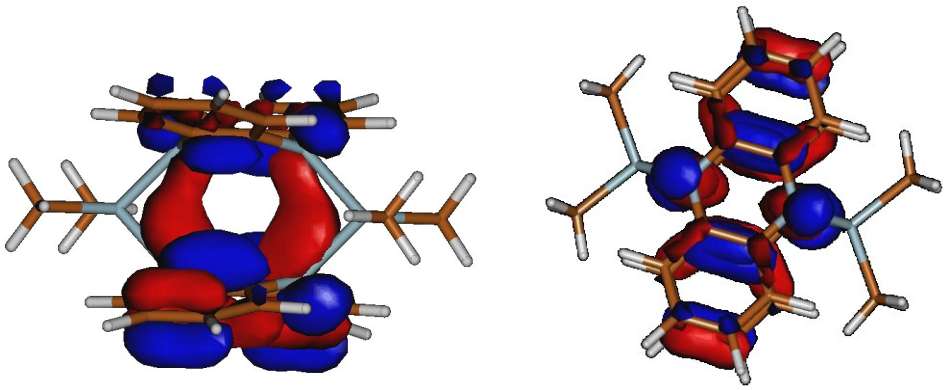

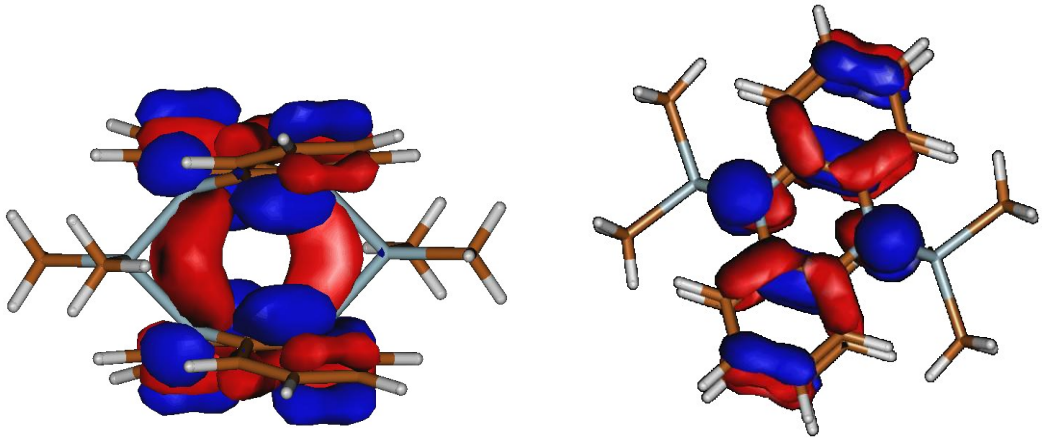

symmetry b3-lyp description, the α electron is mainly distributed on the top ligand while the β electron is on the other ligand (Figure 9).

The formation of complexes **2** does not have a straightforward explanation. Firstly the phenazine ligand has been reduced to its radical monoanionic form. Secondly one alkyl of the aluminate group has been removed through what seemingly appears to be an homolytic cleavage of the Al-C bond. In turn this implies that other products must necessarily be formed during the reaction. While crystalline samples of **2** are ESR-silent in both solid state and solution, we observed that in all cases the reaction mother liquors are paramagnetic, displaying ESR spectra with a single wave and complex hyperfine structure. In the case of **2c**, evaporation to dryness, followed by dissolution of the residue in hexane and crystallization, afforded a new monomeric and paramagnetic material formulated as $(AlEtCl_2)[(\eta^1\text{-}C_{12}H_8NN(Et)]$ **(3c)** (Scheme 35).

The structure of **3c** was yielded by X-ray diffraction (Figure 10) and consists of a phenazine molecule with one nitrogen connected to an $EtAlCl_2$ residue and the second alkylated by one ethyl group. The geometry around each nitrogen atom is trigonal planar and consistent with an $sp^2$ hybridization. The aluminum-nitrogen bond lengths in **3c** [Al(1)-N(1) = 1.962(3) Å] (Table 7), are significantly shorter than the Al-N distances in **1a** [2.144(4) Å and 2.147(4) Å] (Table 2) but comparable to those of **2c** [1.966(2) and 1.965(2) Å], also containing a radical form of the phenazine framework. The N-C bond lengths in **3c** are all in the same narrow range of [1.383(5) Å to 1.398(5) Å], suggesting delocalization of the $\pi$ electrons in the ligand.

**Figure 10**. X-ray Structure of complex $[AlEtCl_2]_2(\eta^1\text{-}C_{14}H_{13}N_2)$ (**3c**). Thermal ellipsoids are drawn at the 50% probability level.

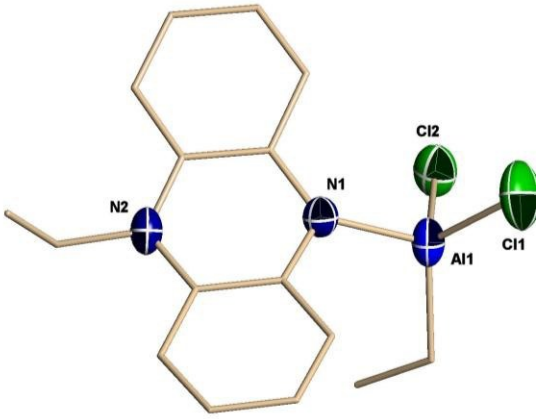


**Table 7**. Selected Bond Distances (Å) and Angles (°) for complex $[AlEtCl_2]_2(\eta^1\text{-}C_{14}H_{13}N_2)$ (**3c**).

| | | | |
|---|---|---|---|
| Al(1)-N(1) | 1.962(3) | N(1)-Al(1)-Cl(1) | 105.44(10) |
| Al(1)-Cl(1) | 2.1525(17) | N(1)-Al(1)-Cl(2) | 106.87(10) |
| Al(1)-Cl(2) | 2.1700(16) | Cl(1)-Al(1)-Cl(2) | 108.35(7) |
| Al(1)-C(13) | 1.955(5) | C(1)-N(1)-C(12)-C(7) | 20.4(4) |
| N(1)-C(1) | 1.391(4) | N(2)-C(6) | 1.383(5) |
| N(1)-C(12) | 1.395(4) | N(2)-C(7) | 1.398(5) |

The elemental analysis of **3c** was consistent with the proposed formulation. The connectivity clearly indicates that this species is an organic radical. Accordingly, **3c** is paramagnetic [$\mu_{eff}$ = 1.9 $\mu_{BM}$] with a proton NMR spectrum only showing broad and overlapping resonances.

**Figure 11**. Simulated (red) and experimental (black) EPR spectra of **3c**.

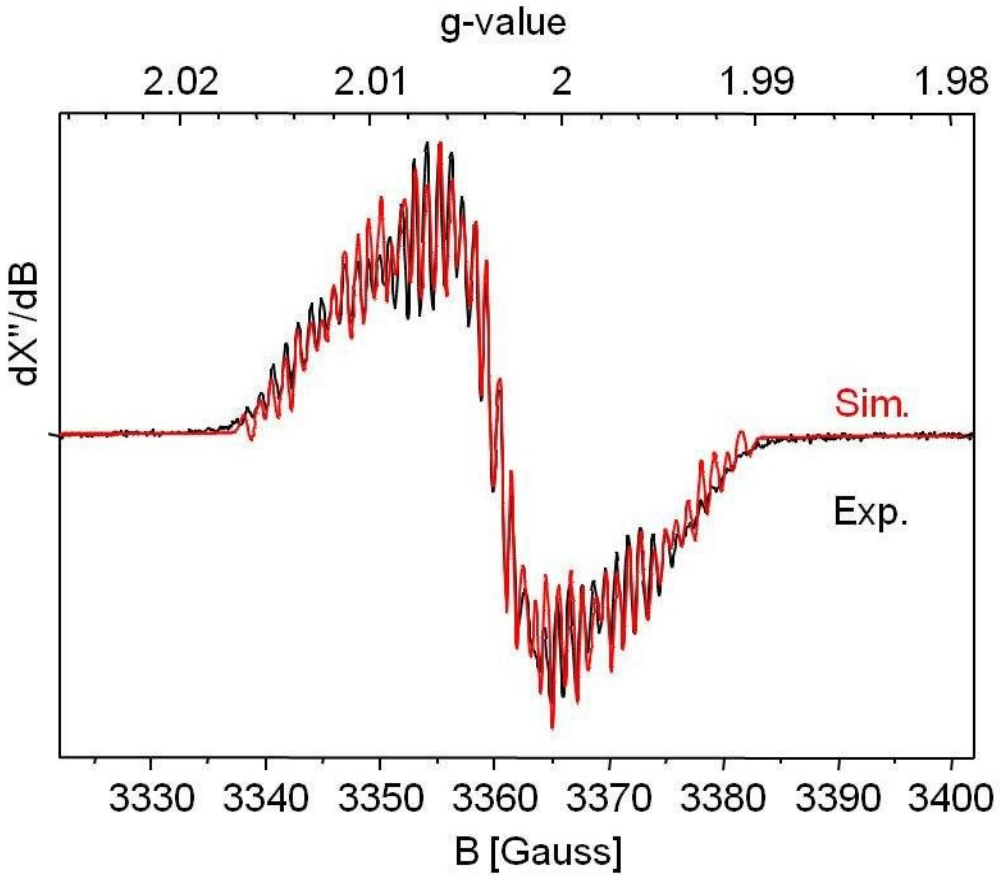


The EPR spectrum of **3c** shows the overall single wave feature expected for an organic radical. A satisfactory simulation of the experimental spectrum (Figure 11) was obtained using parameters consistent with delocalization of spin density over the aromatic rings. Through simulation of the experimental spectrum (Figure 11, Table 8) it is possible to derive the hyperfine couplings to aluminum ($A^{Al}$ = 8.54 MHz; I = 5/2), two non-equivalent nitrogen atoms ($A^{N1}$ = 14.16 MHz, $A^{N2}$ = 8.74 MHz; I = 1), and three different sets of hydrogens ($A^{H1}$ = 3.68 MHz, $A^{H3}$ = 6.85 MHz, $A^{H7}$ = 6.11 MHz; I = 1/2). Other hyperfine couplings were not resolved. The experimental data were in reasonable agreement with the DFT calculated EPR parameters of **3c** (see discussion below and Table 8). A satisfactory simulation was obtained, however the

analyzed solution most probably contained more than one paramagnetic compound leading to some deviations of simulated and experimentally observed EPR spectrum of **3c**.

**Table 8**. Experimental and DFT calculated EPR parameters for complex **3c**.

| | **Experiment** (spectral simulation) | **DFT** (b3-lyp, TZVP) | |
|---|---|---|---|
| **Isotropic g-value** | 2.0034 | *2.0033* | 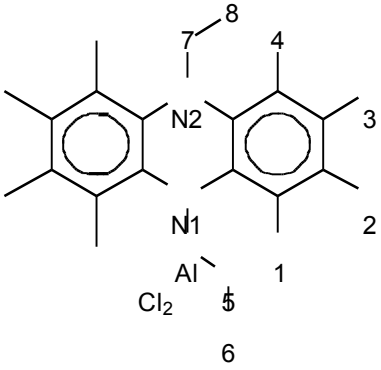 |
| **Hyperfine couplings (MHz)** [(a)] | | | |
| ***Nucleus*** | | | |
| *Al* | -8.535 | *-8.634* | |
| *N1* | 14.156 | *14.716* | |
| *N2* | 8.735 | *10.516* | |
| *H1* | -3.682 | *-5.239* | |
| *H3* | -6.854 | *-7.480* | |
| *H7* | 6.107 | *6.942* | |
| *H2* | *n.r.* | *-0.418* | |
| *H4* | *n.r.* | *+0.815* | |
| *H5* | *n.r.* | *0.410* | |
| *H6* | *n.r* | *0.844* | |
| *H8* | *n.r* | *-0.316* | |
| *Cl* | *n.r.* | *0.144* | |



[(a)] The signs of the experimental hyperfine couplings are taken identical to the DFT values. (b) The geometry of complex was optimized at the BP86 level, the EPR parameters were calculated at the b3-lyp, TZVP level (using the BP86 geometry).

**Figure 12**. Simulated (red) and experimental (black) EPR spectra of **3a**.

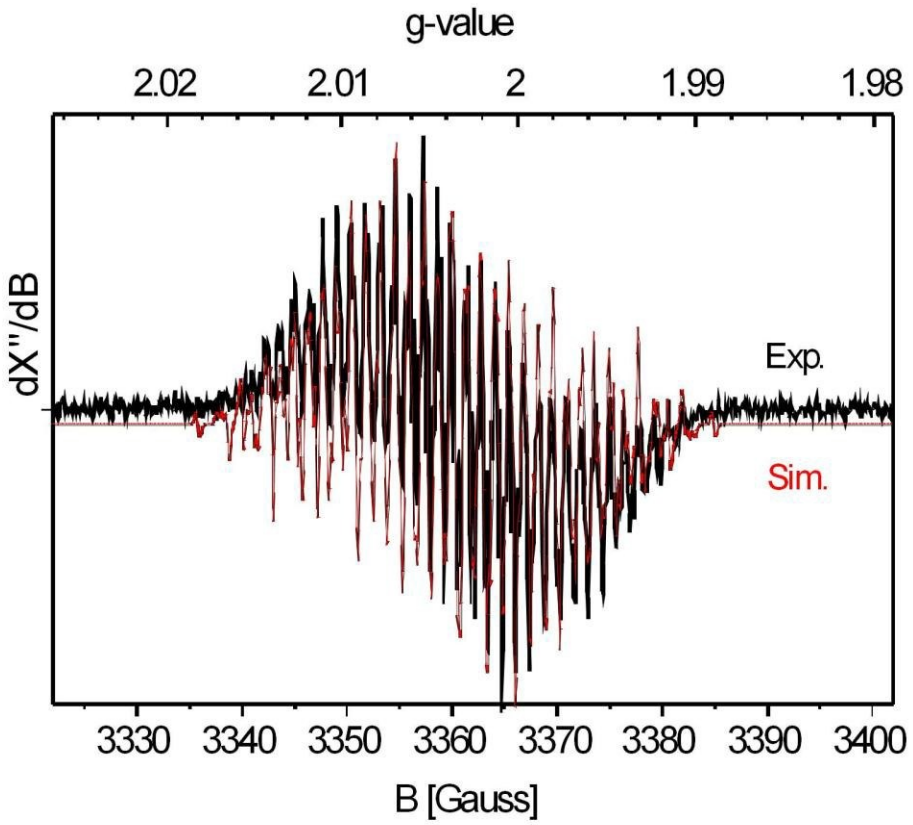


Complex **3c** appears to be indefinitely stable at room temperature under inert atmosphere. Crystalline **3c** did not change appearance by storing in a sealed ampoule over several months.

Similar complexes for the derivatives **a, b** and **d** could not be isolated due to high solubility in all solvents. Nonetheless, the supernatant solutions were always paramagnetic. For example, in the case of the reaction with $AlMe_3$, after separation of the diamagnetic **1a** and **2a** the solution displayed an ESR spectrum (Figure 12) that can be interpreted in terms of $(AlMe_3)[\eta^1\text{-}C_{12}H_8NN(Me)]$ (**3a**) (Figure 13).

**Figure 13**. Optimized geometry of **3a**.

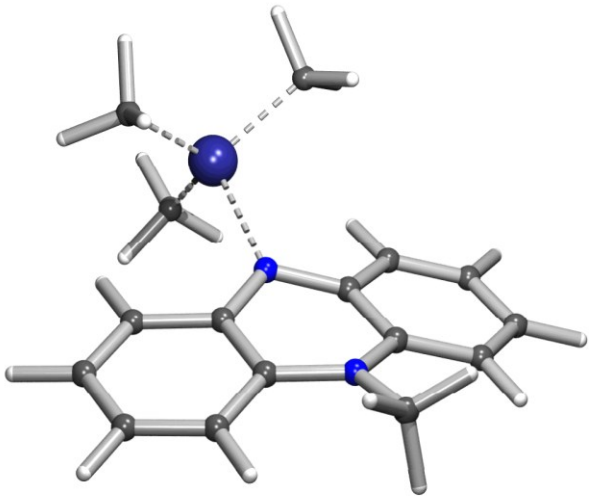

The solution EPR spectrum of **3a** at room temperature shows the complexity expected for an organic radical (Figure 12). A simulation of the experimental spectrum (Figure 12, Table 9) was obtained using parameters consistent with a substantial delocalization of the spin density over the aromatic rings with hyperfine couplings to aluminum ($A^{Al}$ = 5.45 MHz; I = 5/2), two non-equivalent nitrogen's ($A^{N1}$ = 15.17 MHz, $A^{N2}$ = 7.99 MHz; I = 1), two sets of two equivalent hydrogen's ($A^{H1}$ = 6.62 MHz, $A^{H3}$ = 7.70 MHz; I = 1/2) and a set of three equivalent hydrogen's ($A^{H7}$ = 11.80 MHz; I = 1/2).

The assignment of the hydrogen hyperfine couplings (Table 9) is based on the comparison with the DFT calculated EPR parameters for $(AlMe_3)[\eta^1\text{-}C_{12}H_8N_2(Me)]$ (**3a**), and whose structure was optimized by the DFT calculations (Figure 13). The DFT calculated values are in good agreement with the spectral simulation data (Table 9).

**Table 9**. Experimental and DFT calculated EPR parameters of **3a**.

| | **Experimental** (spectral simulation) | **DFT** (b3-lyp, TZVP) | |
|---|---|---|---|
| **Isotropic g-value** | 2.0034 | *2.0032* | 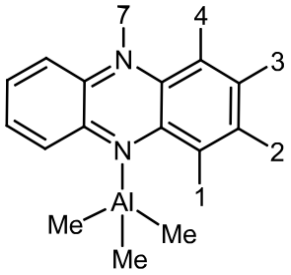 |
| **Hyperfine couplings (MHz)** [(a)] | | | |
| ***Nucleus*** | | | |
| *Al* | -5.45 | *-5.90* | |
| *N1* | 15.17 | *15.41* | |
| *N2* | 7.99 | *9.52* | |
| *H1 (2 eq. H)* | -6.62 | *-6.38* | |
| *H3 (2 eq. H)* | -7.70 | *-8.23* | |
| *H7 (3 eq. H)* | 11.80 | *12.82* | |
| *H2 (2 eq. H)* | *n.r.* | *0.49* | |
| *H4 (2 eq. H)* | *n.r.* | *1.13* | |
| *Al-Me (9 eq. H)* | *n.r* | *<1* | |



[(a)] The signs of the exp. hyperfine couplings are taken identical to the DFT values.

It is clear that at some point in the formation of products **2** and **3**, Al-C bonds have to be cleaved in a homolytic fashion. Bidentate and tridentate imine/pyridine type donors can strongly decrease the energy cost of homolysis of metal-alkyl bonds, by stabilizing the resulting low-valent metal complex through acceptance of the unpaired electron in a low-lying ligand-centered π* orbital (non-innocent behaviour).[15b] In the present case, one could at a first glance expect the phenazine ligand with its extended π-system to play the same role. However, DFT results indicate that the stabilization induced by phenazine is not nearly enough to allow Al-C bond homolysis under normal conditions. The Al-C dissociation free energy is substantially reduced, from about 70 kcal/mol in $AlMe_3$ to about 33 kcal/mol in $(AlMe_3)[\eta^1\text{-}C_{12}H_8N_2]$, but it remains too high for a room temperature reaction. However, the mono-N-alkylated radical ligand $C_{12}H_8N_2(Me)$ turns out to be more effective at promoting hemolysis by reducing the Al-Me bond

strength by a further 11 kcal/mol. Based on this observation, we propose the chain mechanism shown in Scheme 36 to account for the observed chemistry. [16]

**Scheme 36**.

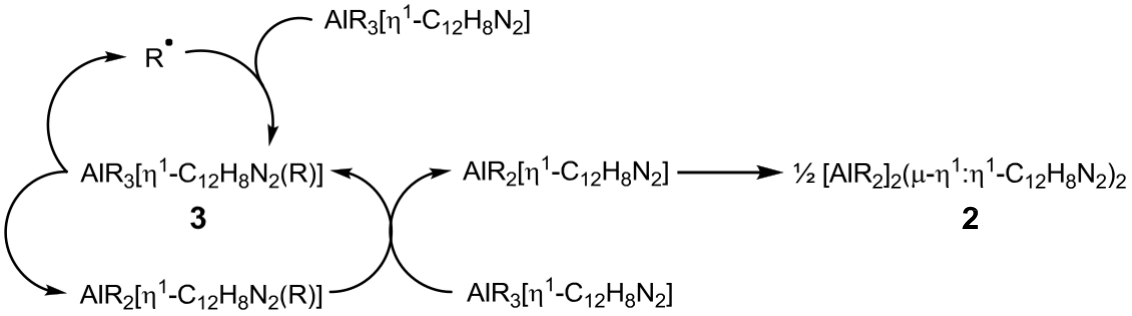


We have only located the intermediates in this cycle, not any of the presumed transition states, so the mechanism must remain somewhat speculative for now. The crucial intermediate is $AlR_3[\eta^1\text{-}C_{12}H_8N_2(R)]$ (**3**). [17] This can undergo Al-C bond homolysis (as noted above) to in turn produce an alkyl radical R and $AlR_2[\eta^1\text{-}C_{12}H_8N_2(R)]$. The alkyl radical attacks $AlR_3[\eta^1\text{-}C_{12}H_8N_2]$ in a highly exergonic step, regenerating **3**. [18] The diamagnetic $AlR_2[\eta^1\text{-}C_{12}H_8N_2(R)]$ can react with an equivalent of $AlR_3[\eta^1\text{-}C_{12}H_8N_2]$ to give $AlR_2[\eta^1\text{-}C_{12}H_8N_2]$ and regenerate **3**. [19] This step is endergonic by about 10 kcal/mol, but will easily go to completion because of the rather exergonic subsequent dimerization of $AlR_2[\eta^1\text{-}C_{12}H_8N_2]$ to **2** (about 15 kcal per mole of monomer).

In order to obtain a clearer picture of the roles of the ligand (phenazine) and Al alkyls, we compared (by DFT) the reactivities of phenazine (Phen) and pyrazine (Pz), in combination with the Al alkyls $AlMe_3$, $AlEt_3$ and $AlEt_2Cl$; relevant data are collected in Table 10. Homolysis of

the Al-Et bond is easier than of the Al-Me bond by about 10 kcal/mol. This means that if $AlMe_3$ needs the assistance of Phen(Me) to undergo homolysis, $AlEt_3$ could conceivably already undergo homolysis with Phen itself. However, ligand-assisted homolysis is much less efficient for $AlEt_2Cl$, so that Phen(Et) assistance would again be required for this alkyl. $AlEt_3$ is a slightly weaker Lewis acid than $AlMe_3$ (for both steric and electronic reasons), but $AlEt_2Cl$ is a somewhat stronger Lewis acid. Pz is a stronger Lewis base than Phen by about 10 kcal/mol. Alkylation at N increases the ligand basicity, by about 3 kcal/mol for Phen and 8 kcal/mol for Pz.

**Table 10**. Calculated reaction free energies (kcal/mol) for steps in Scheme 36 and related reactions.[a]

| Reaction | L = Acr | | | L = Pz | | |
|---|---|---|---|---|---|---|
| | $Me_3Al$ | $Et_3Al$ | $Et_2AlCl$ | $Me_3Al$ | $Et_3Al$ | $Et_2AlCl$ |
| Radical Chain Mechanism Steps | | | | | | |
| $R + LAlR_3 \rightarrow RLAlR_3$ | -25.56 | -20.49 | -21.47 | -18.07 | -15.94 | -16.80 |
| $RLAlR_3 \rightarrow RLAlR_2 + R$ | 21.88 | 12.00 | 19.85 | 39.36 | 31.28 | 39.29 |
| $RLAlR_2 + LAlR_3 \rightarrow RLAlR_3 + LAlR_2$ | 11.37 | 9.38 | 10.35 | 12.06 | 11.11 | 11.16 |
| $LAlR_2 \rightarrow ½ [LAlR_2]_2$ | -13.52 | -15.51 | -17.67 | -22.98 | -23.90 | -28.08 |
| Comparison: Al-R Homolysis | | | | | | |
| $AlR_3 \rightarrow AlR_2 + R$ | 70.75 | 59.83 | 59.79 | 70.75 | 59.83 | 59.79 |
| $LAlR_3 \rightarrow LAlR_2 + R$ | 33.25 | 21.38 | 30.20 | 51.43 | 42.39 | 50.45 |
| $R_3AlLAlR_3 \rightarrow R_3AlLAlR_2 + R$ | 24.99 | 14.74 | 22.44 | 40.59 | 0.00 | 37.55 |
| Comparison: Complexation Energies | | | | | | |
| $L + AlR_3 \rightarrow LAlR_3$ | 0.96 | 2.42 | -2.18 | -8.29 | -7.53 | -12.74 |
| $R_3AlL + AlR_3 \rightarrow R_3AlLAlR_3$ | 4.72 | 5.60 | 1.74 | -4.76 | -3.75 | -8.15 |
| $RL + AlR_3 \rightarrow RLAlR_3$ | -2.91 | -0.09 | -5.67 | -15.58 | -15.64 | -21.71 |

[a] Calculated for gas phase, 273K, entropies scaled by 0.67 to reflect decreased freedom of particles in solution.

Conversely, coordination of an $AlR_3$ unit at one nitrogen decreases the basicity of the other nitrogen, by about 4 kcal/mol for both ligands. The Pz ligand and its N-alkylated radical derivative are much less effective than their Phen analogs (by about 20 kcal/mol) at promoting

Al-C bond homolysis because the resulting ligand-centered electron is not as efficiently stabilized in a ligand π* orbital. As a result, calculations predict the cycle shown in Scheme 36 would not be possible with pyrazine, even though formation of the final product $[AlR_2]_2(\mu{-}\eta^1{:}\eta^1\text{-}C_4H_4N_2)_2$ would be about as favourable as its phenazine analog. Due to the less extensively delocalized π-system of pyrazine, AF coupling between the two halves of the molecule in $[AlR_2]_2(\mu{-}\eta^1{:}\eta^1\text{-}C_4H_4N_2)_2$ is much stronger than in $[AlR_2]_2(\mu{-}\eta^1{:}\eta^1\text{-}C_{12}H_8N_2)_2$, as indicated by the lower $S^2$ values of < 0.05.

In conclusion we have herein reported an unprecedented behaviour of phenazine as a non-innocent ligand in terms of promoting radical cleavage with formation of a stable organic radical. This behaviour is certainly established in the case of transition metals and lanthanides where the drive for the formation of the radical is usually provided by either reducing conditions or instability of a certain metal valence state. In the present case instead, it is the tendency to form stable radicals, which actually promotes this unique case of radical cleavage of a fairly stable Al-C bond. In turn, this might have interesting implications for inducing radical bond cleavage on other more interesting target molecules such as water where hydrogen atom abstraction would eventually lead to the formation of oxygen gas.

## *Experimental Section*

All manipulations were performed under the nitrogen atmosphere with rigorous exclusion of oxygen and water using standard Schlenk and glove-box techniques. Hexane and toluene were purified by passing through the activated $Al_2O_3$ column and deoxygenated prior to use by several

vacuum/nitrogen purges. Benzene-$d^6$ was obtained from "C/D/N isotopes", dried over freshly activated molecular sieves (4A) for 10 days and distilled under $N_2$ atmosphere. $AlMe_3$, $AlEt_3$, $Al^iBu_3$, $AlEt_2Cl$ were purchased from Aldrich and used as received. The ligand phenazine was purchased from Aldrich and used as received. Magnetic susceptibility measurements were performed at room temperature using a Johnson Matthey Gouy balance and corrected to diamagnetism. NMR spectra were recorded on a Bruker AVANCE 300 spectrometer. The analyzed solution was placed in the NMR tubes inside a glove-box and the NMR tube flame sealed under the nitrogen atmosphere. Elemental Analysis was performed using a Perking-Elmer Series II CHN/O 2400 analyser. The EPR measurements were performed with a JEOL FA-100 X-Band EPR spectrometer (Jeol USA, Peabody, MA). The samples were run in a 0.3 mm fused quartz flat cell (Jeol Co.), at room temperature, and in the absence of oxygen.

**Synthesis of $[AlMe_3]_2(\mu\text{-}\eta^1\text{:}\eta^1\text{-}C_{12}H_8N_2)$ (1a)**

Slow addition of a cold solution (- 30 ºC) of phenazine (181 mg, 1 mmol) in toluene (10 mL) to solution of $AlMe_3$ (144 mg, 2 mmol) also in the same solvent (5 mL) afforded immediate color change from orange to red. The resulting clear solution was immediately concentrated in vacuo and left undisturbed at -35$^o$C for one day, affording red crystals of **1a** (239 mg, 0.74 mmol, 74 %). Anal. Calcd. (found) for $C_{18}H_{26}Al_2N_2$: C 66.63 (66.59); H 8.08 (7.97); N 8.64 (8.61). $^1$H NMR ($C_6D_6$,): δ 8.5 (m, 4H, Ar-*H*), 7.0 (m, 4H, Ar-*H*), -0.3 (s, 18H, C*H*$_3$). $^{13}$C NMR ($C_6D_6$,): δ 141.8 (Ar *C*), 131.3 (Ar *C*H), 127.5 (Ar *C*H), -5 (*C*H$_3$ ).

**Preparation of $[AlMe_2]_2(\mu\text{-}\eta^1\text{:}\eta^1\text{-}C_{12}H_8N_2)_2$ (2a)**

A solution of phenazine (181 mg, 1 mmol) in toluene (10 mL) was slowly added to a stirred solution of $AlMe_3$ (144 mg, 2 mmol) in the same solvent (5 mL) and at room temperature. An immediate color change of the solution from orange to red was observed which slowly turned green during 1 h of stirring. The reaction mixture was stirred for further 24 hours at room temperature. The resulting mixture was centrifuged, and the clear surnatant concentrated to small volume in vacuo and left undisturbed at -35$^{o}$C. Green crystals of **2a** deposited upon standing for 24 hours at -35.0 ˚C (251 mg, 0.53 mmol, 53 %). Anal, calcd (found) for $C_{28}H_{28}Al_2N_4$: C 70.86 (70. 78); H 5.95 (5.89); N 11.81 (11.75). $^{1}$H NMR ($C_6D_6$): δ 6.4 (m, 8H, Ar-*H*), 7.1 (m, 8H, Ar-*H*), 0.3 (s, 12H, C*H*$_3$). $^{13}$C NMR ($C_6D_6$): δ 140.5 (Ar *C*), 125.5 (Ar *C*H), 124.0 (Ar *C*H), 1.0 (*C*H$_3$).

**Preparation of $[AlEt_2]_2(\mu\text{-}\eta^1\text{:}\eta^1\text{-}C_{12}H_8N_2)_2$ (2b)**

A solution of phenazine (181 mg, 1 mmol) in toluene (10 mL) was slowly added to a solution of $AlEt_3$ (228 mg, 2 mmol) in the same solvent (5 mL) at room temperature. An immediate color change from orange to red, slowly turning to green, was observed. The reaction mixture was stirred for 24 hours at room temperature and then centrifuged. The clear surnatant was concentrated in vacuuo and left undisturbed at -35$^{o}$ C. An oily material deposited during 24 hours at -35.0 ˚C which was separated, washed with hexanes (2 x 5 ml) and redissolved in toluene (1 mL). The resulting toluene solution was left undisturbed at -35$^{o}$ C overnight. Green crystals of **2b** appeared on the next day which were separated, washed with hexane and dried in vacuo (302 mg, 0.57 mmol, 57 %). Anal, calcd (found) for $C_{32}H_{36}Al_2N_4$: C 72.42 (72.35); H 6.84 (6.78); N

10.56 (10.49). $^{1}$H NMR ($C_6D_6$): δ 6.5 (m, 8H, Ar-*H*), 6.9 (m, 8H, Ar-*H*), 0.2 (q, 8H, C*H*$_2$), 1.1 (t, 12H, C*H*$_3$). $^{13}$C NMR ($C_6D_6$): δ 140.5 (Ar *C*), 125.5 (Ar *C*H), 123.5 (Ar *C*H), 8 (*C*H$_3$), 0.5 (*C*H$_2$).

**Preparation of $[AlEt_{1.6}Cl_{0.4}]_2(\mu\text{-}\eta^1\text{:}\eta^1\text{-}C_{12}H_8N_2)_2$ (2c) and $[AlEtCl_2]_2(\eta^1\text{-}C_{14}H_{13}N_2)$ (3c)**

A solution of phenazine (181 mg, 1 mmol) in toluene (10 mL) was slowly added to a solution of $AlEt_2Cl$ (242 mg, 2 mmol) in the same solvent (5 mL) and at room temperature. An immediate color change from orange to red and eventually to green was observed. The reaction mixture was stirred for 24 hours at room temperature, evaporated to dryness and the residual oil dissolved in hexane (10 mL) leading to a precipitation of a dark green solid while standing for 20 minutes at room temperature. The suspension was centrifuged, the clear solution separated from the solid, transferred to another vial (A). The solid was dissolved in toluene (5 mL) and allowed to stand for 24 hours at -35$^{o}$ C. The green crystalline **2c** separated and which was isolated, washed with hexane, dried in vacuo and characterized (210 mg, 0.4 mmol, 40%). The original mother liquor (A) was evaporated to dryness and the residue redisolved in hexane. Upon standing for 3 days at -35$^{o}$ C purple crystals of **3c** separated (**3c** 105 mg, 0.3 mmol, 31 %).

**2c:** Anal. Calcd. (found) for $C_{30.40}H_{32}Al_2Cl_{0.80}N_4$: C 68.09 (67.78); H 5.97 (5.77); N 10.45 (10.25). $^{1}$H NMR ($C_6D_6$): ä 6.5 (m, 8H, Ar-*H*), 6.9 (m, 8H, Ar-*H*), 0.1 (q, 4H, C*H*$_2$), 1.5 (t, 6H, C*H*$_3$). $^{13}$C NMR ($C_6D_6$,): ä 140.5 (Ar *C*), 125.5 (Ar *C*H), 123.5 (Ar *C*H), 9.0 (*C*H$_3$ ), 1.1 (*C*H$_2$)

**3c:** Anal. Calcd. (found) for $C_{16}H_{18}AlCl_2N_2$: C 57.14 (57.01); H 5.40 (5.31); N 8.33 (8.21) $\mu_{eff}$ = 1.9 $\mu_{BM}$.

**Preparation of $[Al^{i}Bu_2]_2(\mu\text{-}\eta^1\text{:}\eta^1\text{-}C_{12}H_8N_2)_2$ (2d)**

A solution of phenazine (181 mg, 1 mmol) in toluene (10 mL) was slowly added to a solution of $Al^{i}Bu_3$ (400 mg, 2 mmol) in the same solvent (5 mL) and at room temperature. An immediate color change from orange to red, slowly turning green was observed. The reaction mixture was stirred for 24 hours at room temperature and the resulting solution centrifuged. The clear surnatant was concentrated *in vacuo* and left undisturbed at -35° C for 24 hours. Some oily material further separated from the toluene solution which was washed with hexanes (2 x 5 ml), dried and re-dissolved in toluene (1 mL). Upon standing at -35° C for several days, the resulting solution separated green crystals of **2d** contaminated by some residual oil. All attempts to purify the crystalline mass failed and therefore, compound **2d** was characterized exclusively by its X-ray structure.

**Computational**

All calculations used the program Turbomole [20] in combination with the external Baker optimizer.[21] All geometries were fully optimized at the b3-lyp [14]/TZVP [22] level. Vibrational analyses (analytical second derivatives) were carried out to check the nature of all minima (no imaginary frequencies), and to calculate thermal corrections (enthalpy and entropy, gas phase, 273K 1 bar). Since the calculations were not intended to model any specific experiment, no solvent corrections were applied, but entropies were scaled by a factor of 0.67 to represent the effect of reduced freedom in solution.[23]

**Crystal Structure Data**

Appropriate single crystals of compounds were selected under the microscope and mounted on a thin, glass fiber with parathone oil, and cooled to the data collection temperature. X-ray data were collected on a Bruker AXS SMART 1k CCD diffractometer at 200(2) K, equipped with graphite-monochromated Mo-$K_\alpha$ radiation ($\lambda$ = 71.073 pm). Initial unit-cell parameters were determined from 60 data frames collected at different sections of the Ewald sphere. The intensity data were corrected for Lorentz and polarization effects; the data were integrated with SAINT,[24] and an empirical absorption (SADABS) was applied.[25] The structures were solved by direct methods (SHELXS-97)[26] and refined by full-matrix least-squares methods against $F^2$ (SHELXL-97). [27] All non-hydrogen-atoms were refined with anisotropic displacement parameters. The hydrogen atoms were refined isotropically on calculated positions.

**Crystals of $C_{18}H_{26}Al_2N_2$ (1a)** were grown from a toluene. The crystal data and refinement parameters for complex **1a** can be found in Table 11, and interatomic distances and angles are listed in Table 2. The reflection data were consistent with a monoclinic system, space group *P*2(1)/*n*. The largest residual electron density peak (0.280 e/Å$^3$) was associated with the N1 atom. Full-matrix least-squares refinement on $F^2$ gave $R_1$ = 0.0649 and $wR_2$ = 0.1532 at convergence.

**Crystals of $C_{28}H_{28}Al_2N_4$ (2a)** were grown from a toluene. The crystal data and refinement parameters for complex **2a** can be found in Table 11, and interatomic distances and angles are listed in Table 3. The reflection data were consistent with a monoclinic system, space group *P*2(1)/*n*. The largest residual electron density peak (0.282 e/Å$^3$) was associated with the N1

atom. Full-matrix least-squares refinement on $F^2$ gave $R_1$ = 0.0665 and $wR_2$ = 0.1358 at convergence.

**Crystals of $C_{32}H_{36}Al_2N_4$ (2b)** were grown from a toluene. The crystal data and refinement parameters for complex **2b** can be found in Table 11, and interatomic distances and angles are listed in **Error! Reference source not found.**. The reflection data were consistent with a monoclinic system, space group *P*2(1)/*n*. The largest residual electron density peak (0.307 e/Å$^3$) was associated with the N1 atom. Full-matrix least-squares refinement on $F^2$ gave $R_1$ = 0.0675 and $wR_2$ = 0.1388 at convergence.

**Crystals of $C_{30.4}H_{32}Al_2Cl_{0.8}N_4$ (2c)** were grown from a toluene. The crystal data and refinement parameters for complex **2c** can be found in Table 12, and interatomic distances and angles are listed in Table 5. The reflection data were consistent with a monoclinic system, space group *P*2(1)/*n*. The largest residual electron density peak (0.257 e/Å$^3$) was associated with the N1 atom. Full-matrix least-squares refinement on $F^2$ gave $R_1$ = 0.0464 and $wR_2$ = 0.1332 at convergence. The resolved occupancy of clorine in **2c** is 0.8, the chlorine atom is disordered over 4 positions with the equal occupancies 0.2.

**Crystals of $C_{40}H_{52}Al_2N_4$ (2d)** were grown from a toluene. The crystal data and refinement parameters for complex **2d** can be found in Table 12, and interatomic distances and angles are listed in Table 6. The reflection data were consistent with a triclinic system, space group *P*-1. The largest residual electron density peak (0.54 e/Å$^3$) was associated with the Al1-C13 bond. Full-matrix least-squares refinement on $F^2$ gave R1 = 0.0641, wR2 = 0.1504 at convergence.

**Crystals of $C_{16}H_{18}AlCl_2N_2$ (3c)** were grown from a hexane. The crystal data and refinement parameters for complex **3c** can be found in Table 12, and interatomic distances and angles are listed in Table 7. The reflection data were consistent with a triclinic system, space group *P*-1. The largest residual electron density peak (0.355 e/Å$^3$) was associated with the N1 atom. Full-matrix least-squares refinement on $F^2$ gave $R_1 = 0.0639$ and $wR_2 = 0.1790$ at convergence.

**Table 11**. Crystal Data and Refinement Parameters for Complexes **1a** and **2a**, **2b**.

| | **Complex 1a** | **Complex 2a** | **Complex 2b** |
|---|---|---|---|
| Empirical Formula | $C_{18}H_{26}Al_2N_2$ | $C_{28}H_{28}Al_2N_4$ | $C_{32}H_{36}Al_2N_4$ |
| Formula Weight | 324.37 | 474.5 | 530.61 |
| Temperature | 203(2) K | 203(2) K | 200(2)K |
| Wavelength | 0.71073 Å | 0.71073 Å | 0.71073 Å |
| Crystal System | Monoclinic | Monoclinic | Monoclinic |
| Space Group | P2(1)/n | P2(1)/n | P2(1)/n |
| Unit cell Dimensions | a = 10.733(3) Å<br>b = 10.852(3) Å<br>c = 16.540(4) Å<br>α = 90°<br>β= 92.356(4)°<br>γ = 90° | a = 10.145(2) Å<br>b = 14.288(3) Å<br>c = 16.740(4) Å<br>α= 90°.<br>β= 96.505(3)°.<br>γ = 90° | a = 7.678(2) Å<br>b = 17.964(5) Å<br>c = 10.542(3) Å<br>α =90°<br>β= 105.842(5)°<br>γ=90° |
| Volume | 1924.7(8) Å$^3$ | 2411.0(9) Å$^3$ | 1398.9(7) Å$^3$ |
| Z | 4 | 4 | 2 |
| Density (calculated) | 1.119 Mg/m$^3$ | 1.307Mg/m$^3$ | 1.260Mg/m$^3$ |

| | | | |
|---|---|---|---|
| Absorption Coefficient | 0.150 $mm^{-1}$ | 0.145 $mm^{-1}$ | 0.133 $mm^{-1}$ |
| F(000) | 696 | 1000 | 564 |
| Crystal Size $mm^3$ | 0.25 x 0.20 x 0.10 | 0.10 x 0.01 x 0.01 | 0.23 x 011 x 0.10 |
| Theta Range for Data Collection | 2.22 to 23.25° | 1.88 to 24.75° | 2.27 to 24.75° |
| Index Ranges (h,k,l) | ±11, ±12, ±18 | ±11, ±16, ±19 | ±9, ±21, ±12 |
| Reflections Collected/Independent | 10426/2730 | 16809/4060 | 8238/2041 |
| R(int) | 0.0958 | 0.0677 | 0.0835 |
| Completeness to theta = | 23.25° =99.2% | 24.75° =98.3% | 24.75° = 85.5% |
| Max. and Min. Transmission | 0.9535 and 0.9072 | 0.9985 and 0.9856 | 0.9869 and 0.9702 |
| Data/Restraints/ Parameters | 2730 / 0 / 199 | 4060 / 0 / 308 | 2041 / 0 / 172 |
| Goodness-of-Fit on $F^2$ | 1.012 | 1.055 | 1.048 |
| Final R indices [I>2sigma(I)] | R1 =0.0649, wR2 = 0.1523 | R1 = 0.0665, wR2 = 0.1358 | R1 = 0.0675, wR2 = 0.1388 |
| R indices (all data) | R1 = 1137, wR2 = 0.1754 | R1 = 0.1164, wR2 = 0.1621 | R1 = 0.1216, wR2 = 0.1624 |
| Largest Diff. Peak and Hole | 0.329 and -0.280 e. $Å^{-3}$ | 0.282 and -0.341 e.$Å^{-3}$ | 0.307 and -0.210e.$Å^{-3}$ |

**Table 12**. Crystal Data and Refinement Parameters for Complexes **2c**, **2d** and **3c**.

| | **Complex 2c** | **Complex 2d** | **Complex 3c** |
|---|---|---|---|
| Empirical Formula | $C_{30.4}H_{32}Al_2Cl_{0.8}N_4$ | $C_{40}H_{52}Al_2N_4$ | $C_{16}H_{18}AlCl_2N_2$ |
| Formula Weight | 535.72 | 642.82 | 336.03 |

| Temperature | 203(2) K | 204(2) K | 204(2) K |
|---|---|---|---|
| Wavelength | 0.71073 Å | 0.71073 Å | 0.71073 Å |
| Crystal System | Monoclinic | Triclinic | Triclinic |
| Space Group | P2(1)/n | P-1 | P-1 |
| Unit cell Dimensions | a = 7.6232(19) Å<br>b = 17.799(4) Å<br>c = 10.503(3)Å<br>$\alpha$ = 90°.<br>$\beta$ = 105.121(3)°<br>$\gamma$ = 90° | a = 7.178(2) Å<br>b = 10.154(3)Å<br>c = 13.112(4) Å<br>$\alpha$ = 78.495(5)°<br>$\beta$ = 83.990(5) °<br>$\gamma$ = 75.003(5)° | a = 8.232(4) Å<br>b = 9.890(4) Å<br>c = 13.016(6) Å<br>$\alpha$ = 101.478(6)°.<br>$\beta$ = 100.553(3)°<br>$\gamma$ = 103.099° |
| Volume | 1375.8 (3) $Å^3$ | 903.2(5)$Å^3$ | 982.1 (7) $Å^3$ |
| Z | 2 | 1 | 2 |
| Density (calculated) | 1.293 $Mg/m^3$ | 1.182 $Mg/m^3$ | 1.293 $Mg/m^3$ |
| Absorption Coefficient | 0.211 $mm^{-1}$ | 0.114 $mm^{-1}$ | 0.379 $mm^{-1}$ |
| F(000) | 564 | 346 | 400 |
| Crystal Size ($mm^3$) | 0.90 x 0.90 x 0.40 | 0.50 x 0.50 x 0.40 | 0.70 x 0.70 x 0.40 |
| Index Ranges (h,k,l) | ±8, ±20, ±12 | ±8, ±11, ±14 | ±9, ±11, ±15 |
| Reflections Collected/Independent | 7493 / 2274 | 6122 / 2726 | 7144/2976 |
| R(int) | 0.0383 | 0.0523 | 0.0388 |
| Completeness to theta = | 24.73° =97.0% | 23.81° = 98.1 % | 24.72° = 88;4% |
| Max. and Min. Transmission | 0.9205 and 0.8331 | 0.9559 and 0.9452 | 0.9954 and 0.9909 |
| Data/Restraints/ Parameters | 2274 / 3 / 178 | 2726 / 0 / 208 | 2976 / 0 / 241 |
| Goodness-of-Fit on $F^2$ | 1.060 | 1.020 | 1.036 |
| Final R indices [I>2sigma(I)] | R1 =0.056, wR2 = 0.1257 | R1 = 0.0641, wR2 = 0.1504 | R1 = 0.0639, wR2 = 0.1790 |

| | | | |
|---|---|---|---|
| R indices (all data) | R1 = 0.0566, wR2 = 0.1327 | R1 = 0.1030, wR2 = 0.2110 | R1 = 0.0965, wR2 = 0.2053 |
| Largest Diff. Peak and Hole | 0.280 and -0.230 e. $Å^{-3}$ | 0.537 and -0.260 e. $Å^{-3}$ | 0.355 and -0.300 e. $Å^{-3}$ |

## References


[1] Heunisch, G. W. *Anal. Chem*., **1972**, *44*, 741.

[2] Kaim, W. *J. Am. Chem. Soc*. **1984**, *106*, 1712.

[3] Scott, J.; Gambarotta, S.; Korobkov, I.; Knijnenburg, Q.; de Bruin, B.; Budzelaar, P. H. M. *J. Am. Chem. Soc.* **2005**, *127*, 17204.

[4] (a) Foxon, S. P.; Green, C.; Walker, M. G.; Wragg, A.; Adams, H.; Weinstein, J. A.; Parker, S. C.; Meijer, A. J. H. M.; Thomas, J. A. *Inorg. Chem*. **2012**, *51*, 463. (b) Banerjee, P.; Mostafa, G.; Castiñeiras, A.; Goswami, S. *J. Eur. Inorg. Chem*. **2007**, 412. (c) Tschierlei, S.; Karnahl, M.; Presselt, M.; Dietzek, B.; Guthmuller, J.; Gonzalez, L.; Schmitt, M.; Rau, S.; Popp, J. *Angew. Chem. Int. Ed.* **2010**, *49*, 3981. (d) Yang, X.; Hall, M. B. *J. Am. Chem. Soc.* **2010**, *132*, 120. (e) Rau, S.; Schwalbe, M.; Losse, S.; Görls, H.; McAlister, C.; Vos, J. G. *Eur. J. Inorg. Chem.* **2008**, 1031. (f) Hartshorn, R. M.; Barton, J. K. *J. Am. Chem. Soc.,* **1992**, *114,* 5919. (g) Sullivan, B. P.; Salmon, D. J.; Meyer, T. J. *Inorg. Chem.* **1978**, *17*, 3334. (h) Collin, J. P.; Sauvage, J. P. *Inorg. Chem.* **1986**, *25*, 135.

[5] Stender, M.; Eichler, B. E.; Hardman, N. J.; Power, P. P.; Prust, J.; Noltemeyer, M.; Roesky, H. W. *Inorg. Chem.* **2001**, *40*, 2794.

[6] Qian, B.; Ward, D.L.; Smith III, M.R. *Organometallics* **1998**, *17*, 3070.

[7] Waezsada, S. D.; Liu, F.-Q.; Murphy, E. F.; Roesky, H. W.; Teichert, M.; Usón, I.; Schmidt, H.-G.; Albers, T.; Parisini, E.; Noltemeyer, M. *Organometallics* **1997**, *16*, 1260.

[8] Schiefer, M.; Hatop, H.; Roesky, H.W.; Schmidt, H.-G.; Noltemeyer, M. *Organometallics* **2002**, *21*, 1300.

[9] Junk, P. C.; Raston, C. L.; Skelton, B. W.; White, A. H. *Chem. Comm*. **1987**, 1162.

[10] Scholz, J.; Scholz, A.; Weimann, R.; Janiak, C.; Schumann, H. *Angew. Chem., Int. Ed*. **1994**, *33*, 1171.

[11] MacDonald, M. R.; Ziller, J. W.; Evans, W. J. *Inorg. Chem*. **2011**, *50*, 4092.

[12] Sakurada, Y.; Huggins, M. L.; Anderson, Jr. W. R. *J. Phys. Chem*. **1964**, *65*, 1934.

[13] Petrakis, L.; Dickson, F. E. *Appl. Spectroscopy Rev*. **1970**, *4*, 1.

[14] (a) Becke, A. D. *J. Chem. Phys*. **1993**, *98*, 5648; (b) Becke, A. D. *J. Chem. Phys*. **1993**, *98*, 1372; (c) Lee, C. T.; Yang, W. T.; Parr, R. G. *Phys. Rev. B* **1988**, *37*, 785. (d) All calculations were performed using the Turbomole functionals "b3-lyp" and "b-p", which are similar but not identical to the Gaussian "B3LYP" and "BP86" functionals

[15] (a) Zhu, D.; Budzelaar, P. H. M. *Organometallics* **2010**, *29*, 5759; (b) Budzelaar, P. H. M. *Eur. J. Inorg. Chem*. **2012**, 530.

[16] A number of variations of this scheme are conceivable, involving additional coordination and dissociation of $AlR_3$ at various stages. The scheme discussed in the text is the simplest variation we believe to be capable of explaining the observed chemistry.

[17] An initial trace amount of radicals R is needed to start the cycle by combining with PhenazineAl$R_3$ to give (R)PhenazineAl$R_3$.

[18] It is also conceivable that instead of generating a true free radical R the intermediate (R)Phenazine Al$R_3$ directly transfers an Al-bound R group to the free nitrogen of PhenazineAl$R_3$. Transition state searches for such a transfer have so far been unsuccessful due to the extreme flexibility of the dinuclear presumed transition states, but constrained optimizations suggest the barrier for the transfer would not be high.

[19] This is a net alkyl radical transfer. It should be rather easy since the Al atom in (R)PhenazineAlR$_2$ is coordinatively unsaturated.

[20] (a) Ahlrichs, R.; Bär, M.; Baron, H.-P.; Bauernschmitt, R.; Böcker, S.; Ehrig, M.; Eichkorn, K.; Elliott, S.; Furche, F.; Haase, F.; Häser, M.; Hättig, C.; Horn, H.; Huber, C.; Huniar, U.; Kattannek, M.; Köhn, A.; Kölmel, C.; Kollwitz, M.; May, K.; Ochsenfeld, C.; Ohm, H.; Schäfer, A.; Schneider, U.; Treutler, O.; Tsereteli, K.; Unterreiner, B.; Von Arnim, M.; Weigend, F.; Weis, P.; Weiss, H. *Turbomole*, 5 ed., Theoretical Chemistry Group, University of Karlsruhe, **2002**; (b) Treutler, O.; Ahlrichs, R. *J. Chem. Phys.* **1995**, *102*, 346.

[21] (a) Baker, J. *J. Comput. Chem.* **1986**, *7*, 385; (b) Baker, J. *PQS*, 2.4 ed., Parallel Quantum Solutions, Fayetteville, AR, **2001**.

[22] Schafer, A.; Huber, C.; Ahlrichs, R. *J. Chem. Phys.* **1994**, *100*, 5829.

[23] (a) Raucoules, R.; de Bruin, T.; Raybaud, P.; Adamo, C. *Organometallics* **2009**, *28*, 5358; (b) Tobisch, S.; Ziegler, T. *J Am. Chem. Soc.* **2004**, *126*, 9059.

[24] SAINT-NT, Bruker AXS Inc., Madison, W., USA, **2000**

[25] Sheldrick, G. M. *SADABS 2.0,* Universität Göttingen: Göttingen, Germany, **2000**.

[26] Sheldrick, G. M. *Acta Crystallogr. Sect. A* **1990**, *46*, 467.

[27] Sheldrick, G. M. *SHELX-97*: Program for the Solution and Refinement of Crystal Structures; Universität Göttingen: Göttingen, Germany, **1997**.

## Chapter 3

# *Heteromatallic aluminum - chromium phenazine and thiophenazine complexes. Reduction of phenazine, thiophenazine ligands and formation of Cr(I) sandwich complex*

Organic molecules possessing large and delocalized π-systems may occasionally embark in a very substantial charge transfer interaction with a transition metal.[1,2,3,4,5,6,7,8,9,10] This behaviour is well established and is the primary characteristic of the so-called "non innocent" ligands. [1-10] The main result is the ability of the ligand system to act as an electronic reservoir.[10a,b,12] This turns out to be particularly useful in the case of metals that cannot be readily reduced because of high instability and reactivity of their low-valent states. An extreme example is provided by thorium, a metal normally regarded as "irreducible". [13] Provided that the appropriate ligand system is present, it is possible to obtain species that have the appearance of a low-valent complex.[10a,b,12b,14] This is of course a mere deception since the complex is in fact composed of higher valent metal connected to radical anion forms of the ligand system. [3a,b,5b-e,14,10a,b,e-h, 15] While charge transfer phenomena are well established, what is remarkable is that the chemical behaviour truly remains that expected for a low-valent species. These so-called "low-valent synthons" may in fact perform a variety of transformations such as dinitrogen cleavage,[16] hydrogen atom abstraction,[17] aromatic ring openings,[14c,18] *etc*.[10]

Among the molecules with established "non-innocent" behavior, phenazine plays a unique role. Not only it works as an electron reservoir in the classical sense of the term [19,20] but it also promotes performs radical cleavage of stable bonds, e.g. by interaction with the $AlH_3$, [21] $AlMe_3$ [22] and $[Ru_3(CO)_{12}]$ in THF. [17g] We were therefore interested in studying how this behaviour may be modified or affected by transition metals, for example by stabilizing low-valent synthons with enhanced radical behaviour. We were primarily interested in the interaction with chromium given the high reactivity of its low oxidation state and the possibility of finding new venues to catalytic transformations.

In this chapter, we have explored the interaction of phenazine and thiophenazine with both alkylaluminum compounds and chromium salts aiming at obtaining heterometallic complexes of negatively charged ligands. Given the unusual stability of the radicals generated by this polyaromatic molecule, we wondered about the properties of species arising from the simultaneous coordination to a Lewis acid and to an electron rich low-valent transition metal.

## *Results and Discussion*

Treatment of a suspension of phenazine and $CrCl_2(THF)_2$ in toluene with four equivalents of triethylaluminium (Scheme 37) affords the heterobimetallic $[AlEt_2(THF)(\mu^3\text{-}\eta^1\text{:}\eta^2\text{-}C_{12}H_8N_2)(\mu\text{-}\eta^2\text{-}AlEt_2Cl)]_2(\mu\text{-Cr})$ (**1**) which was isolated as brown crystalline material.[23]

The structure (Figure 14) consists of one $CrCl_2$ central unit [Cr-Cl = 2.397(17) Å] σ-bonded to the two nitrogen atoms of two phenazine residues [Cr-N = 2.129(4) Å] (Table 13). In turn, each of these nitrogen atoms bridge one $[AlEt_2]$ unit [N-Al = 1.951(5) Å, Al-Cl = 2.295(2) Å]. Each of the other two nitrogen atoms, placed at the exterior of the molecule, coordinates an

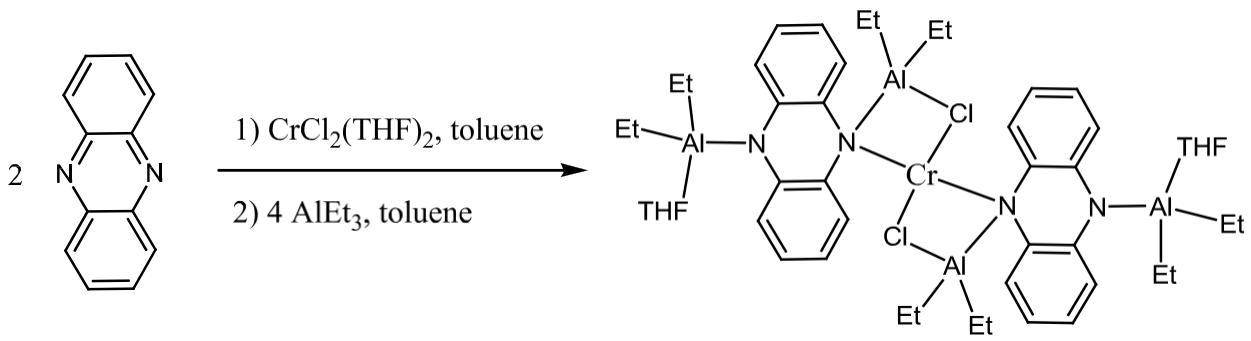


**1**

**Scheme 37.** Preparation of complex $[AlEt_2(THF)(\mu^3\text{-}\eta^1\text{:}\eta^2\text{-}C_{12}H_8N_2)(\mu\text{-}\eta^2\text{-}AlEt_2Cl)]_2(\mu\text{-Cr})$ (**1**).

**Figure 14**. Crystal structure of **1**. Thermal ellipsoids are drawn at the 50% probability level.

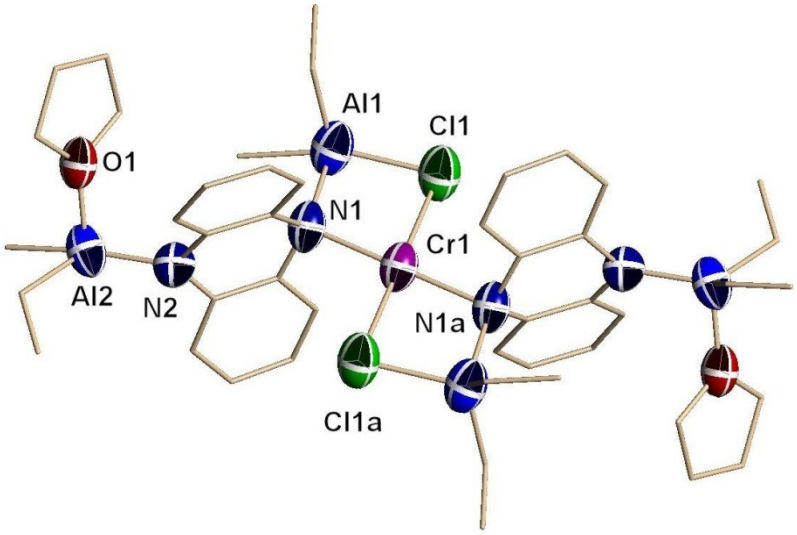


additional $AlEt_2(THF)$ moiety [Al-N = 1.886(4) Å]. The central nearly planar $[(\mu\text{-}AlEt_2Cl)_2(\mu\text{-Cr})]$ moiety in **1** is reminiscent the similar central $[(\mu\text{-}AlEt_2Cl)_2(\mu\text{-Cr})]$ moiety in the $[Cr\{\eta^2\text{-}AlEt_2Cl(2,3,4,5\text{-}C_{12}H_{12}N)\}_2]$. [24] The phenazine residue is no longer planar but folded along the N-N vector as a result of loss of aromaticity of the central ring and as resulting for the re-hybridization of both N atoms.

**Table 13**. Selected Bond Distances (Å) and Angles (°) for complex $[AlEt_2(THF)(\mu^3\text{-}\eta^1\text{:}\eta^2\text{-}C_{12}H_8N_2)(\mu\text{-}\eta^2\text{-}AlEt_2Cl)]_2(\mu\text{-Cr})$ (**1**).

| | | | |
|---|---|---|---|
| Cr(1)-N(1) | 2.129(4) | N(1)-Cr(1)-N(1a) | 179.998(1) |
| Cr(1)-Cl(1) | 2.397(17) | N(1)-Cr(1)-Cl(1) | 84.09 (12) |
| Al(1)-N(1) | 1.951(5) | N(1a)-Cr(1)-Cl(1) | 95.91(12) |
| Al(2)-N(2) | 1.886(4) | C(1)-C(2) | 1.400(8) |
| Al(1)-Cl(1) | 2.295(2) | C(2)-C(3) | 1.346(10) |
| N(1)-C(1) | 1.438(7) | C(3)-C(4) | 1.352(12) |
| N(2)-C(6) | 1.407(6) | C(4)-C(5) | 1.402(11) |
| N(1)-C(7) | 1.460(6) | C(5)-C(6) | 1.363(8) |

The square planar geometry of the chromium atom clearly diagnoses the presence of a $d^4$ divalent chromium. Accordingly, the complex is paramagnetic with a value of the magnetic moment [$\mu_{eff}$ = 4.71 $\mu_{BM}$] as expected for divalent chromium in a square-planar environment. The fact that two $[AlEt_2(THF)]$ moieties are present per each phenazine molecule, indicates that the diazine is in its dianionic form. Consequently, the N2-C and C-C bond lengths in **1** are comparable with those in the magnesium complex $[MgBr_2(C_{12}H_8N_2)(THF)_6]\cdot[MgBr_2(THF)_4]$ [25] (1.396(8) Å and 1.384(7) Å) containing the phenazine dianion. The N1-C distances in **1** (1.460(6) Å and 1.438(7) Å) are the longest observed for the bridging phenazine dianion. The maximal N-C bond length (1.411(9) Å) is reported in the $[C_5Me_5(C_8H_8)U]_2(\mu\text{-}\eta^1\text{:}\eta^1\text{-}C_{12}H_8N_2)$. [20j] In turn, the formation of such a dianion implies that a two-electron reduction took place likely at the expenses of the two alkyl functions from the aluminum atoms. It is well conceivable that the

reaction initially proceeds by following the radical pathway previously observed for the radical cleavage of $AlR_3$ as promoted by this ligand and where in this case the $CrCl_2$ moiety acts only as a templating agent (Scheme 38).[see the previous chapter]

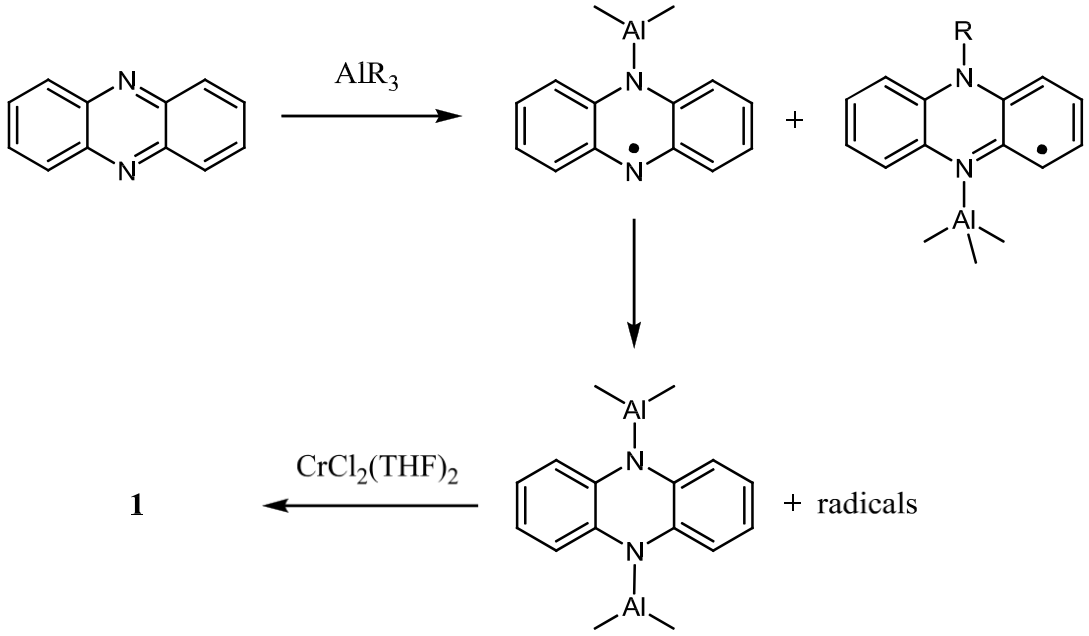


**Scheme 38**.

Complex **1** is stable at room temperature and does not decompose upon storage in a sealed ampoule during several months.

A similar reaction was investigated with thiophenazine. In this particular case the reaction is more straightforward given that the nitrogen atom carries a proton on the nitrogen atom which can be easily removed via treatment with either BuLi or $AlR_3$ itself. The reactions afforded the new complex $[(\eta^1{:}\eta^1\text{-}C_{12}H_8NS)(\mu\text{-}\eta^2\text{-}AlEt_2Cl)]_2(\mu\text{-}Cr)$ (**2**) (Scheme 39) in crystalline form.

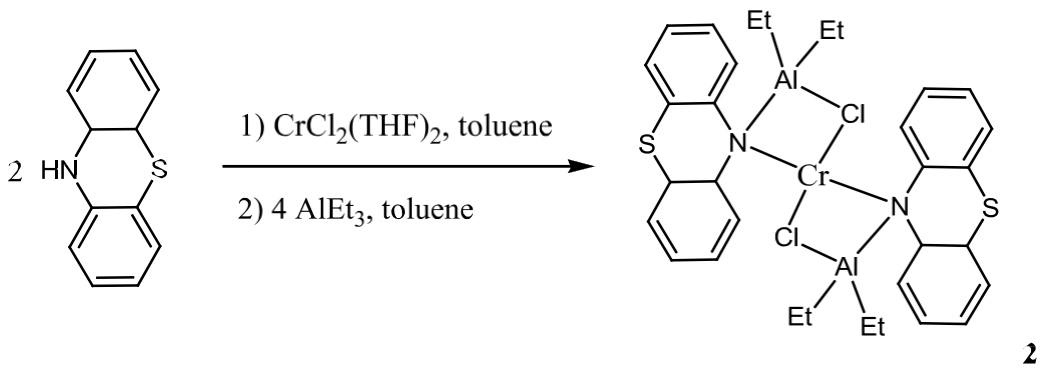


**2**

**Scheme 39**. Synthesis of complex $[(\eta^1{:}\eta^1\text{-}C_{12}H_8NS)(\mu\text{-}\eta^2\text{-}AlEt_2Cl)]_2(\mu\text{-}Cr)$ (**2**).

**Figure 15**. Crystal structure of **2** with thermal ellipsoids drawn at the 50% probability level.

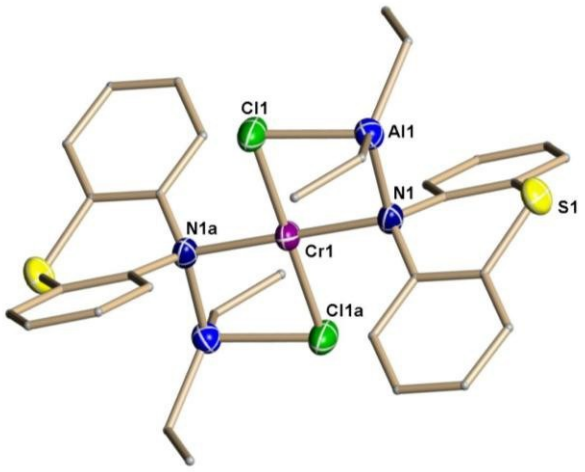


The structure of **2** (Figure 15) is closely related to that of **1** except for the absence of second aluminate residues attached in this case to the neutral sulphur atom. The central chromium atom displays the characteristic square-planar coordination geometry, as expected for high-spin $d^4$ $Cr^{II}$ ion. The Cr-Cl and Cr-N distances [2.370(8) Å and 2.131(2) Å respectively]

compare well with the corresponding values of **1**. The tricyclic structure is severely bent along the N-S vector, the angle between the phenyl wings is 42.7º.

**Table 14**. Selected Bond Distances (Å) and Angles (°) for $[(\eta^1{:}\eta^1\text{-}C_{12}H_8NS)(\mu\text{-}\eta^2\text{-}AlEt_2Cl)]_2(\mu\text{-}Cr)$ (**2**).

| | | | |
|---|---|---|---|
| Cr(1)-N(1) | 2.131(2) | N(1)-Cr(1)-N(1a) | 180.00 |
| Cr(1)-Cl(1) | 2.370(8) | N(1)-Cr(1)-Cl(1) | 85.05 (7) |
| Al(1)-N(1) | 2.006(3) | Cl(1)-Cr(1)-Cl(1a) | 180.00 |
| Al(1)-Cl(1) | 2.3161(12) | Al(1)-Cl(1)-Cr(1) | 85.31(3) |
| S(1)-C(1) | 1.763(3) | | |
| N(1)-C(12) | 1.459(4) | | |

Analytical data of **2** were consistent with the $C_{32}H_{36}Al_2Cl_2CrN_2S_2$ formulation. The magnetism of **5** [$\mu_{eff}$ = 3.97 $\mu_{BM}$] is lower than that in a high-spin Cr(II) complexes [$\mu_{eff}$ = 4.7 - 4.9 $\mu_{BM}$]. In turn, chromium atom has a four contacts with the hydrogen and carbon atoms (Cr1-H5A 2.561 Å and Cr1-H11A 2.625 Å, Cr1-C5 3.118 Å, Cr1-C11 3.169 Å; sum of vdW Radii Cr and H 3.09 Å, Cr and C is 3.7 Å) [26] of aromatic rings, implying an ligand mediated AF coupling. Complex **2** is stable at room temperature and does not decompose upon storage in a sealed ampoule during several months.

When the preparation of **1** was carried out in the presence of excess of $Et_3Al$, the reaction took a different pathway (or underwent a further transformation of initially formed **1**) affording the *formally* monovalent $[AlEt_2]_2(\mu\text{-}\eta^1{:}\eta^1\text{-}\eta^6{:}\eta^6\text{-}C_{12}H_8N_2Cr)_2$ (**3**) (Scheme 40) isolated in analytically pure form in 31% yield.

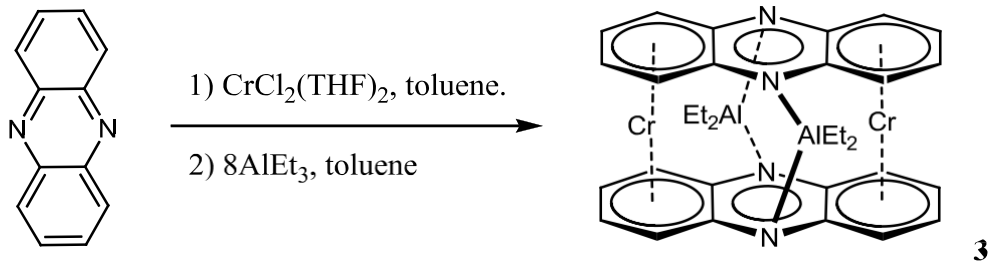


**3**

**Scheme 40**. Synthesis of complex $[AlEt_2]_2(\mu\text{-}\eta^1\text{:}\eta^1\text{-}\eta^6\text{:}\eta^6\text{-}C_{12}H_8N_2Cr)_2$ (**3**).

The structure of **3** (Figure 16) displays the characteristic sandwich coordination geometry, commonly observed for a low-spin $d^5$ $Cr^I$ ion bonded to aromatics. [27] The complex features two phenazine rings parallel to each other and eclipsed. Two $Et_2Al$ residues bridge each a pair of nitrogen atoms from the two ligands [Al(1)-N(1) = 1.972(8) Å; Al(1)-N(2) = 1.945(7) Å] (Table 15) in an overall sort of $\{Et_2Al(\mu\text{-}C_{12}H_8N_2)_2AlEt_2\}$ cage structure. Two chromium atoms are encapsulated in the cage structure and are held between each pair of parallel aromatic rings [Cr1-centroid = 1.64(5) Å; centroid-Cr1-centroid = 176.2(5)°]. Therefore the coordination geometry around chromium clearly appears that of slightly bent bis-arene chromium. The presence of the two chromium atoms in the interior of the cage reflects into slightly larger N-Al-N angle [N(2)-Al(1)-N(1) = 91.5(3)°] with respect to the chromium-free species [87.03(14)° for complex $[AlEt_2]_2(\mu\text{-}\eta^1\text{:}\eta^1\text{-}C_{12}H_8N_2)_2$]. Curiously, the phenazine units deviate from planarity [folding angle along the N..N vector 171.5°] substantially less than in $[AlEt_2]_2(\mu\text{-}\eta^1\text{:}\eta^1\text{-}C_{12}H_8N_2)_2$ (158.1°)]. The nitrogen-carbon distances in **3** (N(1)-C(1) 1.402(10) Å and N(1)-C(12A) 1.380(10) Å; N(2)-C(6A) 1.402(10) Å and N(2)-C(7) 1.418(11) Å) (Table 15) fall in the same range as nitrogen-carbon bonds in the complexes $\{R_2Al(\mu\text{-}C_{12}H_8N_2)_2AlR_2\}$ (range 1.387(5) Å to 1.397(5) Å, R =

Me, Et, $^{i}$Pr) and in the magnesium complex $[MgBr_2(C_{12}H_8N_2)(THF)_6]\cdot[MgBr_2(THF)_4]$ (1.396(8) Å and 1.384(7) Å). [25]

**Figure 16**. Crystal structure of **3** with thermal ellipsoids are drawn at the 50% probability level.

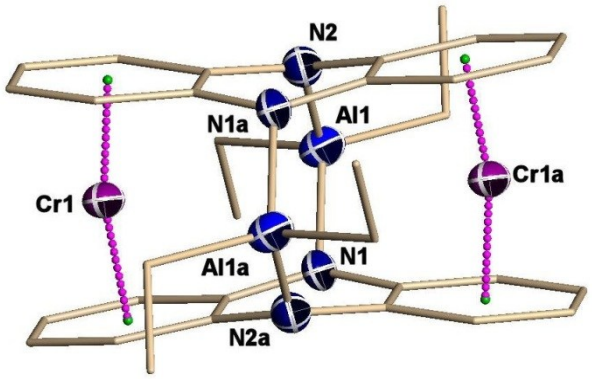


**Table 15**. Selected Bond Distances (Å) and Angles (°) for complex $[AlEt_2]_2(\mu\text{-}\eta^1\text{:}\eta^1\text{-}\eta^6\text{:}\eta^6\text{-}C_{12}H_8N_2Cr)_2$ (**3**).

| | | | |
|---|---|---|---|
| Cr-Cnt1 | 1.673(5) | Cnt1-Cr-Cnt2 | 171.5(5) |
| Cr-Cnt1 | 1.658(5) | N(2)-Al(1)-N(1) | 91.5(3) |
| Al(1)-N(1) | 1.978(8) | N(1)-Al(1)-C(13) | 118.2(3) |
| Al(1)-N(2) | 1.930(8) | C(15)-Al(1)-C(13) | 101.2(4) |
| N(1)-C(1) | 1.402(10) | C(11)-Cr(1)-C(1) | 133.3(3) |
| N(1)-C(12A) | 1.380(10) | C(8)-Cr(1)-C(1) | 106.7(4) |
| N(2)-C(6A) | 1.402(10) | C(9)-Cr(1)-C(1) | 140.8(4) |
| N(2)-C(7) | 1.418(11) | C(5)-Cr(1)-C(1) | 66.8(4) |

Cnt1 = C1C2C3C4C5C6, Cnt2 = C7C8C9C10C11C12

The electronic structure of **3** is intriguing. Our previous work has indicated that the $\{Et_2Al(\mu\text{-}C_{12}H_8N_2)_2AlEt_2\}$ cage compound is diamagnetic in spite of the fact that each phenazine molecule is present in the form of a radical dianion. A strong AF coupling between the two molecules is responsible for the diamagnetism. Therefore if one considers the aluminate cage compound prior to the coordination of chromium as a neutral species, it would be natural to attribute the zero valent state to the two transition metals. On the other hand, it is also conceivable to regard the complex as constructed by two phenazine dianions coordinated to two $Et_2Al$ cationic residues. In that event the two transition metals must be regarded as monovalent. In this event however, the complex may be expected to be paramagnetic. The magnetic moment of **3** [$\mu_{eff}$ = 1.25 $\mu_{BM}$] is substantial although is below the normal range for low-spin $d^5$ Cr(I) complexes [$\mu_{eff}$ = 1.6 - 1.9 $\mu_{BM}$]. There are two possible interpretations for this. One possibility could be that an antiferromagnetic exchange occurs between the two monovalent chromium atoms but it is also possible that two diamagnetic Cr(0) simply disrupt the efficient antiferromagnetic exchange responsible for the diamagnetism of the cage.

DFT calculations were performed to address these issues. Geometries were optimized for $\{Me_2Al(\mu\text{-}C_{12}H_8N_2)_2AlMe_2\}$ (**A**), $\{Me_2Al(\mu\text{-}\eta^1\text{:}\eta^1\text{-}\eta^6\text{:}\eta^6\text{-}C_{12}H_8N_2Cr)_2AlMe_2\}$ (**B**) and $(C_6H_6)_2Cr^+$ (**C**) at the unrestricted b3-lyp/SV(P) level; spin density plots are shown in Figure 17. $\{Me_2Al(\mu\text{-}C_{12}H_8N_2)_2AlMe_2\}$ prefers a broken-symmetry solution ($S^2$ = 0.30, see Figure 17A); the triplet is substantially higher in energy than the singlet (by 7.3 kcal/mol, respectively). When regarding this as consisting of two phenazine radical anions bridged by the $Me_2Al^+$ fragments, it is clear that there is significant antiferromagnetic coupling between these radicals. For the bis(chromium) complex, on the other hand, the singlet-triplet splitting is negligible, and the spin density is predominantly located on the Cr atoms (Figure 17B). The broken-symmetry solution

has $S^2$ = 1.13, best interpreted as two independent Cr(I) centres (ideal value $S^2$ = 1.00) and some spin contamination; $(C_6H_6)_2Cr^+$ has $S^2$ = 0.80, to be compared with the ideal value of 0.75 for a single unpaired electron. In fact, the spin density on each half of {$Me_2Al(\mu\text{-}\eta^1\text{:}\eta^1\text{-}\eta^6\text{:}\eta^6\text{-}C_{12}H_8N_2Cr)_2AlMe_2$} is virtually identical to that in an isolated $(C_6H_6)Cr^+$ molecule (Figure 17C). This makes it evident that {$Me_2Al(\mu\text{-}\eta^1\text{:}\eta^1\text{-}\eta^6\text{:}\eta^6\text{-}C_{12}H_8N_2Cr)_2AlMe_2$} is best described as containing two nearly independent Cr(I) centres and doubly reduced phenazine ligands.

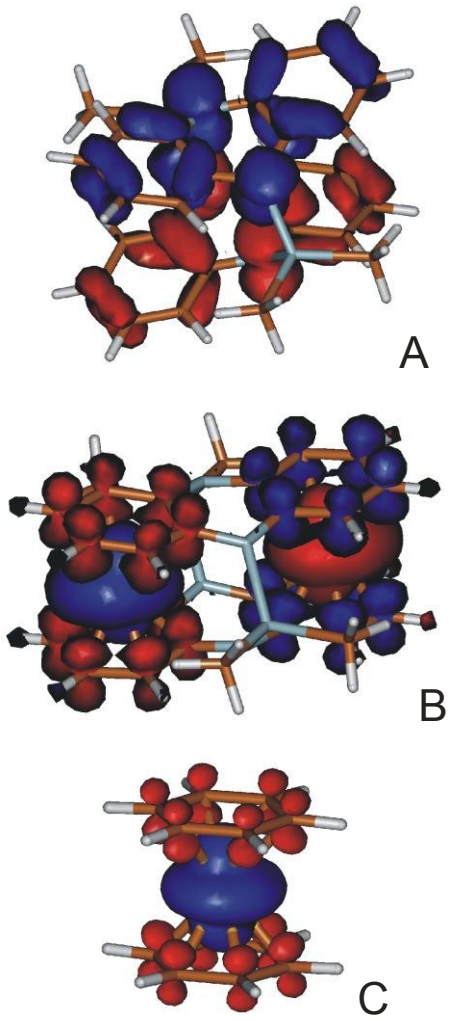


**Figure 17**. Calculated spin densities for (**A**) {$Me_2Al(\mu\text{-}C_{12}H_8N_2)_2AlMe_2$}; (**B**) {$Me_2Al(\mu\text{-}\eta^1\text{:}\eta^1\text{-}\eta^6\text{:}\eta^6\text{-}C_{12}H_8N_2Cr)_2AlMe_2$}; (**C**) $(C_6H_6)_2Cr^+L_2(AlMe_2)_2$. **A** and **B** are broken-symmetry solutions.

Given the ambiguity of the phenazine ligand as either radical mono anion or simple dianion, we have also attempted the preparation of **3** by using the doubly deprotonated form of dihydrophenazine. The reaction was carried out by using the usual reaction conditions used for the preparation of **3** and by using the dihydrophenazine dilithium salt obtained via in situ treatment with two equivalent of *n*-BuLi. The reaction afforded **3** only in 11% yield and heavily contaminated with the phenazine dilithium salt crystallized as a dark purple LiCl adduct $[(Li(THF)_2)_2(\mu\text{-Cl})]_2(\mu\text{-}\eta^2\text{:}\eta^2\text{-}C_{12}H_8N_2)$ (**4**) (Scheme 41).

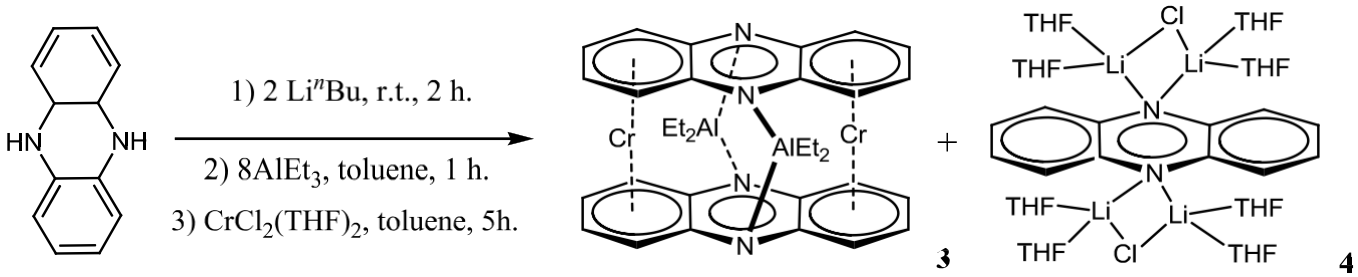


**Scheme 41**. Synthesis of complex $[AlEt_2]_2(\mu\text{-}\eta^1\text{:}\eta^1\text{-}\eta^6\text{:}\eta^6\text{-}C_{12}H_8N_2Cr)_2$ (**3**) and $[(Li(THF)_2)_2(\mu\text{-Cl})]_2(\mu\text{-}\eta^2\text{:}\eta^2\text{-}C_{12}H_8N_2)$ (**4**).

Even in the case of $[(Li(THF)_2)_2(\mu\text{-Cl})]_2(\mu\text{-}\eta^2\text{:}\eta^2\text{-}C_{12}H_8N_2)$ (**4**) the connectivity was obtained by an X-ray crystal structure. The complex **4** (Figure 18) consists of one phenazine molecule where each N atom bridges two lithium of a Li-Cl-Li unit [Li(1)-Cl(1) = 2.365(6); Li(2)-Cl(1) = 2.371(6) Å]. The Li-N and Li-Cl distances [Li(1)-N(1) = 2.038(6); Li(2)-N(1) = 2.095(6) Å] are close to those in $Li_2(\mu\text{-Cl})(\mu\text{-}\eta^2\text{-}NC_{12}H_8NH)(THF)_4$ [28] and are within the normal range of lithium amides (e.g. in $[Li(\mu\text{-Cl})(2\text{-methylpyridine})_2]_2$ (2.378(8), 2.383(9) Å), [29] in

$Li_2(\mu\text{-}Cl)(\mu\text{-}\eta^2\text{-}NC_{12}H_8NH)(THF)_4$ (2.09(1) and 2.06(1) Å), [28] $[Li(\mu\text{-}N(Me)Ph(tmeda))]_2$ (2.082(6) Å)[30]).

**Figure 18**. Crystal structure of **4**. Thermal ellipsoids are drawn at the 50% probability level.

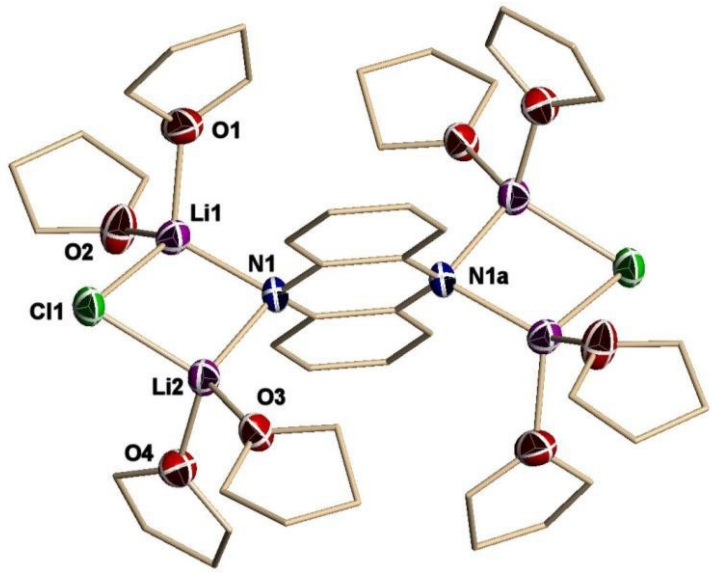


**Table 16**. Selected Bond Distances (Å) and Angles (°) for complex $[(Li(THF)_2)_2(\mu\text{-}Cl)]_2(\mu\text{-}\eta^2\text{:}\eta^2\text{-}C_{12}H_8N_2)$ (**4**).

| | | | |
|---|---|---|---|
| Li(1)-Cl(1) | 2.365(6) | Li(1)-Cl(1)-Li(2) | 69.66(18) |
| Cl(1)-Li(2) | 2.371(6) | O(2)-Li(1)-O(1) | 99.2(3) |
| Li(1)-N(1) | 2.038(6) | Li(2)-N(1)-Li(1) | 81.7(2) |
| Li(2)-N(1) | 2.095(6) | C(1)-N(1)-Li(2) | 117.0(2) |
| Li(1)-Li(2) | 2.705(8) | C(1)-N(1)-Li(1) | 118.5(2) |
| Li(1)-O(1) | 1.976(6) | N(1)-Li(1)-Cl(1) | 103.8(2) |
| Li(1)-O(2) | 1.957(6) | N(1)-Li(2)-Cl(1) | 101.8(2) |

| | | | |
|---|---|---|---|
| N(1)-C(4) | 1.398(4) | | |
| N(1)-C(1) | 1.404(4) | | |

In conclusion, the ability of phenazine to extract radical may be used to generate ligand cage capable of encapsulating two chromium atoms. The interaction of phenazine or thiophenazine, with $CrCl_2(THF)_2$ and triethylaluminum in toluene is initially accompanied by the reduction of phenazine ligand leading to the heterometallic Cr(II) - aluminum complexes containing a formally dinegative phenazine or thiophenazine ligands. In a second step, the interaction of phenazine, $CrCl_2(THF)_2$ and excess of triethylaluminum in toluene is accompanied by the reduction of phenazine ligand and chromium leading to the heterometallic multinuclear Cr(I) - aluminum complex containing a formally dinegative phenazine ligands and two chromium atoms.

## *Experimental section*

All manipulations were performed under the nitrogen atmosphere with rigorous exclusion of oxygen and water using standard Schlenk and glove-box techniques. Hexane, toluene and THF were purified by passing through the activated $Al_2O_3$ column and deoxygenated prior to use by several vacuum/nitrogen purges. Benzene-$d^6$ was obtained from "C/D/N isotopes", dried over freshly activated molecular sieves (4A) for 10 days and distilled under $N_2$ atmosphere. $AlEt_3$, $AlEt_2Cl$ and solution of Li$^n$Bu in hexane were purchased from Aldrich and used as received. $CrCl_2(THF)_2$ was prepared by extraction the commercially available $CrCl_2$ with the dry THF under the nitrogen atmosphere. The ligands phenazine, phenothiazine were purchased from

Aldrich and used as received. Dihydrophenazine was prepared according to the established procedure. [31] Magnetic susceptibility measurements were performed at room temperature using a Johnson Matthey Gouy balance and corrected to diamagnetism. Elemental Analysis was performed using a Perking-Elmer Series II CHN/O 2400 analyser.

**Preparation of [$AlEt_2(THF)(\mu^3$-$\eta^1$:$\eta^2$-$C_{12}H_8N_2)(\mu$-$\eta^2$-$AlEt_2Cl)]_2(\mu$-Cr) (1)**

Neat triethylaluminium (456 mg, 4 mmol) was added drop wise to a stirred suspension of phenazine (181 mg, 1 mmol) and $CrCl_2(THF)_2$ (133 mg, 0.5 mmol) in toluene (10 mL). The color of the solution turned red during the addition of $AlEt_3$. The reaction mixture was stirred for 5 minutes and then centrifuged. The clear solution was separated and concentrated in vacuum. The resulting solution was left undisturbed for crystallization at -35$^o$C. Red crystals of **1** appeared in 24 hours and which were separated, washed with hexane and dried in vacuum (295 mg, 0.37 mmol, 37 %). Anal. Calcd. (found) for $C_{48}H_{72}Al_4Cr_2N_4O_2$: C 60.73 (60.59); H 7.65 (7 53); N 5.91 (5.78). $\mu_{eff}$ = 4.71 $\mu_{BM}$

**Preparation of [($\eta^1$:$\eta^1$-$C_{12}H_8NS)(\mu$-$\eta^2$-$AlEt_2Cl)]_2(\mu$-Cr) (2)**

Method A. Neat $AlEt_3$ (570 mg, 50 mmol) was added drop wise to a solution of thiophenazine (2.0 g, 10 mmol) in toluene (30 mL). An immediate discoloration of the reaction mixture was observed during the addition. The resulting solution was stirred for 3 hours and then $CrCl_2(THF)_2$ (1.33 g, 5 mmol) was introduced in small portions. The color changed immediately to blue. After 30 min of stirring, the mixture was centrifuged and the clear solution was separated from the solid, transferred to another vial and concentrated in vacuum. The concentrated solution was left undisturbed at -35$^o$C. Blue crystals of **2** appeared on the next day and which were

separated from the supernatant solution, washed with hexane and dried in vacuum (1.55 g, 2.25 mmol, 45 %). Anal, calcd (found) for Anal, calcd (found) for $C_{32}H_{36}Al_2Cl_2CrN_2S_2$: C 55.73 (55.63); H 5.26 (5.08); N 4.06 (4.05). $\mu_{eff}$ =3.90 $\mu_{BM}$

Method B. A solution of *n*-BuLi (6.3 mL, 1.6 M, 10 mmol) in hexane was added drop wise to a suspension of $CrCl_2(THF)_2$ (2.66 g, 10 mmol) and thiophenazine (3.96 g, 20 mmol) in toluene (10 mL) at room temperature. The resulting mixture was stirred for two hours at room temperature and then added with $AlEt_2Cl$ (6.8 g, 40 mmol) drop wise. The reaction mixture was further stirred for 4 hours and then centrifuged. The clear toluene solution was separated, concentrated and left undisturbed for crystallization at -35$^o$C. Blue crystals of **2** appeared on the next day and which were separated, washed with hexane and dried in vacuum (4.89 g, 7.09 mmol, 71 %). Anal, calcd (found) for $C_{32}H_{36}Al_2Cl_2CrN_2S_2$: C 55.73 (55.59); H 5.26 (5.14); N 4.06 (4.05). $\mu_{eff}$ =3.97 $\mu_{BM}$

**Preparation of $[AlEt_2]_2(\mu\text{-}\eta^1\text{:}\eta^1\text{-}\eta^6\text{:}\eta^6\text{-}C_{12}H_8N_2Cr)_2$ (3)**

Method A. A suspension of phenazine (181 mg,1 mmol) and $CrCl_2(THF)_2$ (267 mg, 1 mmol) in toluene (10 mL), was treated with triethylaluminun (912 mg, 8 mmol) affording immediate color change of the solution to dark brown. Stirring was continued for 5 hours followed by centrifugation. The clear toluene solution was separated, concentrated and left undisturbed for several days at -35$^o$C. Oily material deposited at that temperature. The oil was washed with hexanes (3 x 5 ml) and then dissolved in toluene (2 mL) at room temperature. Crystalline **3** separated upon standing at -35$^o$C for 1 week which was separated, washed with hexane and dried

in vacuum (197 mg, 0.31 mmol, yield 31%). Anal. Calcd. (found) for $C_{32}H_{36}Al_2Cr_2N_4$: C 60.54 (60.40); H 5.72 (5.58); N 8.83 (8.71). $\mu_{eff}$ =1.3 $\mu_{BM}$

Method B. A solution of *n*-BuLi (2 mmol, 0.8 ml, 2.5 M in hexane) was added drop wise to a stirred solution of dihydrophenazine (182 mg, 1 mmol) in toluene (10 ml) producing an orange solution. After 10 minutes, triethylaluminum (918 mg, 8 mmol) was also added drop wise to the stirred mixture affording a color change from orange to green. After 1h of stirring, $CrCl_2(THF)_2$ (0.267 mg, 1 mmol) was added to the mixture causing a darkening of the color. The resulting mixture was stirred for 5 h, and then centrifuged. The clear toluene solution was separated and allowed to stand at –35˚ C. Oily material deposited at that temperature which was washed with hexanes (3 x 5 ml) and then dissolved in 2 mL of toluene at room temperature. The solution was left for crystallization at -35$^{o}$C yielding a mixture of red crystals of **3** and purple crystals of **4**. Analytically pure crystals of **3** (69 mg, 0.11 mmol, yield 11 %) were obtained after recrystallization. Anal. Calcd. (found) for $C_{32}H_{36}Al_2Cr_2N_4$: C 60.54 (60. 47); H 5.72 (5.69); N 8.83 (8.70). $\mu_{eff}$ =1.2 $\mu_{BM.}$ Complex **4** could not be isolated in analytically pure form.

**Crystal Structure Data**

Appropriate single crystals of compounds were selected under the microscope and mounted on a thin, glass fiber with parathone oil, and cooled to the data collection temperature. X-ray data were collected on a Bruker AXS SMART 1k CCD diffractometer at 200(2) K, equipped with graphite-monochromated Mo-$K_\alpha$ radiation ($\lambda$ = 71.073 pm). Initial unit-cell parameters were determined from 60 data frames collected at different sections of the Ewald sphere. The intensity data were corrected for Lorentz and polarization effects; the data were integrated with SAINT,[32] and an empirical absorption (SADABS) was applied.[33] The structures were solved by direct

methods (SHELXS-97)[34] and refined by full-matrix least-squares methods against $F^2$ (SHELXL-97). [35] All non-hydrogen-atoms were refined with anisotropic displacement parameters. The hydrogen atoms were refined isotropically on calculated positions.

**Crystals of $C_{48}H_{72}Al_4Cr_2N_4O_2$ (1)** were grown from a toluene. The crystal data and refinement parameters for complex **1** can be found in Table 17, and interatomic distances and angles are listed in Table 13. The reflection data were consistent with a monoclinic system, space group *C*2/*c*. The largest residual electron density peak (0.419 e/Å$^3$) was associated with the N1 atom. Full-matrix least-squares refinement on $F^2$ gave $R_1 = 0.0692$ and $wR_2 = 0.1842$ at convergence.

**Crystals of $C_{32}H_{36}Al_2Cl_2CrN_2S_2$ (2)** were grown from toluene. The crystal data and refinement parameters for complex **2** can be found in Table 17, and interatomic distances and angles are listed in Table 14. The reflection data were consistent with a triclinic system, space group *P*-1. The largest residual electron density peak (0.744 e/Å$^3$) was associated with a Cr atom. Full matrix least-squares refinement on $F^2$ gave $R_1 = 0.0422$ and $wR_2 = 0.1373$ at convergence.

**Crystals of $C_{39}H_{44}Al_2Cr_2N_4$ (3)** were grown from toluene. The crystal data and refinement parameters for complex **3** can be found in Table 17, and interatomic distances and angles are listed in Table 15. The reflection data were consistent with triclinic system, space group *P*-1. The largest residual electron density peak (0.367 e/Å$^3$) was associated with a disordered Cr1 atom. Full-matrix least-squares refinement on $F^2$ gave $R_1 = 0.0792$ and $wR_2 = 0.0982$ at convergence.

**Crystals of $C_{44}H_{72}Cl_2Li_4N_2O_8$ (4)** were grown from THF. The crystal data and refinement parameters for complex **4** can be found in Table 17, and interatomic distances and angles are listed in Table 16. The reflection data were consistent with a triclinic system, space group *P*-1. The largest residual electron density peak (0.290 e/Å$^3$) was associated with a C12 atom of ethyl group. Full matrix least-squares refinement on $F^2$ gave $R_1$= 0.0525, $wR_2$ = 0.1263 at convergence.

**Table 17**. Crystal Data and Refinement Parameters for Complexes **1 - 4**.

| **Identification Code** | **Complex 1** | **Complex 2** | **Complex 3** | **Complex 4** |
|---|---|---|---|---|
| Empirical Formula | $C_{48}H_{72}Al_4Cr_2N_4O_2$ | $C_{32}H_{36}Al_2Cl_2CrN_2S_2$ | $C_{39}H_{44}Al_2Cr_2N_4$ | $C_{44}H_{72}Cl_2Li_4N_2O_8$ |
| Formula Weight | 948.48 | 689.61 | 726.74 | 855.7 |
| Temperature | 202(2) K | 200(2)K | 203(2) K | 203(2)K |
| Wavelength | 0.71073 Å | 0.71073 Å | 0.71073 Å | 0.71073 Å |
| Crystal System | Monoclinic | Triclinic | Triclinic | Triclinic |
| Space Group | *C*2/*c* | *P*-1 | *P*-1 | *P*-1 |
| Unit cell Dimensions | a = 20.431(8) Å<br>b = 14.075(6) Å<br>c = 20.975(9) Å<br>α = 90°<br>β= 91.185(7)°<br>γ = 90° | a = 9.3503(13) Å<br>b = 9.9256(14) Å<br>c = 10.0618 (14) Å<br>α =106.479(2)°<br>β= 95.036(2)°<br>γ=107.048(2)° | a = 7.109(5) Å<br>b = 10.030(6) Å<br>c = 13.068(8) Å<br>α= 71.206(10)°.<br>β= 86.810(10)°.<br>γ = 70.680(9)° | a = 10.272(3) Å<br>b = 11.348(4) Å<br>c = 11.912 (4) Å<br>α =104.347(4)°<br>β= 102.760(5)°<br>γ=109.161(4)° |
| Volume | 6030(4) Å$^3$ | 841.1(2) Å$^3$ | 831.1 (9) Å$^3$ | 1199.4(7) Å$^3$ |
| Z | 4 | 1 | 1 | 1 |
| Density (calculated) | 1.168 Mg/m$^3$ | 1.361Mg/m$^3$ | 1.452Mg/m$^3$ | 1.185Mg/m$^3$ |

| | | | | |
|---|---|---|---|---|
| Absorption Coefficient | 0.377 $mm^{-1}$ | 0.700 $mm^{-1}$ | 0.743 $mm^{-1}$ | 0.185 $mm^{-1}$ |
| F(000) | 2256 | 358 | 380 | 460 |
| Crystal Size $mm^3$ | 0.33 x 0.21 x 0.17 | 0.20 x 0.20 x 0.15 | 0.20 x 0.20 x 0.05 | 0.10 x 0.02 x 0.01 |
| Index Ranges (h,k,l) | ±21, ±14, ±21 | ±11, ±11, ±11 | ±7, ±10, ±14 | ±12, ±13, ±14 |
| Reflections Collected/Independent | 14748/3324 | 7840/2807 | 5023/2179 | 11861/4049 |
| R(int) | 0.0408 | 0.0339 | 0.1581 | 0.0486 |
| Completeness to theta = | 21.49° =95.9% | 24.79° = 97.5% | 22.72° =97.5% | 24.78° = 98.1% |
| Max. and Min. Transmission | 0.9387 and 0.8858 | 0.9023 and 0.8727 | 0.9638 and 0.8657 | 0.9982 and 0.09818 |
| Data/Restraints/ Parameters | 3324 / 0 / 277 | 2807 / 0 / 187 | 2179 / 43 / 214 | 4049 / 45 / 280 |
| Goodness-of-Fit on $F^2$ | 1.052 | 1.028 | 1.002 | 1.028 |
| Final R indices [I>2sigma(I)] | R1 =0.0692, wR2 = 0.1842 | R1 = 0.0422, wR2 = 0.1373 | R1 = 0.0792, wR2 = 0.0982 | R1 = 0.0525, wR2 = 0.1263 |
| R indices (all data) | R1 = 0.0919, wR2 = 0.1972 | R1 = 0.0466, wR2 = 0.1426 | R1 = 0.1926, wR2 = 0.1211 | R1 = 0.1077, wR2 = 0.1540 |
| Largest Diff. Peak and Hole | 0.419 and -0.178 e. $Å^{-3}$ | 0.744 and -0.395 e.$Å^{-3}$ | 0.367 and -0.398 e.$Å^{-3}$ | 0.290 and -0.203 e.$Å^{-3}$ |

## References


[1] Selected reviews: (a) Vlcek A. Jr. *Chemtracts* **1998**, *11*, 352. (b) McCleverty, J. A.; Ward, M. D.; Jones, C. J. *Comments Inorg. Chem*. **2001**, *22*, 293. (c) Mezailles, N.; Mathey, F.; Le Floch, P.; *Progr. Inorg. Chem*. **2001**, *49*, 455. (d) Butin, K. P.; Beloglazkina, E. K.; Zyk, N. V. *Rus. Chem. Rev*. **2005**, *74*, 531. (e) Lyaskovskyy, V.; de Bruin, B. *ACS Catal*. **2012**, *2*, 270. f) Lever, A. B. P.; Gorelsky, S. I. "*Optical Spectra and Chemical Bonding in Transition Metal Complexes*" Book Series: *Structure and Bonding* **2004**, *107*, 77.

[2] Selected reviews for complexes with oxygen-containing ligands based on pyrocatechols: (a) Ward, M. D.; McCleverty, J. A. *Dalton Trans*. **2002**, 275. (b) Pierpont, S. G. *Coord. Chem. Rev*. **2001**, *216-217*, 99. (c) Pierpont, S. G. *Coord. Chem. Rev*. **2001**, *219-221*, 415.

[3] Selected references for complexes containing the bis-pyridyl ligands: (a) Adarsh, N. N.; Dastidar, P. *Chem. Soc. Rev*. **2012**, *41*, 3039. (b) Hughes, M. C.; Macero, D. J. *Inorg. Chem*. **1976**, *15*, 2040. (c) Fees, J.; Kaim, W.; Moscberosch, M.; Matheis, W.; Klima, J.; Krejcik, M.; Záliš, S. *Inorg. Chem*. **1993**, *32*, 166. (d) Rau, S. ; Schwalbe, M. ; Losse, S.; Görls, H. ; McAlister, C. ; MacDonnell, F. M. ; Vos, J. G. *Eur. J. Inorg. Chem*. **2008**, 1031. (e) Banerjee, P.; Mostafa, G.; Castiñeiras, A.; Goswami, S. *Eur. J. Inorg. Chem*. **2007**, 412. (f) Deb, A. K.; Goswami, S. *Dalton Trans*. **1989**, 1635. (g) McGuire Jr., R.; McGuire, M. C.; McMillin, D. R. *Coord. Chem. Rev*. **2010**, *254*, 2574. (h) McKinleya, A. W.; Lincoln, P.; Tuite, E. M. *Coord. Chem. Rev*. **2011**, *255*, 2676.

[4] Selected reviews for complexes supported by the bis-phenoxide ligands: Storr, T.; Verma, P.; Pratt, R. C.; Wasinger, E. C.; Shimazaki, Y.; Stack, T. D. P. *J. Am. Chem. Soc*. **2008**, *130*,

15448. Imido ligands: Ignatov, S. K.; Rees, N. H.; Merkoulov, A. A.; Dubberley, S. R.; Razuvaev, A. G.; Mountford, P.; Nikonov, G. I. *Chem. Eur. J.* **2008**, *14*, 296.

[5] Selected reviews for complexes supported by the dithiolene ligands: (a) Fourmigué, M. *Acc. Chem. Res*. **2004**, *37*, 179. (b) Szilagyi, R. K.; Lim, B. S.; Glaser, T.; Holm, R. H.; Hedman, B.; Hodgson, K. O.; Solomon, E. I. *J. Am. Chem. Soc*. **2003**, *125*, 9158 ditiolines mentioned in progr see b. (c) Karlin, K. D.; Stiefel, E. I. (Eds.), *Prog. Inorg. Chem*. **2004**, 52. (d) Burgmayer, S. J. N. *Progr. Inorg. Chem*. **2004**, *52*, 491. (e) Hughes, M. C.; Macero, D. J. *Inorg. Chem*. **1976**, *15*, 2040.

[6] Selected reviews for complexes supported by the ligands based on aromatic diamines: (a) Mederos, A.; Dominguez, S.; Hernardez-Molina, R.; Sanchiz, J.; Brito, F. *Coord. Chem. Rev*. **1999**, *193-195*, 913. (b) Mederos, A.; Dominguez, S.; Hernandez-Molina, R.; Sanchiz, J.; Brito, F. *Coord. Chem. Rev*. **1999**, *193-195*, 857. (c) Khusniyarov, M. M.; Bill, E.; Weyhermuller, T.; Bothe, E.; Harms, K.; Sundermeyer, J.; Wieghardt, K. *Chem. Eur. J.* **2008**, *14*, 7608.

[7] Selected review for complexes supported by the $\alpha$-diimines: Khusniyarov, M. M.; Weyhermuller, T.; Bill, E.; Wieghardt, K. *J. Am. Chem. Soc*. **2009**, *131*, 1208.

[8] Selected reviews for complexes supported by the quinone based ligands: (a) Uhlig, E. *Z. Chem*. **1989**, *29*, 305. (b) Das, D.; Das, A. K.; Sarkar, B.; Mondal, T. K.; Mobin, S. M.; Fiedler, J.; Zalis, S.; Urbanos, F. A.; Jimenez-Aparicio, R.; Kaim, W.; Lahiri, G. K. *Inorg. Chem*. **2009**, *48*, 11853. (c) Boyer, J. L.; Rochford, J.; Tsai, M. K.; Muckerman, J. T.; Fujita, E. *Coord. Chem. Rev*. **2010**, *254*, 309.

[9] Selected reviews for complexes containing Corrole ligands: (a) Ghosh, A.; Steene, E.; *J. Inorg. Biochem*. **2002**, *91*, 423. (b) Ye, S. F.; Tuttle, T.; Bill, E.; Simkhovich, L.; Gross, Z.; Thiel, W.; Neese, F. *Chem. Eur. J*. **2008**, *14*, 10839.

[10] Selected references for DIMPY and related ligands: (a) Gibson, V. C.; Redshaw, C.; Solan, G. *Chem. Rev*. **2007**, *107*, 1745. (b) Knijnenburg, Q.; Gambarotta, S.; Budzelaar, P. H. M. *Dalton Trans*. **2006**, 5442. (c) Gallagher, M; Wieder, N. L.; Dioumaev, V. K.; Carroll, P. J.; Berry, D. H. *Organometallics* **2010**, *29*, 591. (d) Zhu, D.; Thapa, I.; Korobkov, I.; Gambarotta, S.; Budzelaar, P. H. M. *Inorg. Chem*. **2011**, *50*, 9879. (e) Sylvester, K. T.; Chirik, P. J. *J. Am. Chem. Soc*. **2009**, *131*, 8772. (f) Bart, S. C.; Chłopek, K.; Bill, E.; Bouwkamp, M. W.; Lobkovsky, E.; Neese, F.; Wieghardt, K.; Chirik, P. J. *J. Am. Chem. Soc*. **2006**, *128*, 13901. (g) Zhu, D.; Janssen, F. F. B. J.; Budzelaar, P. H. M. *Organometallics* **2010,** *29*, 1897. (h) Zhu, D.; Budzelaar, P. H. M. *Organometallics* **2010**, *29*, 5759.

[11] The term "non-innocent" was introduced in chemistry by Jørgensen in 1966: Jørgensen, C. K. *Coord. Chem. Rev*. **1966**, *1*, 164.

[12] (a) Burgmayer, S. J. N.; Kaufmann, H. L.; Fortunato, G.; Hug, P.; Fischer, B. *Inorg. Chem*. **1999**, *38*, 2607. (b) Sugiyama, H.; Korobkov, I.; Gambarotta, S.; Möller, A.; Budzelaar, P. H. M. *Inorg. Chem*. **2004**, *43*, 5771.

[13] Korobkov, I.; Gambarotta, S. *Organometallics* **2010**, *29*, 692.

[14] (a) Wissing, E.; Van der Linden, S.; Rijnberg, E.; Boersma, J.; Smeets, W. J. J.; Spek, A. L.; Van Koten, G. *Organometallics* **1994**, *13*, 2602. (b) De Bruin, B.; Bill, E.; Bothe, E.; Weyhermüller, T.; Wieghardt, K. *Inorg. Chem*. **2000**, *39*, 2936. (c) Budzelaar, P. H. M.; De

Bruin, B.; Gal, A. W.; Wieghardt, K.; Lenthe, J. H. *Inorg. Chem*. **2001**, *40*, 4649. (d) Reardon, D.; Aharonian, G.; Gambarotta, S.; Yap, G. P. A. *Organometallics* **2002**, *21*, 786. (e) Sugiyama, H.; Aharonian, G.; Gambarotta, S.; Yap, G. P. A.; Budzelaar, P. H. M. *J. Am. Chem. Soc*. **2002**, *124*, 12268. (f) Knijnenburg, Q.; Hetterscheid, D. G. H.; Kooistra, T. M.; Budzelaar, P. H. M. *Eur. J. Inorg. Chem*. **2004**, 1204. (g) Scott, J.; Gambarotta, S.; Korobkov, I.; Knijnenburg, Q.; De Bruin, B.; Budzelaar, P. H. M. *J. Am. Chem. Soc*. **2005**, *127*, 17204. (h) Bailey, P. J.; Dick, C. M.; Fabre, S.; Parsons, S.; Yellowlees, L. J. *Dalton Trans*. **2006**, 1602.

[15] (a) Gibson, V. C.; Humphries, M. J.; Tellmann, K. P.; Wass, D. F.; White, A. J. P.; Williams, D. J. *Chem. Commun*. **2001**, 2252. (b) Kooistra, T. M.; Knijnenburg, Q.; Smits, J. M. M.; Horton, A. D.; Budzelaar, P. H. M.; Gal, A. W. *Angew. Chem. Int. Ed*. **2001**, *40*, 4719.

[16] (a) Vidyaratne, I.; Scott, J.; Gambarotta, S.; Budzelaar, P. H. M. *Inorg. Chem*. **2008**, *47*, 896. (b) Vidyaratne, I.; Crewdson, P.; Lefebvre, E.; Gambarotta, S.; *Inorg. Chem*. **2007**, *46*, 8836. (c) Vidyaratne, I.; Scott, J.; Gambarotta, S.; Budzelaar, P. H. M. *Inorg. Chem*. **2007**, *46*, 7040.

[17] Selected references: (a) Hoff, C. D. *Coord. Chem. Rev*. **2000**, *206*, 451. (b) Bart, S. C.; Lobkovsky, E.; Chirik, P. J. *J. Am. Chem. Soc*. **2004**, *126*, 13794. (c) Bart, S. C.; Lobkovsky, E.; Bill, E.; Chirik, P. J. *J. Am. Chem. Soc*. **2006**, *128*, 5302. (d) Bouwkamp, M. W.; Lobkovsky, E.; Chirik, P. J. *Inorg. Chem*. **2006**, *45*, 2. (e) Knijnenburg, Q.; Horton, A. D.; van der Heijden, H.; Kooistra, T. M.; Hetterscheid, D. G. H.; Smits, J. M. M.; de Bruin, B.; Budzelaar, P. H. M.; Gal, A. W. *J. Mol. Catal. A*. **2005**, *232*, 151. (f) Sattler, A.; Zhu, G.;

Parkin, G. *J. Am. Chem. Soc*. **2009**, *131*, 7828. (g) Cabeza, J. A.; García-Álvarez, P.; Pruneda, V. *Organometallics* **2012**, *31*, 941.

[18] (a) Diaconescu, P. L. *Comments Inorg. Chem*. **2010**, *31*, 196. (b) Knijnenburg, Q.; Smits, J. M. M.; Budzelaar, P. H. M. *Organometallics* **2006**, *25*, 1036.

[19] Reduction of phenazine by the metallic lithium or sodium: (a) A. Minsky, Y. Cohen, M. Rabinovitz, *J. Am. Chem. Soc*., **1985**, *107*, 1501. (b) Y. Cohen, A. Y. Meyer, M. Rabinovitz, *J. Am. Chem. Soc*., **1986**, *108*, 7039.

[20] Reduction of phenazine by the lanthanide and actinide complexes (a) Scholz, J.; Scholz, A.; Weimann, R.; Janiak, C.; Schumann, H. *Angew. Chem., Int. Ed*. **1994**, *33*, 1171. (b) Evans, W. J.; Gonzales, S. L.; Ziller, J. W. *J. Am. Chem. Soc*. **1994**, *116*, 2600. (c) Evans, W. J.; Lorenz, S. E. ; Ziller, J. W. *Inorg. Chem*. **2009**, *48*, 2001. (d) Berg, D. J.; Boncella, J. M.; Andersen, R. A. *Organometallics* **2002**, *21*, 4622. (e) Evans, W. J.; Lee, D. S.; Ziller, J. W.; Kaltsoyannis, N. *J. Am. Chem. Soc*. **2006**, *128*, 14176. (f) Lorenz, S. E.; Schmiege, B. M.; Lee, D. S.; Ziller, J. W.; Evans, W. J. *Inorg. Chem*. **2010**, *49*, 6655. (g) Evans, W. J.; Miller, K. A.; Lee, D. S.; Ziller, J. W. *Inorg. Chem*. **2005**, *44*, 4326. (h) Evans, W. J.; Champagne, T. M.; Ziller, J. W. *Organometallics* **2007**, *26*, 1204. (i) Evans, W. J.; Walensky, J. R.; Champagne, T. M.; Ziller, J. W.; DiPasquale, A. G.; Rheingold, A. L. *J. Organomet. Chem*. **2009**, *694*, 1238. (j) Evans, W. J.; Takase, M. K.; Ziller, J. W.; DiPasquale, A. G.; Rheingold, A. L. *Organometallics* **2009**, *28*, 236.

[21] Kaim, W. *J. Am. Chem. Soc*. **1984**, *106*, 1712.

[22] (a) Heunisch, G. W. *Anal. Chem*., **1972**, *44*, 741. (b) Kaim, W. *J. Organomet. Chem*. **1981**, *215*, 337.

[23] A given synthetic protocol has been commonly used for preparation of heterometallic alkylaluminum – chromium complexes: (a) Temple, C.; Jabri, A.; Crewdson, P.; Gambarotta, S.; Korobkov, I.; Duchateau, R. *Angew. Chem. Int. Ed*. **2006**, *45*, 7050. (b) Jabri, A.; Temple, C.; Crewdson, P.; Gambarotta, S.; Korobkov, I.; Duchateau, R. *J. Am. Chem. Soc*. **2006**, *128*, 9238. (c) Vidyaratne, I.; Nikiforov, G. B.; Gorelsky, S. I.; Gambarotta, S.; Duchateau, R.; Korobkov, I. *Angew. Chem. Int. Ed.* **2009**, *48*, 6552.

[24] A. Jabri, C. B. Mason, Y. Sim, S. Gambarotta, T. J. Burchell, R. Duchateau, *Angew. Chem. Int. Ed*., **2008**, *47*, 9717.

[25] Junk, P. C.; Raston, C. L.; Skelton, B. W.; White, A. H. *J. Chem. Soc., Chem. Comm*. **1987**, 1162.

[26] Cambridge crystallographic data centre, http://www.ccdc.cam.ac.uk/products/csd/radii/table.php4

[27] For reviews of chromium (I) arene complexes, see: (a) Seyferth, D. *Organometallics* **2002**, *21*, 1520. (b) Seyferth, D. *Organometallics* **2002**, *21*, 2800.

[28] Engelhardt, L. M.; Jacobsen, G. E.; White, A. H.; Raston, C. L. *Inorg. Chem*. **1991**, *30*, 3978.

[29] Raston, C. L.; Whitaker, C. R.; White, A. H. *J. Chem. Soc., Dalton Trans.* **1988**, 991.

[30] Barr, D.; Clegg, W.; Mulvey, R. E.; Snaith, R.; Wright, D. S. *J. Chem. Soc., Chem. Commun.* **1987**, 716.

[31] a) M. Mikulla, R. Mülhaupt, *Chem. Ber.*, **1994**, *127*, 1723 - 1728; b) A. Claus, *Liebigs Ann. Chem*., **1873**, *168*, 1.

[32] SAINT-NT, Bruker AXS Inc., Madison, W., USA, **2000**

[33] Sheldrick, G. M. *SADABS 2.0,* Universität Göttingen: Göttingen, Germany, **2000**.

[34] Sheldrick, G. M. *Acta Crystallogr. Sect. A* **1990**, *46*, 467.

[35] Sheldrick, G. M. *SHELX-97*: Program for the Solution and Refinement of Crystal Structures; Universität Göttingen: Göttingen, Germany, **1997**.

# Chapter 4.

## *Conclusions*

Valuable new information has been generated by this thesis work and we believe that the data obtained will be important for the future development of an electron storage materials or materials having intense photochemical properties.

Firstly, we have documented that the alkylaluminum compounds reduce phenazine with formation of dialuminum cage type compounds containing two formally mononegative phenazine ligand. Moreover, reaction of phenazine and alkylaluminum compounds is leading to the paramagnetic compounds, containing an organic radical resulted from the transfer of the alkyl group R$^{\bullet}$ from an aluminum atom of $AlR_3$ to the nitrogen atom of phenazine molecule. All this illustrates an unprecedented behaviour of phenazine as a non-innocent ligand in terms of promoting radical cleavage with formation of stable organic radical. This behaviour is certainly established in the case of transition metals and lanthanides where the drive for the formation of the radical is usually provided by either reducing conditions or instability of a certain metal valence state. In the present case instead, it is the tendency to form stable radicals, which actually promotes this unique case of radical cleavage of a fairly stable Al-C bond in the $AlR_3$ compounds. In turn, this might have interesting implications for inducing radical bond cleavage on other more interesting target molecules such as water where hydrogen atom abstraction would eventually lead to the formation of oxygen gas. From the other side the stable radicals might possess intensive photochemical properties and serve as candidates for assembling of materials for light conversion in to electricity, a key components of the dye sensitized solar cells.

In the third chapter, we have explored the interaction of phenazine and thiophenazine with both alkylaluminum compounds and chromium salt. We have isolated and characterized the heterometallic complexes containing an alkylaluminum moiety, chromium and a negatively charged phenazine ligand.

The interaction of phenazine or thiophenazine, with $CrCl_2(THF)_2$ and triethylaluminum in toluene is initially accompanied by the reduction of phenazine ligand leading to the heterometallic Cr(II) - aluminum complexes containing a formally dinegative phenazine or thiophenazine ligands. The formation of such a dianion implies that a two-electron reduction took place likely at the expenses of the two alkyl functions from the aluminum atoms. It is well conceivable that the reaction initially proceeds by following the radical pathway previously observed for the radical cleavage of $AlR_3$ as promoted by this ligand and where in this case the $CrCl_2$ moiety acts only as a templating agent

When the excess of $Et_3Al$ is used, the interaction of phenazine, $CrCl_2(THF)_2$ and excess of triethylaluminum in toluene is accompanied by the reduction of phenazine ligand and chromium leading to the heterometallic multinuclear Cr(I) - aluminum complex containing a formally dinegative phenazine ligands and two chromium atoms. This means, that the ability of phenazine to extract radical may be used to generate a ligand cage capable of encapsulating two chromium atoms.

## *Future perspectives*

A present investigation aimed to study interaction between the phenazine and aluminum alkyls and chromium source in order to explore behaviour of phenazine molecule in the reaction systems and achieve a rational design of complexes with the negatively charged phenazine ligand or stable radical complexes containing a non-derivatized or derivatized phenazine moiety, potentially important for the photochemical applications. Although the synthetic goals were achieved the practical applications are still pending.

The first obvious future strep would be investigation of interaction between the titanium or aluminum oxide and the obtained in the present work complexes as well as finding an optimal way of grafting the complexes on the titania or alumina support. Titanium and aluminum oxide are classical materials for the nanocrystalline semiconductor film electrode in the dye sensitized solar cell.

The next step is studying a photochemical behaviour of these complexes grafted on titanium or aluminum oxide. Depending on performance a further improvement of photochemical properties might be achieved by synthesis of complexes containing a derivatized phenazine ligand. Another issue is stability of complexes on the titania or alumina support. An increase in stability of complexes in turn might be achieved by derivatization of phenyl groups of phenazine molecule. Therefore an intensive future synthetic work is needed to expand a given class of complexes and to find a best material for the photochemical applications.